# New Methodology for Evaluating Incompatibility of Concrete Mixes in Laboratory: A Feasibility Study

FINAL REPORT
August 2019

Submitted by:

Benjamin Arras, BSCE
Graduate Research Assistant
Center for Transportation Infrastructure Systems
The University of Texas at El Paso

Evan Wolf, Ph.D., MAJ, USA
Doctoral Research Assistant
Center for Transportation Infrastructure Systems
The University of Texas at El Paso

Danniel D. Rodriguez, Ph.D.
Research Assistant Professor
Center for Transportation Infrastructure Systems
The University of Texas at El Paso

Soheil Nazarian, Ph.D., P.E., D.GE
Professor/Director
Center for Transportation Infrastructure Systems
The University of Texas at El Paso

The University of Texas at El Paso
500 W. University Ave, El Paso, TX 79968

External Project Manager
Richard B. Rogers, P.E.

# Disclaimer Statement

| 1. Report No. CAIT-UTC-NC37 | 2.Government Accession No. | 3. Recipient's Catalog No. |
|---|---|---|
| 4. Title and Subtitle New Methodology for Evaluating Incompatibility of Concrete Mixes in Laboratory: A Feasibility Study | | 5. Report Date August 2019 |
| | | 6. Performing Organization Code CAIT / The University of Texas at El Paso |
| 7. Author(s) Benjamin Arras, Evan Wolf , Danniel Rodriguez, Soheil Nazarian | | 8. Performing Organization Report No. CAIT-UTC-NC37 |
| 9. Performing Organization Name and Address Center for Transportation Infrastructure Systems The University of Texas at El Paso 500 W. University Ave., El Paso, Texas, 79968-0516 | | 10. Work Unit No. |
| | | 11. Contract or Grant No. DTRT13-G-UTC28 |
| 12. Sponsoring Agency Name and Address Center for Advanced Infrastructure and Transportation Rutgers, The State University of New Jersey 100 Brett Road, Piscataway, NJ 08854 | | 13. Type of Report and Period Covered Final Report June 1, 2016 – August 31, 2019 |
| | | 14. Sponsoring Agency Code |

16. Abstract

The early-age behavior and properties of portland cement concrete change rapidly over time as a result of the hydration process. Comprised of a series of chemical reactions, this process accelerates nonlinearly with the curing temperature. Gaining knowledge and understanding of the phases of the hydration process (i.e., dormant, setting, and hardening) plays an important role in the timely opening of roads, resuming of construction, and achieving long-term performance. Standard tests such as ASTM C403 arbitrarily define the time of initial and final setting of concrete. Despite decades of studies concerning setting times, actual predictions still span hours, while the quality of concrete is customarily evaluated by its compressive strength at 28-days. New technologies provide an accurate and detailed understanding of the hydration process. In this research, maturity concept, along with seismic and infrared technologies, were used to measure and evaluate portland cement concrete properties. Two different sources of aggregates, dolomite (partly crushed limestone) and gravel (partly crushed, siliceous) were considered. The setting times and quality of early age concrete were evaluated using seismic and maturity tests. The thermal profiles of the gravel-based concrete specimens were observed during the first 48-hours to monitor the heat dissipation during the hydration process. The versatility of the approach was studied by conducting tests under varied environmental curing conditions on a reference mix as well varying the water-cement ratio, chemical admixtures, and gradation of coarse aggregates. Correlations of both the maturity and seismic modulus to conventional compressive strength test at 1, 3 and 7-days are presented. Additionally, thermal profiles of concrete for different curing conditions and mixes are shown. Lastly, an approach for determining the initial and final sets is provided, when coupled with the strength testing, validates the need for redefining sets based on measureable concrete properties.

| 17. Key Words Concrete, Concrete Setting, PCC Modulus, Concrete Hydration, PCC Maturity, Thermal Profile, Early-age Strength Development | | 18. Distribution Statement | |
|---|---|---|---|
| 19. Security Classif (of this report) Unclassified | 20. Security Classif. (of this page) Unclassified | 21. No of Pages 149 | 22. Price |

Form DOT F 1700.7 (8-69)

# Acknowledgements

**Abstract**

The early-age behavior and properties of portland cement concrete change rapidly over time as a result of the hydration process. Comprised of a series of chemical reactions, this process accelerates nonlinearly with the curing temperature. Gaining knowledge and understanding of the phases of the hydration process (i.e., dormant, setting, and hardening) plays an important role in the timely opening of roads, resuming of construction, and achieving long-term performance. Standard tests such as ASTM C403 arbitrarily define the time of initial and final setting of concrete. Despite decades of studies concerning setting times, actual predictions still span hours, while the quality of concrete is customarily evaluated by its compressive strength at 28-days. New technologies provide an accurate and detailed understanding of the hydration process. In this research, maturity concept, along with seismic and infrared technologies, were used to measure and evaluate portland cement concrete properties. Two different sources of aggregates, dolomite (partly crushed limestone) and gravel (partly crushed, siliceous) were considered. The setting times and quality of early age concrete were evaluated using seismic and maturity tests. The thermal profiles of the gravel-based concrete specimens were observed during the first 48-hours to monitor the heat dissipation during the hydration process. The versatility of the approach was studied by conducting tests under varied environmental curing conditions on a reference mix as well varying the water-cement ratio, chemical admixtures, and gradation of coarse aggregates. Correlations of both the maturity and seismic modulus to conventional compressive strength test at 1, 3 and 7-days are presented. Additionally, thermal profiles of concrete for different curing conditions and mixes are shown. Lastly, an approach for determining the initial and final sets is provided, when coupled with the strength testing, validates the need for redefining sets based on measureable concrete properties.

# Table of Contents

# List of Tables

# List of Figures

# Chapter 1: Introduction

## 1.1 Problem Statement

Portland cement concrete (PCC) is one of the most widely used construction materials due to its versatility and ability to be produced with different characteristics and under variable placement conditions with inherent constraints. Achieving these desired characteristics and proper placement requires a knowledge of fresh concrete behavior as it contributes to the long-term performance of the fully-cured concrete. This knowledge contributes to understanding the various processes that occur as fresh concrete hydration leads to setting and hardening. Understanding these processes is necessary to comprehend the strength development in concrete.

In today's fast-paced culture, finding ways to shorten construction project timelines is always sought, whether for monetary benefit for the contractor and owner or convenience for facility users. Predicting concrete mechanical properties through early-age methods can streamline the construction process.

The rate at which concrete develops strength depends on a number of variables related to environmental conditions and mixture components. Variable, system conditions and mixture constituent properties influence the on-going chemical reactions during concrete setting; directly impacting the rate of strength development and the long-term performance. This assortment of variables yields inherent complexities in strength prediction. Most strength predictions are derived from laboratory-based procedures performed prior to final mix production. These early-age methods are confirmed with destructive testing of the specimens produced, considering they are stored under the similar field conditions. Likewise, similar procedures employ cored specimens from placed concrete. A significant amount of research has been conducted that has led to far-more robust methods for understanding and observing the concrete curing process. However,

robust methods for early-age strength prediction is still undergoing further research and development.

A number of variables, either mix-related or environment-related, affect the rate of strength development and the short and long-term strength. Mix-related variables include the type of aggregate/aggregate properties, type of cement, chemical and mineral admixture characteristics, and mix proportions (e.g. water-cement ratio and gradation). The rate of hydration during curing is affected by environmental variables (e.g. humidity levels, mixing, placement and curing temperatures) which ultimately influence the rate of strength development.

Because of the inherent variability of project design and construction conditions-ultimately influencing the required and actual strength development, it is difficult to develop a single mix design that will completely meet the service and constructability requirements for every project. Availability and selection of mixture components varies by location, and environmental conditions are beyond our control. However, by having a thorough understanding of the effects that mixture constituents and environmental parameters have on the PCC curing process and strength development, then mixing, placement and quality methods and processes can be accommodated and modified in order to achieve the desired or optimum concrete properties. Conventionally, confirmation of concrete strength is dependent on the 28-day compressive strength testing of either extracted cores from the placed concrete, or cast specimens produced and cured in the same conditions. Both of these methods require an extensive waiting period; ultimately resulting in time delays, and accumulating project and user-costs.

To understand, predict, and model concrete characteristics in an early stage(s) requires the use of nondestructive testing (NDT) approaches. Employing concrete maturity methods and seismic technologies for characterizing the behavior of early-age concrete has been studied

previously (Nazarian et al., 1997; Yuan et al., 2003, 2005; Yi et al., 2005; Nazarian et al., 2006; Yikici and Chen, 2015; Benaicha et al., 2016; Collier et al., 2017). Seismic and maturity methods provide insight to early-age concrete behavior and pertinent relationships to strength development through the use of standard test procedures. Use of an infrared camera allows capturing the thermal profile of the specimen during the hydration process. Past research studies have provided further insight to understanding the relationships between temperature, modulus of elasticity, and strength development considering the first hours after concrete pouring.

This study employs a NDT-based approach, paired with observing concrete maturity metrics as modes to understand the early-age strength development of concrete as different mix and system variables are adjusted. These experimental relationships can eventually lead to models for predicting strength. The developed method will enable for concrete mix adjustments to fit the time and monetary requirements of the project.

## 1.2    Objective

The objective of this research is to develop a laboratory system based on nondestructive methods to monitor the early-age behavior of concrete considering environmental and mixture variations. Monitoring of temperature and seismic modulus of the concrete during early-age can potentially provide comprehensive measurements of the initial and final sets and the rate of hydration.

A component of this study will focus on the mixture variations, namely: commonly specified admixtures in varying quantities, maximum aggregate size, gradation and aggregate types (dolomite versus gravel mix). Comparison of the early-strength and curing trends among the various mixtures provides the opportunity to identify if the different admixtures and associated dosages enhance or hinder concrete strength development. Additionally, curing specimens at

3

varying temperature and humidity levels provide greater understanding of the strength development under different environmental conditions. This was performed in entirety for a dolomite aggregate PCC mixture. A gravel mixture also underwent testing and analysis for comparison to the dolomite mix, however this comparative analysis considers only variable environmental conditions.

## 1.3    Organization

A background on the parameters and processes that affect the strength development of portland cement concrete (PCC) is presented in Chapter Two. In addition to explaining the hydration process and setting, that chapter overviews the most common supplementary cementitious materials (SCMs) and chemical admixtures. Chapter Two also covers a literature review of studies related to concrete maturity and overall strength development.

Chapter Three details the methodology followed in this research. The experimental design, preparation and testing of the mixes, as well as the evaluated environmental and mix-related parameters are discussed.

Data analysis is presented in Chapter Four. The effects of environmental and mix-related parameters on concrete setting, and strength and modulus growth are shown. Additionally, the obtained relationships between time and maturity, and strength and seismic modulus are presented. Developed methods are proposed in Chapter Five. Approaches for defining the initial and final set in terms of seismic modulus with time and maturity are described. Further, discussion follows with *alternative maturity*, and assessment of thermal profiles of the early-age concrete.

Summary of the findings, conclusions, and recommendations for further research are discussed in Chapter Six.

# Chapter 2: Literature Review

## 2.1    Early-Age Processes and Characteristics of Cast Portland Cement Concrete

Several processes occur during the early-age of placed PCC that can affect its properties. As a result of these processes, concrete properties may change by orders of magnitude over a period of hours (Bertagnoli et al., 2009). Strength increases, from an almost negligible value to several hundred or thousand pounds per square inch (psi). For this to occur, concrete must undergo a hydration process; causing the concrete to stiffen, set and ultimately harden. Definitions of stiffening, setting and hardening vary based on literature source, but the end meanings can be consolidated as the following:

- *Stiffening* – the loss of consistency of the plastic cement paste (Mehta and Monteiro, 2006).

- *Setting* – the process, due to chemical reactions, that results in a gradual development of rigidity of a cementitious mixture (ASTM C125, 2019).

- *Hardening* – the gain of strength of a cementitious mixture as a result of hydration that occurs after final setting (ASTM C125, 2019).

These three processes are controlled by the rate of hydration, which is ultimately dictated by the curing conditions. The concrete progresses from one process to the next, with the rate of hydration dictating the time for each process to occur.

### 2.1.1    Hydration

As water is added to a cement mixture, a chemical reaction occurs; initiating the hydration process. The process of hydration continues as long as moisture is present. The continuous strengthening of PCC can cease when there is not sufficient moisture in the system. Typically, this occurs when the relative humidity in the concrete drops below 80% (Mindess et al., 2003). During a series of chemical reactions, two key products are created: *heat* and the *hydrates* (or bonding

agents). The formation of the hydrate results from the reaction of water with the calcium silicates in the cement (Newman and Choo, 2003a). Hydration is primarily a chemical reaction between water and cement, both the individual particles and those attached to aggregates, and secondarily by diffusion and penetration of the hydrate already formed (Yi et al., 2005).

The hydration process is influenced by the mix, cement quantity, water-cement ratio, and ambient temperature, humidity and wind. Variations in those factors affect the rate and duration of hydration. Mindess et al. (2003) reported that complete hydration occurred at a water-cement ratio of 0.42, indicating that primary hydration of all the cement particles was complete and any further hydration was of the already formed hydrate. As hydration progresses, concrete continues to develop strength as a result of the hydrates fixing to both the aggregates and one-another; effectively forming a solid structure (Newman and Choo, 2003b). The speed with which strength is developed depends on the rate of hydration. Increasing the temperature, or using a cement with finer particles generally increases the rate of hydration (Lin and Meyer, 2009). Two functions generally express the rate of hydration. The first i) is based on the rate of heat of hydration per unit mass of cement under specific hydration conditions and the second ii) is thermal activity of each mineral compound in cement (Swaddiwudhipong et al., 2002).

The rate of hydration, $a$, at a specific time, $t$, is approximated as:

$$a(t) \approx \frac{Q(t)}{Q_{max}}$$ 

EQN 2.1

Where $Q(t)$ is the amount of heat of hydration generated per unit mass of cement at time $t$, and $Q_{max}$ is the specific heat of hydration per unit mass of cement (cal/g). This method provides a linear relationship between the amount hydrated and heat generated. Use of thermal activity allows the calculation of an equivalent maturity for each compound, $M_i$

$$M_i(T,t) = \int_0^t exp \left\{ \frac{-E_i(Q_i)}{R} \left[ \frac{1}{T(t)} - \frac{1}{T_0} \right] \right\} d\tau$$ 

EQN 2.2

where $E_i$ $(Q_i)$ is the activation energy per mol of mineral compound, $i$ (cal/mol). $R$ is the gas constant, $T_0$ is the reference temperature, and $T$ $(t)$ is the actual temperature of hydration at time $t$. When summed, Equation 2.2 provides an exponential function in the form of

$$Q(t) = \Sigma \left( \int_0^M q_i dM_i \right) \qquad \text{EQN 2.3}$$

where $q_i$ is the reference rate of hydration.

Neville (1996) and Glisic and Simon (2000) described the hydration as a three-stage process. Figures 2.1 and 2.2 summarize the process. The *early stage*, or Stage I, is the initial hydration that occurs after the addition of water. During this stage, there is a short period of rapid chemical dissolution causing a high evolution of heat, followed by a one to two-hour dormant period. During Stage II, or the *middle stage*, the setting of PCC occurs. In this stage, growing layers of hydration products in the PCC begin to contact one-another; effectively forming a solid structure. The evolution of heat continues to increase from the end of the dormant period until it peaks at the point where all of the primary reactions between water and cement have occurred. The *late stage*, or Stage III, is the longest stage. In this stage, diffusion controls the renewal of reaction. This stage continues as long as water and hydration products are available to react; the concrete continues to harden as the pores in the system continue to shrink and hydration products grow and fill the spaces. The process continues to produce heat, but the highest point is at the beginning of this stage and decreases as hydration continues.
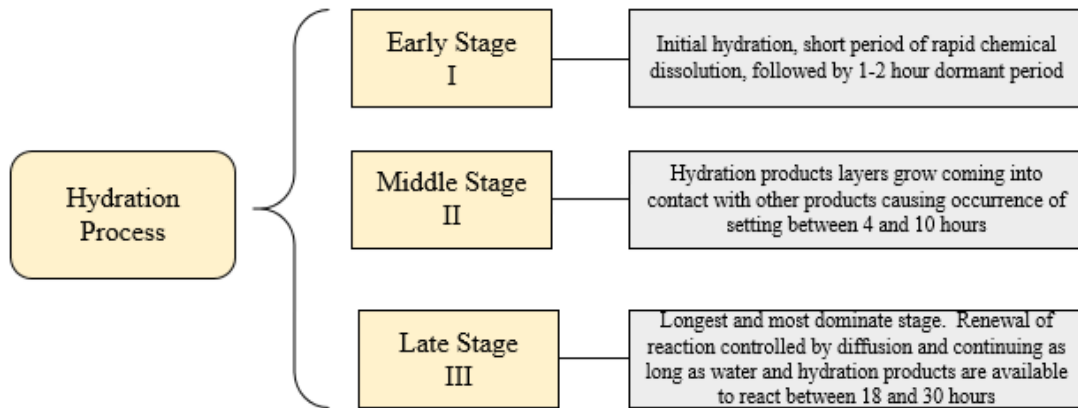
**Figure 2.1 Phases in Hydration Process**
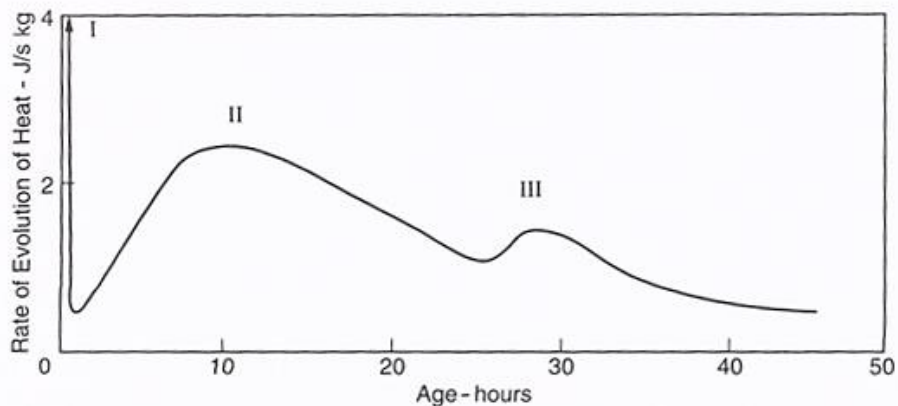


**Figure 2.2 Three-Stage Heat Evolution of Portland Cement (Neville, 1996)**

As seen in Figure 2.3, Mindess et al. (2003) depicted the rate of heat evolution in a similar

manner to Neville (1996), but categorized as five stages. They further explained the relevance of

each stage to the concrete properties. They described Neville's early stage as the *initial hydrolysis*

and *induction period*. The *initial hydrolysis* period occurs when water comes in contact with the

mix as a result a rapid heat evolution stage occurs. The *induction* or *dormant* period determines

the initial set of the concrete. The *acceleration* period most closely relates to the middle stage,

since this phase is a chemically controlled reaction and sees the formation of hydration creating

bonds. This formation determines the final set, as well as the rate of initial hardening. The late

stage is the combination of what Mindess et al. (2003) labeled as the *deceleration* and *steady state*

8

stages. Both stages experience diffusion-controlled reactions, which occur at a slower rate and produce less heat. Deceleration is the stage that the rate of early strength gain is determined, while steady state determines the long-term strength gain.
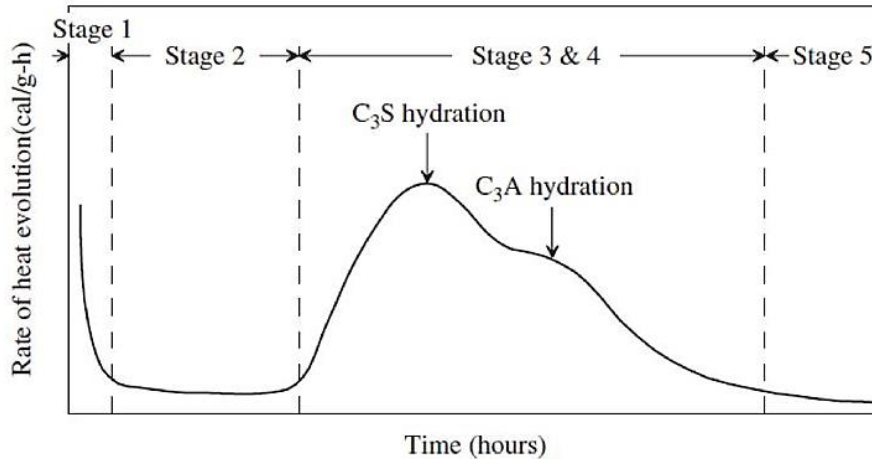


**Figure 2.3 Five-Stage Heat Evolution of Portland Cement (Mindess et al., 2003)**

### 2.1.2 Setting and Hardening

Concrete setting is characterized by initial setting time and final setting time, as determined by the penetration resistance of cement paste obtained with the Vicat apparatus (ASTM C191, 2019). A separate method uses a penetrometer to determine penetration resistance of cement mortar (ASTM C403, 2016). Although both methods are considered as the standard procedures for determining concrete set time, they are destructive methods that either damage the placed concrete or require producing test specimens. Gams and Trtnik (2013) suggested the use of longitudinal waves as a nondestructive, alternative approach for determining setting times. Two advantages of their approach is that i) the method is testable on in-situ concrete and ii) it is unaffected by the presence of fine and coarse aggregates. They found that the ratio between maximum amplitudes at different dominate frequencies could provide accurate determination of the setting times.

The *initial set*, which typically occurs between two and four hours from mixing, is defined as the time when the paste stiffens to a point where it is no longer workable. The *final set* is defined as the time when the concrete has hardened to a point it can sustain a load, this typically occurs between five and eight hours (Mindess et al., 2003; Mehta and Monteiro, 2006). Variables such as the composition of the cement, water-cement ratio, temperature, and the use of admixtures, all influence the time it takes for concrete to set. Cements with finer particles set faster since their higher surface area yields increased reaction between the water and cement. Bentz (2008) stated that higher water-cement ratio caused a greater amount of reaction, but slowed down the setting time. The extra water in the system slows the rate that the hydrates encounter each other and form a mutual bond. Decreases in temperature typically decrease the setting times. The addition of admixtures can either increase or decrease the setting time, depending on the type of admixture used.

Figure 2.4 depicts the hardening of cement paste, displaying the various processes of setting and hardening. Concrete hardening occurs subsequent to setting and is the phase where the mechanical properties develop, specifically strength.
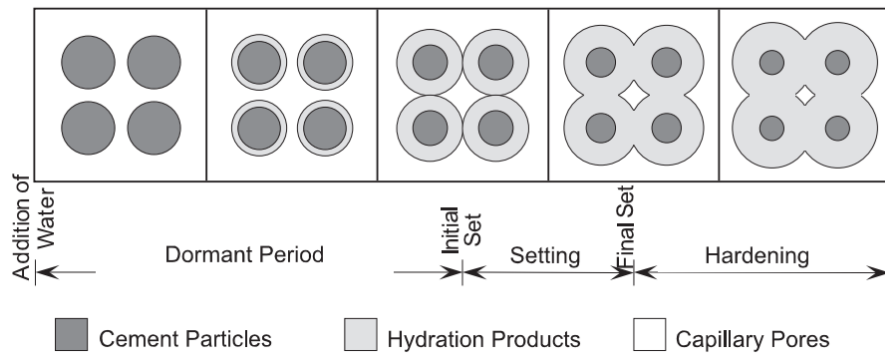


**Figure 2.4 Hardening of Cement Paste (Glisic and Simon, 2000)**

Figure 2.5 illustrates the typical strength gain over time, as well as where setting occurs in relation to limits of handling and hardening. Although the final set typically occurs after approximately eight hours, it still takes one to two days for concrete to achieve appreciable strength (Mehta and Monteiro, 2006). As hardening progresses, hydrates continue to form yielding reduction of pores in the system and causing strength gain. During the dormant stage, there is no mutual contact which results in negligible strength. Once the initial set occurs, the cement paste begins to come into contact and bond with other hydration products. This results in a reduction of pores as it reaches final set, and transitions into hardening.
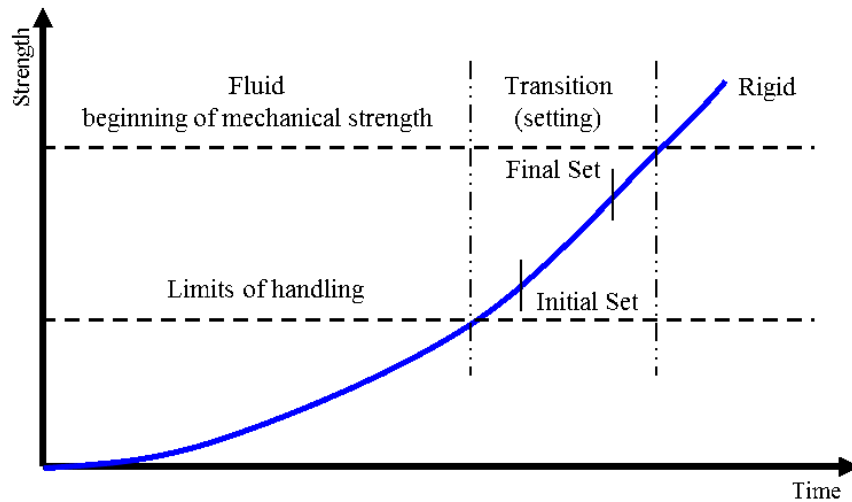


**Figure 2.5 Process of Setting and Hardening (Mindess et al., 2003)**

### 2.1.3 Curing

To promote proper curing, the temperature and the movement of moisture have to be controlled (Neville, 1996). Mehta and Monteiro (2006) further stated that controlling the temperature and preventing moisture loss must occur for the concrete to reach a desired strength. It is during this process that PCC develops its hardened properties. Use of various laboratory and field-based methods during curing enables control of the temperature and moisture. Application of the specific method employed depends on time and cost constrains, and ambient conditions.

Table 2.1 provides further discussion of these effects. In general, higher temperatures and prolonged exposure to moisture result in increased strength development at early stages.

**Table 2.1 Literature Discussing Concrete Curing, Hardening and Strength Development**

| Source | Discussion |
|---|---|
| Burg, 1996 | • As an approximation, setting time will change approximately 50% for each 10ºC change in temperature from a reference temperature. Lower temperatures increase set times; higher temperatures decrease set times<br>• Strength development at low temperatures is lengthy and small change, although later age strength is equal or exceeded that of the reference temperature mix<br>• At high temperatures early strength has a reversed effect after 7 days which the reference temperature mix has a higher strength than the high temperature mix |
| Neville, 1996 | • Standard curing temperature ranges between 64 and 70 degrees Fahrenheit.<br>• Higher temperatures at curing increases hydration reactions by reducing the dormant period, thus promoting early strength<br>• High pressure steam curing has resulted in 28 day strength at 24 hours |
| Mindess et al., 2003 | • Higher curing temperature causes higher early strength, but lower ultimate strength<br>• Sealed concrete gains strength slower than continuously moist cured<br>• To reach 70% specified strength 7 days moist curing should be prescribed |
| Yi et al., 2005 | • Increasing initial curing temperature increases early strength, but decreased long-term strength<br>• Changes in curing temperatures influence the diffusion and penetration of hydrates affecting strength development; generally, as temperature increases diffusion and penetration increases. |
| Mehta and Monteiro, 2006 | • The longer moist curing occurs, the higher strength of concrete will be<br>• Higher temperature promotes faster hydration and thus faster strength development |
| Yikici & Chen, 2015 | • Higher curing temperatures speed up the hydration process and leads to early strength gain<br>• Larger mass concrete structures have variable concrete temperatures throughout the structure which affect the curing history<br>• High curing temperatures at early-age lead to a lower ultimate strength when compared to lower early-age curing temperatures |

## 2.2    Strength Estimation and Development

Concrete strength develops over time based on various factors. Regardless of these factors, the 28-day strength determines the concrete strength rating. At this point, assessing strength development is lengthy in time, however the measured strength is obtained with high confidence. Project managers, contractors, and owners, alike, all desire to complete projects rapidly. A 28-day wait period seems to pose a common obstacle and presents a relatively constant, time constraint.

Possessing the capability to estimate the 28-day strength, with certainty, at earlier stages is highly desirable. Estimating the final strength with a high degree of certainty requires a thorough understanding of the early-age behavior. Being able to estimate the strength, in situ, of the placed concrete represents the ideal scenario. Assessing strength, without causing damage to the concrete, is a necessary attribute. Two such methods that are employed for assessing strength and stiffness development with curing, are a) the maturity test (which relates the time and temperature of the concrete to the strength) and b) seismic method to determine the concrete elastic modulus. In the laboratory, a seismic method includes use of the Free-Free Resonant Column (FFRC), while field-testing has employed the Portable Seismic Property Analyzer (PSPA). Since this research is focused on a laboratory-based procedure, the FFRC method will remain a focal point.

### 2.2.1 Free-Free Resonant Column Method

The Free-Free Resonant Column (FFRC) test method utilizes wave propagation principles to determine the modulus and Poisson's ratio by measuring the resonant frequencies of a cylindrical specimen. Based on the recorded resonant frequencies and dimensions of the specimen, the modulus is calculated.

Components of the FFRC apparatus include a data acquisition system, an accelerometer, and an instrument hammer (shown in Figure 2.6). Generation of compressive waves occurs by the impact from the instrumented hammer. These waves propagate through the specimen and the accelerometer collects them to determine the resonant frequencies. Shown in a frequency versus amplitude graph, two peak frequencies appear. The lower peak represents the shear frequency ($f_s$) while the higher peak indicates the longitudinal frequency ($f_L$). These frequency correspond to the shear wave and compression wave, respectively, as seen in Figure 2.6.
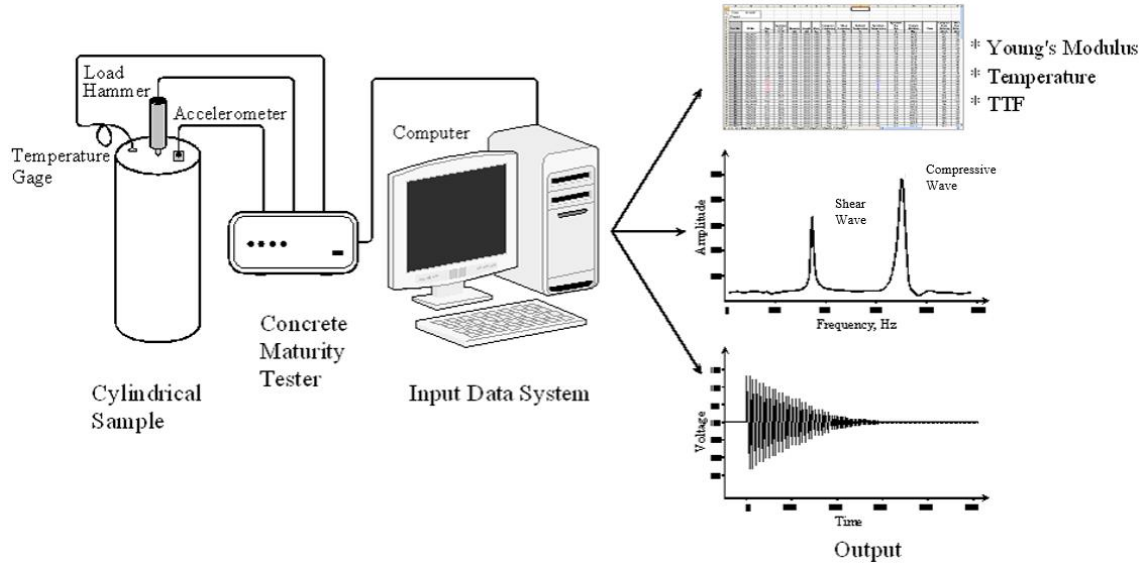
**Figure 2.6 Free-Free Resonant Column Test Layout Apparatus**

With the known mass ($M$), length ($L$), and cross sectional area of the specimen ($A_s$) of the specimen, the density ($\rho$) is calculated from;

$$\rho = \frac{M}{LA_s} \hspace{4cm} \text{EQN 2.4}$$

Young's modulus ($E$) is estimated by the following equation:

$$E = \rho(2f_L L)^2 \hspace{4cm} \text{EQN 2.5}$$

Poisson's ratio ($v$) is estimated from:

$$v = \frac{(0.5\lambda - 1)}{(\lambda - 1)} \hspace{4cm} \text{EQN 2.6}$$

where

$$\lambda = \left[\frac{f_L}{f_s}\right]^2 C_{L/D} \hspace{4cm} \text{EQN 2.7}$$

$C_{L/D}$ is a correction factor when the length-to-diameter ratio is not 2 (see ASTM C 215).

Nazarian et al. (1997) found strong correlations between the moduli obtained through FFRC method and the compressive and tensile strengths of the specimens. Yuan et. al (2003) showed that the relationship between the compressive strength and Young's modulus appeared to be independent of the concrete mixture for the same aggregate source. Nazarian et al. (2006) later

14

confirmed that the laboratory calibration curve between the seismic modulus and compressive strength can be developed with confidence. This allows the FFRC apparatus to be a useful tool to assess the concrete strength during the hardening process.

### 2.2.2 Maturity

Since time and temperature both affect the hydration process, and thus the strength development of concrete, developing a function that is defined as the product of these factors is the basis for the maturity method. This method defined in Equation 2.8 (ASTM C1074, 2017):

$$M(t) = \sum (T_\alpha - T_0) \Delta t \qquad \text{EQN 2.8}$$

where $T_\alpha$ = average concrete temperature, $T_0$ = datum temperature, and $\Delta t$ = time interval. Use of the maturity function aids in determining an equivalent age (at a reference temperature) which considers effects of both time and temperature. Mehta and Monteiro (2006) presented the following equation to determine the equivalent age, $t_e$, based on temperature during a time interval:

$$t_e = \frac{\sum (T_\alpha - T_0) \Delta t}{(T_r - T_0)} \qquad \text{EQN 2.9}$$

where $T_r$ = reference temperature.

Yuan et. al (2003) studied the strengths, Young's modulus, and maturity parameters of several slabs and cores. They reported good correlations between compressive strength, flexural strength, and seismic modulus with maturity values (as judged by the coefficients of determination, $R^2$ around 0.90). This is shown in Figure 2.7. Tensile strength had a slightly weaker correlation, as suggested by the $R^2$ value of 0.81 (see Figure 2.7c). Overall, a good correlation between the maturity values and Young's modulus was found, as observed by an $R^2$ of 0.94 (see Figure 2.7d).
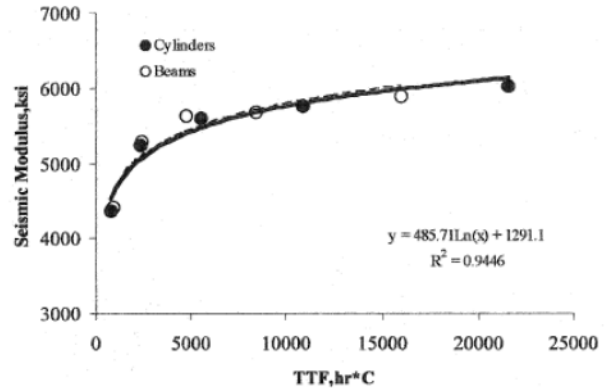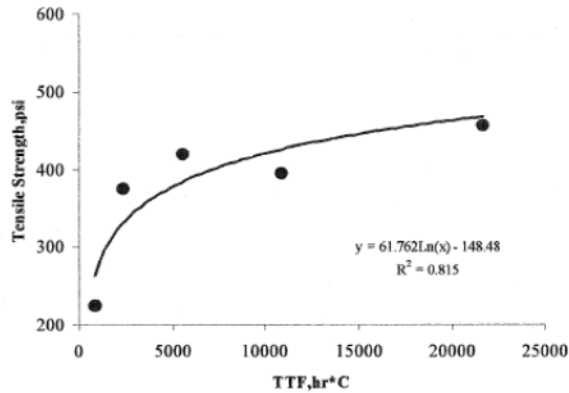
a) Compressive strength vs maturity parameters    b) Flexural strength vs maturity parameters
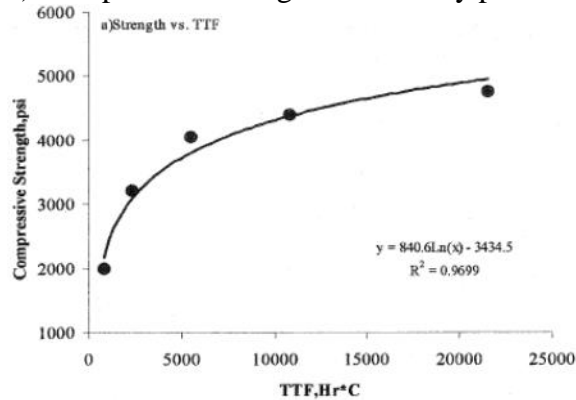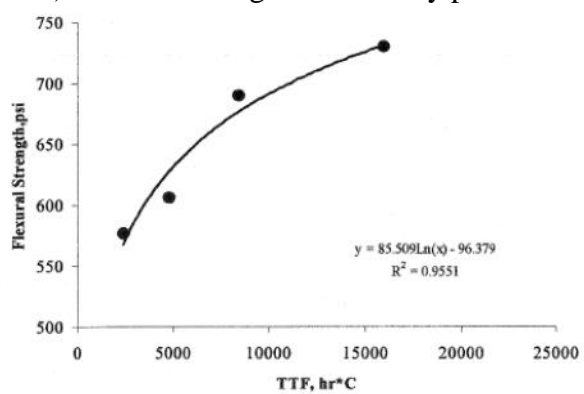
c) Tensile strength vs maturity parameter    d) Seismic modulus vs maturity parameters

**Figure 2.7 Correlations Determined by Yuan et al. (2003)**

## 2.3    Imaging

Infrared imaging provides a nondestructive method for the evaluation of subsurface defects in concrete structures. These methods are commonly used to identify cracks and delamination, as well as locate steel reinforcement (Pla-Rucki and Eberhard, 1995). The principle behind infrared imaging is that subsurface anomalies cause localized difference at the object surface due to varying rates of heat transfer (Weil, 1991; Büyüköztürk, 1998). Although all three modes of heat transfer, radiation, conduction, and convection affect the surface temperature of the material, radiation serves as the measurement used for infrared imaging. The infrared detector measures the emitted infrared radiation, which is then converted to a visual image based on the Stefan Boltzmann law (Maser and Roddis, 1990; Clark et al., 2003). Radiation is calculated from:

$$E_r = \epsilon \sigma T^4$$                                                        EQN 2.10

16

where $E_r$ = radiation emissive power, T = temperature, $\epsilon$ = emissivity, and σ = Stefan-Boltzmann constant.

Hiasa et al. (2014) noted that the ambient temperature surrounding the specimen during infrared imaging creates thermal noise, affecting the temperature reading. Weil (1991) reported that the surface conditions and subsurface configuration also affected the readings during infrared imaging. Although these shortcomings are the result of conduction and convection, they are more prominent during field-testing. During field testing, environmental conditions are not controlled and the potential for presence of anomalies in the large sections of concrete is higher than in cylindrical lab specimens.

Use of infrared imaging on early-age concrete is limited. One study that used infrared imaging on early age concrete was completed by Azenha et al. (2011). That study sought to verify the feasibility of applying thermography to early-age concrete during hydration, and to validate a model to predict temperature development. The research not only validated their model, but also showed that the temperatures measured by the internal thermocouples were correlated with those measured with the infrared devices. A drawback found during the study was the need for visual contact with the specimen, as formwork would prevent temperature measurement or degrade the confidence of the results.

## 2.3    Concrete Mix Design

Three considerations drive the concrete mixture design. The primary criteria being a hardened concrete with a desired compressive strength. Design of concrete based on a specified compressive strength is the dominant criterion, regardless of the intended use. American Concrete Institute (ACI) Committee 211 (Kosmatka et al., 2002) indicated that the absolute volume method provides the most accurate proportioning for obtaining the target compressive strength. The

17

flexural strength of PCC is calculated from the compressive strength; with the generally accepted conversion factor being 7.5 to 10 times the square root of the compressive strength [psi] (Kosmatka et al., 2002).

The second criterion considered is the setting time. Having a concrete that sets rapidly allows for continued construction and lower delay in the opening of the project. Producing a faster or slower setting time is typically accomplished through adjusting the amount of fines or chemical admixtures. Increasing fines (which have larger surface areas) increase the rate of hydration; accelerating the setting time.

Workability of the concrete, the third criterion for a mix design, is largely associated with the water-to-cement ratio. The rapid hydration of concrete can occur with a low water-to-cement ratio, however, lowering the ratio generally results in workability issues. A decrease in workability typically yields a faster setting time, but is much more labor intensive to pour and provides less time for finishing. Ashraf and Noor (2011) found that compressive strength and workability of concrete are highly affected by its aggregate gradation.

Since the compressive strength is a primary factor driving a concrete mix design, an understanding of the effects caused by the different components of PCC is necessary. The characteristics of PCC admixtures and their effects on constructability and short and long-term mechanical properties will be discussed. While this study is focused on assessing early-strength development of concrete mixes given various mix constituents and curing conditions, it should be noted that designing for a high degree of durability is necessary in order to achieve a long-lasting concrete.

### 2.3.1 Mixture Variables and Strength Development

Aggregate, cement, and water serve as the three core components needed for producing concrete. The cement-aggregate ratio, water-cement ratio, and sand-coarse[1] aggregate ratio are three of the four controllable variables in mixture design. Variability in these components can either help or hinder the strength development of concrete. Understanding their impact on strength, as well as cost, can influence the type and quantity of these components used in the mixture.

*Aggregate*

The particle gradation, shape, texture, strength and stiffness impact the concrete strength (Neville, 1996). The properties of the aggregates used have small effect on the strength development rate, but do influence the actual strength. The type of aggregate used in concrete mixtures is considered the most uncertain constituent, in terms of composition, due to sourcing variability. Typically, locally-sourced aggregates are used for convenience and economic reasons.

The particle gradation of the aggregates determines the entrapped air in the mixture, and as a result; the amount of cement needed to create the bond between the particles. Higher entrapped air yield a lower strength, while an increase in the cement content increases cost. The shape and texture of the aggregates determine the level of bonding between the cement paste and aggregate particles. Rougher, angular surface particles provide increased bonding with the cement paste; while smooth, spherical particles impact the workability (Neville, 1996; Mindess et al., 2003). An increased bond between the cement paste and aggregate particles provides higher strength because of improved ability to transfer stress throughout the concrete. If a weak bond occurs, or the particle has low strength, then the load-induced stress causes failure at the weaker point.

---

[1] Except for an optimized gradation, where an intermediate grade is important.

*Portland Cement*

The type and amount of portland cement in a concrete mixture is typically the greatest contributor of cost of the core components. Each chemical component of cement plays a role in the strength development. Typical chemical components include tricalcium silicate ($C_3S$), dicalcium silicate ($C_2S$), tricalcium aluminate ($C_3A$), tetracalcium aluminoferrite ($C_4AF$), and calcium sulfate dihydrate ($CSH_2$), in addition to other minor impurities (Mindess et al. 2003). The quantities of these compounds and the fineness of the cement determine cement classification (shown in Table 2.2). Each type of cement possesses characteristics that employed for certain purposes. Type I is typically associated with general construction. Type II is utilized for moderate sulfate resistance and Type V is applied for high sulfate resistance. Type III is best when rapid strength development is desired. When controlling heat of hydration, Type IV is used.

$C_3S$ is the chemical compound that contributes the most to the strength of concrete, particularly, rapid initial strength (Newman and Choo, 2003b). $C_2S$ normally contributes to the long-term strength of concrete (Newman and Choo, 2003b; Caldarone, 2009).

**Table 2.2 Chemical Composition and Properties of Portland Cements (Mindess et al. 2003)**

| Component | Type I | Type II | Type III | Type IV | Type V |
|-----------|--------|---------|----------|---------|--------|
| $C_3S$ | 55 | 55 | 55 | 42 | 55 |
| $C_2S$ | 18 | 19 | 17 | 32 | 22 |
| $C_3A$ | 10 | 6 | 10 | 4 | 4 |
| $C_4AF$ | 8 | 11 | 8 | 15 | 12 |
| $CSH_2$ | 6 | 5 | 6 | 4 | 4 |
| Fineness | 365 | 375 | 550 | 340 | 380 |
| 1 Day Strength (psi) | 2200 | 2000 | 3500 | 600 | 1750 |

Aside from the chemical compounds in cement, the fineness of the cement plays a significant role in the hydration and strength development of concrete. Finer cements provide an increased surface area; resulting in a higher rate of hydration and increased strength development (Mindess et al., 2003; Lin and Meyer, 2009). As seen in Table 2.2, Types I and III portland cements

have nearly identical chemical compositions with the exception that Type III is 50% finer and yields a one-day strength of almost 60% higher than Type I. Neville (1996) states that cement containing 95% of particles, between 3 and 30-microns, is best for rapid hydration and strength development. Mindess et al. (2003) states that particles below 3-microns have the greatest influence on 1-day strength. Alexander (1972) stated that hydration throughout the first two days, occurred mainly with the fines and the outermost layers of coarser particles. This hydration of the fines improves the early-strength development, and shortens the setting time.

*Water-Cement Ratio*

Water serves two primary roles in the production of concrete. First, it initiates and maintains the hydration process. Once the there is no more moisture, the hydration process ceases; thus ending strength development. The water-cement ratio ultimately determines the degree of hydration of the mixture, with amount of water necessary typically being below normal water-cement ratio. The reason water-cement ratios are usually higher than the amount needed for full hydration is to increase the workability. Although this has less to do with strength development, it is extremely important when considering the placement of the concrete. However, higher water content typically yields more pore space in the mixture, which means lower strength and durability (Newman and Choo, 2003b). Bentz (2008) indicated that the higher water content yielded greater hydration, but increases the setting time. A balance is necessary when considering the desired strength, and the required workability of the concrete. Understanding the inverse relationship between strength and the water-cement ratio enables one to make the necessary adjustments to other controlled variables in order to obtain the desired strength with needed workability (Mehta and Monteiro, 2006). According to Mindess et al. (2003), the typical water-cement ratios used for high-strength concrete varies from 0.22 to 0.50. This wide range indicates the adjustment of either

the cement-aggregate ratio or sand-coarse aggregate ratio; but more than likely the inclusion of the fourth controllable ratio, the use of admixtures.

## 2.4    Admixtures

The use of admixtures in PCC influences the processes that occur in early age concrete, thus affecting the characteristics of the hardening concrete. Mineral admixtures, also called supplementary cementitious materials (SCMs), generally serve as additional cementing material or as a replacement for a portion of the cement. The properties of mineral admixtures also influence concrete characteristics, as well as aid in limiting deterioration of the concrete at later stages of its life. Chemical admixtures, on the other hand, generally influence the early-age process of concrete to affect setting time, rate of hydration, or the amount of entrained air.

### 2.4.1   Mineral Admixtures

Commonly used mineral admixtures, or SCMs, are either naturally occurring or by-products from other industries. Their use typically benefits concrete by increasing the resistance to chemical attack and/or adding cementitious effect; allowing for either replacement of portland cement or addition of cementitious material to improve strength. Strength improvements result from the effects the SCMs have on the hydration process caused by the chemical composition, particle size distribution, particle shape, and reactivity (Neville, 1996). The ability to replace portland cement with a SCM, especially those that are by-products, helps conserve resources while reducing waste from other industries.

Table 2.3 lists the source and common material traits of each SCM. The most common SCMs include slag, fly ash, (FA), silica fume (SF), and natural materials. All but the natural materials are by-products of other industries and require their own classification based on

processes and controls used by each specific source, while natural materials are products from volcanic rock and minerals.

**Table 2.3 Common Mineral Admixtures (Neville, 1996; Mindess et al., 2003; Newman and Choo, 2003a; Mehta and Monteiro, 2006; Parande et al., 2009)**

| Name | Source | Material traits |
|---|---|---|
| Slag | By-product of iron blast furnace | • Chemically same oxides as cement, but different proportions<br>• Physical structure and composition vary based on manufacturing processes and cooling method used |
| FA | Waste product of coal burning electric plants | • Spherical with very high fineness<br>• Classification based on type of coal using ASTM C 618 |
| SF | By product of alloy manufacturing, produced by electric arc-furnace | • Extremely fine particles<br>• Composition varies based on type of alloy produced and furnace used<br>• Expensive<br>• Most commonly associated with high early strength |
| Metakaolin | Kaolin clay | • Higher purity due to controlled refining process<br>• Comparable effects as SF, but lower cost |

Table 2.4 details the effects of common SCMs on the concrete, as well as their typical content ranges. Natural materials used as mineral admixtures are typically categorized as volcanic glasses, volcanic tuffs, calcined clays or shales, or diatomaceous earth. Regardless of which category the material belongs to, the presence of pozzolans made the use of natural materials as mineral admixtures ideal due of the benefits from the pozzolanic reaction; slow rate of heat of liberation, reaction consumes lime, and efficiency at filling capillary spaces (Mehta and Monteiro 2006). However, their use is less prevalent than GGBS, FA, and SF due to economic and environmental reasons. For that reason, and the diversity of potential natural minerals, there is little literature on the various types of natural minerals. One natural mineral studied outside the United States is metakaolin, which is produced by thermal activation of kaolin clay and is considered comparable to silica fume. Although first studied in the 1990's, metakaolin is not widely used in industry due to limited and, at times, contradictory results. Badogiannis et al.

(2002); Ding and Li (2002); Babu and Apparao (2003); Ganesh Babu and Dinakar (2006); Parande et al. (2009); Ismael and Ghanim (2015) evaluated the use of metakaolin as an admixture in concrete. Largely, conclusions were that its use increased concrete strength due to filler effect and reactivity (with 15% to 20% replacement being optimal).

**Table 2.4 SCM Effects on Concrete (Popovics, 1982; Payá et al., 1995; Neville, 1996; Ding and Li, 2002; Langan et al., 2002; Papadakis and Tsimas, 2002; Targan et al., 2002; Mindess et al., 2003; Newman and Choo, 2003a; Ganesh Babu and Dinakar, 2006; Mehta and Monteiro, 2006; Caldarone, 2009)**

| Name | Effects | Range |
|---|---|---|
| GGBFS | • Resistant to chemical attack<br>• Controls early development of heat of hydration, thus low rate of strength gain, but improved long-term strength<br>• Increased workability<br>• Increased sensitivity to changes in water content<br>• Retardation effect on setting up to 1 hour<br>• Reduced heat evolution | 35-65% |
| FA | • Reduces water demand up to 15% with no change in workability<br>• Delays initial setting by about 1 hour<br>• Hydration process more sensitive to temperature than pure Portland cement concrete<br>• Reduces early strength, especially at low temperatures<br>• Increases curing time at cold temperatures<br>• Low strength development<br>• Reduce heat generation<br>• Strength enhance when particles smaller than 10 microns | 20-50% |
| SF | • High fineness improves packing near aggregate<br>• Higher modulus of elasticity<br>• Requires increased mixing time to ensure uniform dispersion<br>• Accelerates hydration if GGBFS is in the mix, also sensitive to water-cement ratio<br>• Increased water requirement<br>• Increased rate of strength development | 3-15% |
| Metakaolin | • Very rapid hydration process<br>• Increased strength<br>• Increased rate of strength gain<br>• Improved workability<br>• Higher early strength due to filler effect | 5-20% |

### 2.4.2 Chemical Admixtures

According to Neville (1996), the main characteristic of chemical admixtures are that the chemical product (typically added in quantities of less than 5% mass of cement) achieve

alteration(s) or modification(s) of normal concrete properties. Modified properties and characteristics affected, include: setting time, rate of strength development, and workability to name a few. Regardless of the desired property modification, the effectiveness depends on the amount added to the mix and the other constituents. Selection of chemical admixtures depends on the desired effect sought at the location of the project. Table 2.5 list the different types of chemical admixtures approved for use by TxDOT. Table 2.5 also describes admixture intended effects and the known advantages and disadvantages.

**Table 2.5 TxDOT Approved Chemical Admixtures (Neville, 1996; Mehta and Monteiro, 2006; Caldarone, 2009; Transportation, 2016)**

| Name | Desired Effect | Advantages | Disadvantages |
|---|---|---|---|
| Water Reducing | Reduce water content while maintaining workability | • Reduce water content by 5-10%<br>• Improves hydration causing higher rate of early strength<br>• Reduce required amount of cement | |
| Retarding | Retard the setting of concrete | • Prolongs time to transport, place, and compact concrete in hot weather<br>• Increased strength beyond 7 days | • Severely reduces early strength<br>• Incorrect quantities can inhibit setting and hardening |
| Accelerating | Accelerate setting and early strength development | • Allows placement at low temperatures. (35-40 F)<br>• Allows early finishing<br>• Allows structure to be placed in service earlier | • At high temps can cause shrinkage cracking<br>• Degrades long-term strength development |
| High-Range Water Reducing (HRWR) / Superplasticizers | Reduce the quantity of mixing water by 12% or greater | • Better hydration<br>• Rapid placing<br>• Extreme high strength at lower water content with normal workability<br>• Reduce water content 25-35%; increase 24 hr. strength 50-75% | |
| Air Entraining | Increase entrained air in the concrete | • Increased resistance to freeze-thaw<br>• Improved workability | • Increased porosity<br>• Decreases strength |

## 2.5 Alkali Silica Reaction

Although not the focus of this project, the authors felt it necessary to provide a general overview of the causes and preventative measures for alkali silica reaction (ASR). As-related to this project, a conscience awareness of ASR characteristics ensures that preventive measures are established concerning mix selection for this study, as there is little benefit to early-strength if service life is reduced due to ASR. Symptoms often associated with ASR include map cracking, expansion, discoloration, pop-outs, and gel exudations (Fournier et al., 2010; Thomas et al., 2013). Although primarily aesthetic, these symptoms can be concerning to the populace. The presence of ASR also has an effect on other properties of the concrete. Fournier et al. (2010) describes the effects of ASR on concrete mechanical properties (shown in Table 2.6).

**Table 2.6 Effect on Mechanical Properties Due to ASR (Fournier et al., 2010)**

| Property | Effect |
|---|---|
| Compressive Strength | up to 60% reduction |
| Splitting Strength | up to 60% reduction |
| Elastic Modulus | up to 60% reduction |
| Direct Tensile Strength | up to 80% reduction |

Defined as a chemical reaction between the alkalis in the concrete and silica from aggregate, producing a gel, ASR requires moisture to occur (Kreitman, 2011; Giannini et al., 2013; Thomas et al., 2013; Nixon et al., 2016). This gel causes the symptoms discussed above. For the reaction to occur all three components (alkali, silica, and moisture) must be present. Alkali sources include Portland cement, aggregates, chemical admixtures, and supplementary cementitious materials (SCMs). The alkali content of the cement was originally thought to be the controlling source, but more recently, the concrete mix constituents and characteristics was found to be more important (Thomas et al., 2013). Silica contributions by aggregates vary by type, while the reactivity varies by the chemical structure of the aggregate (Thomas et al., 2013). The initial reaction typically occurs when the internal relative humidity of the concrete is over 80% (Fournier

et al., 2010). Reaction gel expansion causing cracks. This enables the migration of water from external to the structure, inward, thus allowing the reaction to continue.

  With only three components necessary for ASR to occur, prevention focuses on removing or reducing one of these components, or adding a chemical admixture to prevent the reaction. Use of non-reactive aggregates is not always feasible due to cost constraints, particularly in cases where aggregate sources are far in distance or inaccessible. Limiting moisture generally occurs by treating the concrete after construction to prevent external migration of water, but addition of some admixtures or SCMs are effective in limiting the initial reaction. Use of low-alkali cement is a widely used approach to lowering the alkaline content; however, increased importance on the alkali content in concrete is more dominate, with recommendation being below 3 kg/m$^3$ (Thomas et al., 2013). Aside from low-alkali cement, a more efficient option is to include SCMs in the mix. The addition of SCMs replaces a percentage of the cement used in the mix. SCMs (e.g. slag and silica fume) limit water permeability, while fly ash reduces alkali availability; thus limiting components necessary for ASR to occur (Kreitman, 2011). The amount of SCMs required depends on several factors. Thomas et al. (2012) and Thomas et al. (2013) provide general guidelines for the common types of SCMs. These guidelines detail the positive effects of adding SCMs to the mixture and associated effective accumulative effects from various combination. There is discussion on SCMs use and potential consequences that affect the environment. Table 2.7 summarizes the general guidelines for mix design to prevent ASR.

**Table 2.7 Summary of Mix Design Guidelines**

| Guidelines | | Notes | Reference |
|---|---|---|---|
| Alkali Limit | 1.8 to 3.0 kg./m³ | Level dependent on | Thomas et al., 2013 |
| | 3.0 to 5.0 lb./yd³ | prevention level required | |
| | Alkali content of concrete = cement content of concrete x alkali content of cement (Thomas et al., 2012) | | |
| Low-calcium fly ash | 20 to 30% | | Thomas et al., 2013 |
| Moderate calcium fly ash | 25 to 35% | | |
| High Calcium fly ash | 40 to 60% | | |
| Silica fume | 8 to 15% | | |
| Slag | 35 to 65% | | |
| Ternary blend | $\dfrac{f_a}{FA} + \dfrac{s_g}{SG} + \dfrac{s_f}{SF} \geq 1$ | See below | Thomas et al., 2012 |

$f_a$ – Fly ash to be used in combination　　　　　$FA$ – minimum fly ash used on its own
$s_g$ – Slag to be used in combination　　　　　　$SG$ – minimum slag used on its own
$s_f$ – Silica fume to be used in combination　　　$SF$ – minimum silica fume used on its own

## 2.6　Summary

The hydration of concrete is the controlling factor of both early-age and long-term concrete strength development. Although the time of setting and onset of hardening is useful when working with concrete, understanding how hydration can affect them is important. Adjustment of several variable results in a concrete with changing setting and hardening characteristics. Either the mix design can be adjusted, curing conditions can be changed, or both.

When considering the mix design selection of the aggregate, in terms of gradation, shape, texture, and size; these properties affect strength. Rough, angular aggregate of smaller size that are well graded, are preferred for high-strength concrete. Portland cement with a higher fineness increases the rate of hydration due to the increased surface area available to react with water and to bond with other particles and aggregate. A higher water-cement ratio can increase the rate of hydration, but the excess, unreacted, water can prevent the hydrate products from bonding. This ultimately yields larger pores and lower strength. Addition of admixtures, whether mineral or chemical, also affects the rate of hydration and strength development. Mineral admixtures provide an increased amount of fines in the mixture to increase the rate of hydration, as well as cementing

ability (depending on the admixture used). Chemical admixtures, such as accelerators and water reducers, can increase the rate of hydration (decreasing setting time), while also yield an equivalent workability at a reduced water-cement ratio. The increase in curing temperature, prolonging of moisture on the concrete (or both), encourages an increase in hydration. This results in increased strength development. Once the relative humidity of the concrete drops below 80%, hydration stops. The longer the temperature and humidity are controlled, the longer hydration occurs. However, but in order to expedite opening of pavements for service, the curing duration must be shortened.

The 28-day strength determines the classification of final strength, however alternative methods should be explored to shorten this duration period. Therefore, methods have been developed to measure the concrete at early-ages to predict the 28-day strength. The maturity method estimates the strength based on a time-temperature factor. This corresponds to understanding the rate of hydration of the concrete. Use of the Free-Free Resonant Column (FFRC) is used to measure the frequency of seismic waves to determine the modulus; this in turn, can be related to concrete strength. Potential of ASR, in the long term, for concrete is less of a concern when mineral admixtures are used in the mix. Based on the reference mix used throughout this research, no further discussion of ASR is necessary. This will be further discussed in the next chapter.

# Chapter 3: Methodology

## 3.1    Introduction

To achieve the objective of this research, an experimental design plan was developed to consider test matrices composed of adjusting both: environmental conditions and mix-related parameters. Two concrete mix designs were employed: dolomite aggregate mixture and gravel aggregate mix). These mixes were evaluated at six different environmental conditions in order to assess hydration characteristics, and strength and stiffness development as a comparison between the dolomite and gravel aggregate mixtures. The environmental conditions were simulated by varying the temperature and humidity during curing and testing. The experimental design represented curing conditions at controlled temperatures (50 °F, 70 °F, 90 °F) and humidity levels (40% and 80%). Gravel mixes were only tested to assess environmental impact, and not mix-related parameters. The dolomite mixture underwent evaluation considering impacts of, both, environmental and mix-related parameters. The mix-related parameters were adjusted based on the quantities/proportioning of chemical admixtures and coarse aggregates. The assessment of the rate of hydration and strength development occurred by monitoring the internal temperature and seismic modulus of the specimens through a nondestructive method. Empirical relationships between the time, temperature, and seismic modulus to strength were established by conducting compressive strength tests at one, three, and seven days and through continuous acquisition of FFRC over the seven-day period. The evolution of heat throughout the specimen over the first 48-hours was monitored for the dolomite mix design utilizing infrared imagery.

The concept and procedures for this research follow ASTM and TxDOT standards. Testing procedures used included cylinder preparation, determination of set, compressive testing, maturity, and seismic modulus. The ASTM and TxDOT methods are largely similar, with a few minor

exceptions. TxDOT does not have a procedure for FFRC test. TxDOT also makes use of a different datum temperature for determining maturity. ASTM C1074 states to use a datum of 32°F for curing temperatures between 32°F and 104°F. Tex-426-A states to use a datum temperature of 14°F (TxDOT Designation: Tex-426-A, 2010; ASTM C1074, 2017). This research used the datum temperature prescribed by ASTM C1074.

## 3.2    Experimental Design

Laboratory tests were carried out to measure the compressive strength, standard maturity, setting characteristics, and seismic modulus growth. In addition, the dolomite mix went through thermal imaging techniques. Standard 6-inch by 12-inch cylindrical specimens were used throughout this study.

Figure 3.1 displays an overview of experimental study. Both the dolomite and gravel mixes underwent testing to assess the impacts of environmental conditions on the hydration process and strength and stiffness development. The portion of the experiment assessing the impacts through adjustment of the mix-related parameters was only applied on the dolomite mixture. The mix-related parameters considered variants in the presence and quantity of several chemical admixtures, change in coarse aggregate gradation as well as adjustments to the water-to-cementitious ratio.
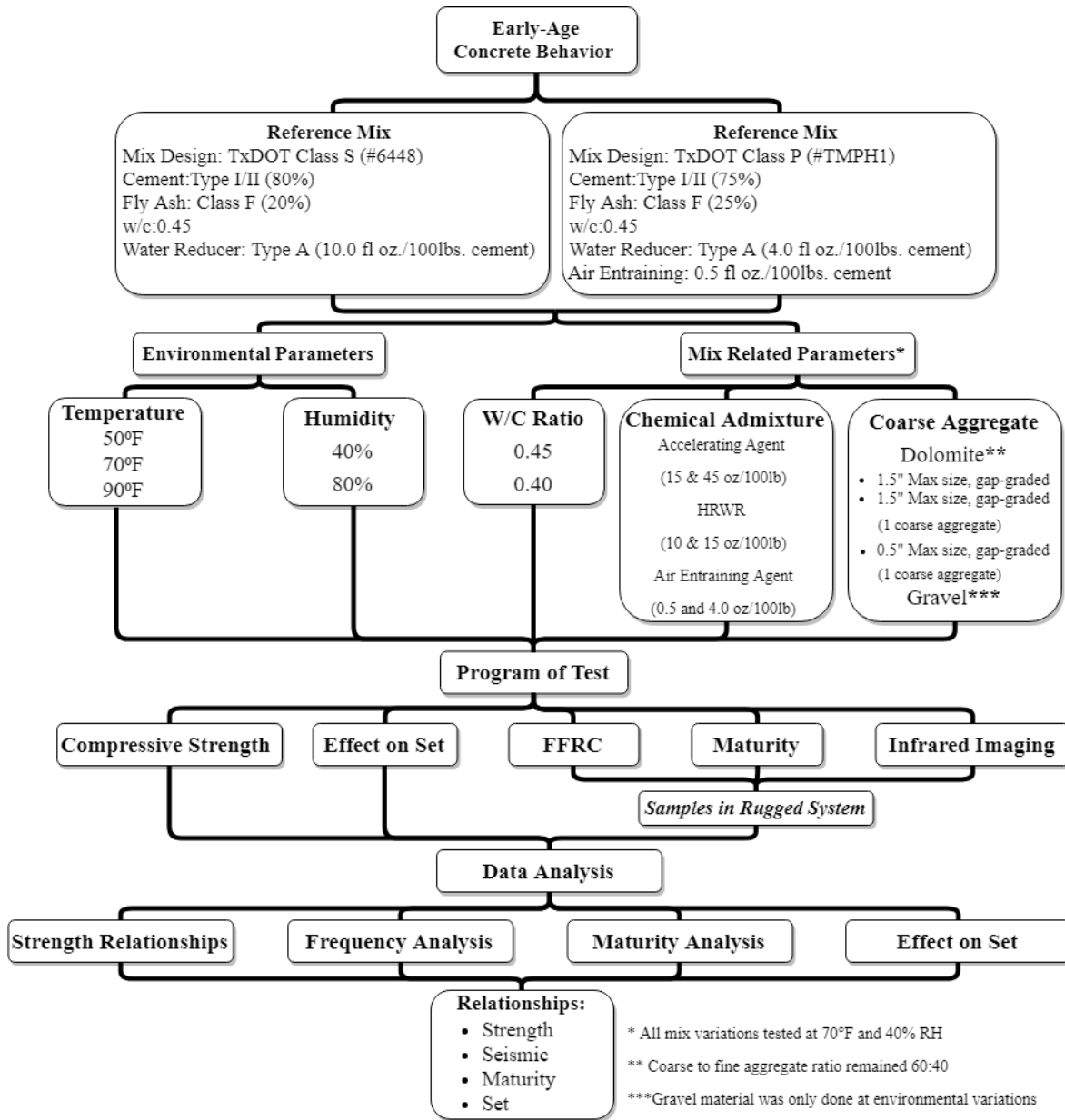
**Figure 3.1 Project Work Plan**

A detailed description of each reference mix is found in Tables 3.1, while Table 3.2 illustrates the aggregate gradation followed for both mixes. Six dolomite mixture variants were evaluated to assess impacts on early-strength and maturity from variable. Twelve dolomite mixture variants were evaluated to assess these impacts from mix-related parameters. In total, this comprises of twenty-four different mix variants, beyond the reference mixes, were evaluated. Table 3.3 outlines the mix proportions for the twelve dolomite mixes tested. For both

environmental and mix parameters each mix tested consisted of 12 cylinders. Of the cylinders, three were placed in an environmental chamber and cured under standard curing conditions (70°F and 100% humidity). The remaining nine were placed in a temperature control room at the specified temperature (50°F or 70°F or 90°F) and humidity  and humidity levels (40% or 80%). Three cylinders had thermocouples inserted during preparation. In addition to collecting internal temperature data, these cylinders were also used to collect continuous seismic data through FFRC. These same cylinder also underwent data acquisition of infrared imaging. Imaging occurred for 48-hours, while temperature and seismic data was collected for seven-days. The data acquisition system utilized for monitoring of specimen internal temperature and seismic response was also configured to monitor the controlled, ambient air temperature. The ambient air temperature was collected through use of a separate thermocouple. FFRC and compressive strength testing occurred on three cylinders from the temperature room and one cylinder from the environmental chamber at one-, three- and seven-days.

**Table 3.1 Reference Mixes**

| Mix Components | Dolomite Mix Design | | | Gravel Mix Design | | |
|---|---|---|---|---|---|---|
| | Type/ Class/ Grade | Producer / Source | % or Dosage | Type/ Class/ Grade | Producer / Source | % or Dosage |
| Portland Cement | I / II | GCC Rio Grande/Samalayuca | 80 | I / II | GCC Rio Grande/Samalayuca | 75 |
| Fly Ash | F | Salt River Materials/Escalante | 20 | F | Boral / Monticello | 25 |
| Water Reducer | A | Euclid Chemical Eucon X-15 | 10 | A | Euclid Chemical Eucon X-15 | 4 |
| Air Entraining | - | - | - | - | Aucon AEA-92 | 0.5 |
| Coarse Agg. 1 | 3 | Jobe Materials, L.P./Avispa | 13 | 3 | Hanson / Little River | 13 |
| Coarse Agg. 2 | 5(67) | Jobe Materials, L.P./Avispa | 42 | 5(67) | Hanson / Little River | 42 |
| Int. Agg. | | Jobe Materials, L.P./Avispa | 5 | | Hanson / Little River | 5 |
| Fine Agg. | | Jobe Materials, L.P./Dyer | 40 | | Hanson / Little River | 40 |
| w/c | 0.45 | | | 0.45 | | |

## Table 3.2 Aggregate Gradation

| Sieve Size | Sieve Size (in) | Coarse Agg. 1 % Passing | Coarse Agg. 2 % Passing | Intermediate Agg. % Passing | Fine Agg. % Passing |
|---|---|---|---|---|---|
| 2 ½ in | 2.500 | 100 | 100 | 100 | 100 |
| 2 in | 2.000 | 100 | 100 | 100 | 100 |
| 1 ½ in | 1.500 | 76 | 100 | 100 | 100 |
| 1 in | 1.000 | 17 | 100 | 100 | 100 |
| ¾ in | 0.750 | 2 | 96 | 100 | 100 |
| ½ in | 0.500 | 1 | 62 | 98 | 99 |
| 3/8 in | 0.375 | | 35 | 65 | 95 |
| No. 4 | 0.187 | | 3 | 4 | 93 |
| No. 8 | 0.093 | | 1 | 1 | 86 |
| No. 16 | 0.047 | | | 1 | 71 |
| No. 30 | 0.024 | | | | 56 |
| No. 50 | 0.012 | | | | 22 |
| No. 100 | 0.006 | | | | 2 |
| No. 200 | 0.003 | | | | 0.3 |

## Table 3.3 Test Mix Proportions (Dolomite Mix)

| Batch | Cement | Fly Ash | Water Reducer | Accelerating Agent | High Range Water-Reducer | Air-Entraining Agent | Coarse Agg. 1 | Coarse Agg. 2 | Intermediate Agg. | Fine Agg. | w/c |
|---|---|---|---|---|---|---|---|---|---|---|---|
| | % | | oz./100 lbs. cement | | | | % | | | | |
| Reference | 80 | 20 | 10 | - | - | - | 13 | 42 | 5 | 40 | 0.45 |
| 0.40 w-c | 80 | 20 | 10 | - | - | - | 13 | 42 | 5 | 40 | 0.40 |
| 15 oz. AA | 80 | 20 | 10 | 15 | - | - | 13 | 42 | 5 | 40 | 0.45 |
| 45 oz. AA | 80 | 20 | 10 | 45 | - | - | 13 | 42 | 5 | 40 | 0.45 |
| 45 oz. AA; 0.40 w-c | 80 | 20 | 10 | 45 | - | - | 13 | 42 | 5 | 40 | 0.40 |
| 10 oz. HRWR | 80 | 20 | 10 | - | 10 | - | 13 | 42 | 5 | 40 | 0.45 |
| 15 oz. HRWR | 80 | 20 | 10 | - | 15 | - | 13 | 42 | 5 | 40 | 0.45 |
| 10 oz. HRWR; 0.40 w-c | 80 | 20 | 10 | - | 10 | - | 13 | 42 | 5 | 40 | 0.40 |
| 0.5 oz. AE | 80 | 20 | 10 | - | - | 0.5 | 13 | 42 | 5 | 40 | 0.45 |
| 4 oz. AE | 80 | 20 | 10 | - | - | 4 | 13 | 42 | 5 | 40 | 0.45 |
| 0.5 oz. AE; 0.40 w-c | 80 | 20 | 10 | - | - | 0.5 | 13 | 42 | 5 | 40 | 0.40 |
| Large Agg. | 80 | 20 | 10 | - | - | - | 60 | - | - | 40 | 0.45 |
| Small Agg. | 80 | 20 | 10 | - | - | - | - | - | 60 | 40 | 0.45 |

34

In addition, three mortar mix cylinders were prepared to check the sets using the penetration resistance method. These specimens were also placed in the temperature control room where the nine concrete cylinders were maintained.

An apparatus was designed and built for continuous acquisition of seismic modulus data (as per ASTM C 215) and heat of hydration/maturity information (derived from ambient air temperature and specimen internal temperature) over a 7-day period.  The construction of a frame was necessary to house the impact hammers, accelerometers, and thermocouples. The frame configuration also accounted for the cylinder spacing required for effective thermal imaging. Figure 3.2a displays the frame built for testing the dolomite mix. The frame consisted of 2in. x 4-in. plywood boards connecting a threaded rod. Cylinders were placed atop a 1-in. mat of hard foam to limit interference during collection of seismic data. Figure 3.2b displays an upgraded prototype of this system with aluminum extrusions. This system was utilized for testing of the gravel mix. The frame, base supports, and instrumentation housings were. Figure 3.3a displays the configuration of the thermocouple, impact source and accelerometer. Impact hammers were connected to a turnbuckle and adjusted, as necessary, to provide impact at the center of the specimen. The turnbuckle provided means of vertical adjustment to ensure proper impact occurred. Figure 3.3b is a view of the thermocouple, impact source and accelerometer on the upgraded acquisition system. Components for the system remained the same, however the frame was replaced by aluminum extrusions. Data acquisition of the specimens occurred continuously for seven-days with data recorded at specified intervals. Further explanation of each test is found in the following sections.

**Figure 3.2 Specimen Testing Frame**


**Figure 3.3 Seismic Modulus and Internal Temperature Monitoring**

Figure 3.4 is a schematic of the complete data acquisition system and test apparatus. Output from the system consisted of ambient air temperature, internal specimen temperature, compression wave frequency, and shear wave frequency of each cylindrical specimen. The data acquisition system provided modulus values as early as 90 minutes from the initial water-cement contact during mixing.
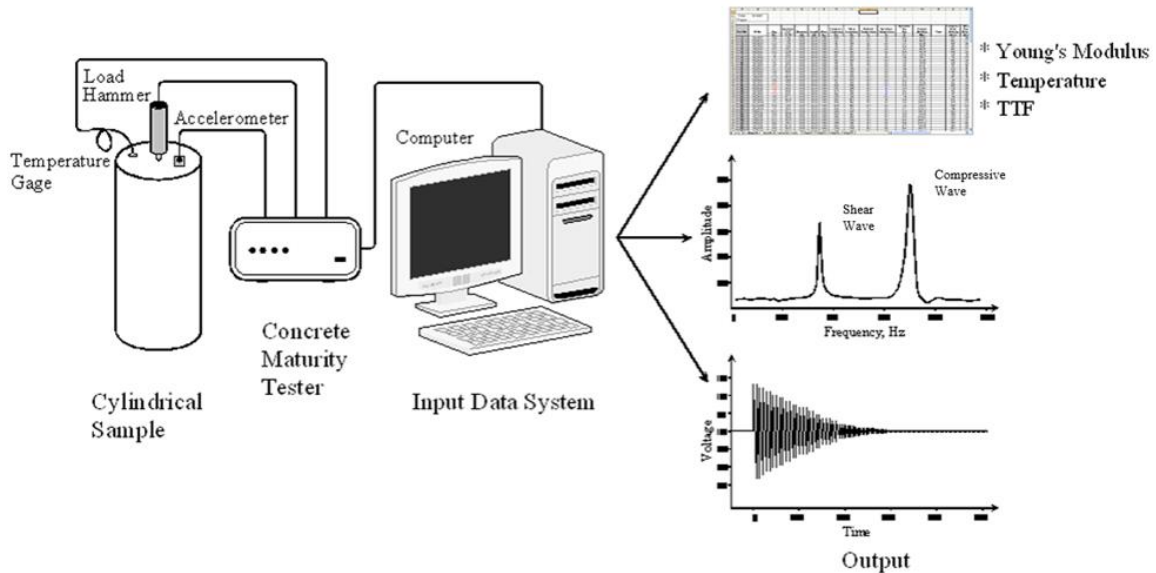
**Figure 3.4 Schematic of Data Acquisition System and Test Apparatus**

### 3.2.1 Reference Mixes

TxDOT specifications, which provided the basis for the selection of the reference mixes, mandates a compressive strength of i) 3,200-psi for traffic opening and ii) 4,000 psi as the 28-day strength for Class-S (TxDOT, 2014). TxDOT specifications also mandates a compressive strength of 3,500-psi, 7-day strength and 4,400-psi, 28-day strength for Class-P (TxDOT, 2014). The maximum time to achieve 3,200-psi for opening is seven-days, however this can be as early as 24-hrs-48 hours for high early-strength concrete. With these requirements, approximately 15 high early strength (HES) and Class P mixes tested by TxDOT El Paso District Laboratory were reviewed. The final selection depended on the mixtures that had the fewest constituents of admixtures. These comparable gravel and dolomite mixes maintained several mixture parameters as a control in order to provide direct, comparable analyses. The mix parameters that remained unchanged during the research were the type of cement, sources for chemical admixtures and aggregate gradation.

The dolomite mix was comprised of three different coarse aggregates, and one fine aggregate. The aggregate was obtained from a local supplier. Table 3.2 shows the aggregate

gradations. The absorption of Coarse Aggregate 1 and Coarse Aggregate 2 were 0.5%, the intermediate aggregate was 0.6%, and the fine had an absorption of 0.7%. The gravel mix is comprised of one coarse aggregate and one fine aggregate from a quarry in Texarkana, TX. The same aggregate gradation from the dolomite mix was followed for the gravel mix. The absorption of the coarse aggregate was 1.11% while the fines had an absorption of 0.24%. The type I/II portland cement and Class F fly ash used adhered to ASTM C150 and ASTM C618, respectively. To minimize the potential variability of aggregate properties during source sampling, all materials utilized for this study were stockpiled from the start of the project.

Eucon X-15, a mid-range water-reducer, produced by Euclid Chemical was used in both reference mixes. The mixes contained a dosage of 10-fluid ounces per every 100 pounds of cementing material for the dolomite material. The gravel mix utilized 4 fluid ounces per every 100 pounds of cementing material. These dosages remained constant for all other mixes evaluated. Eucon AEA-92, an air entraining agent, produced by Euclid Chemical was only used in the gravel reference mix. The gravel mix utilized 0.5 fluid ounces per every 100 pounds of cementitious material.

The inclusion and amount of chemical admixtures (i.e., accelerating agent, high range water reducer, and air-entraining agent) were varied in dolomite mixtures. The water-cement ratio was also adjusted. To study the impact of the gradation, the proportions of the materials from different bins were varied for the dolomite mix. The amount of fly ash, type of cement, and coarse-to-fine aggregate ratio remained constant for each mixture variant.

### 3.2.2 Specimen Preparation

The specimens were cast in 6-inch by 12-inch cylindrical molds in compliance with ASTM C470. Prior to mixing, all aggregates were oven dried to prevent the presence of excess moisture

in the mixture. Once dried, the aggregates were cooled to room temperature prior to mixing. Mixing and consolidation of each mix followed the procedure listed in ASTM C192. A distinct difference between mixture preparations, the dolomite mixes were mixed outdoors. The gravel mixes were mixed indoors, at room temperature (70°F). All cylinders were cured for seven-days at a specific nominal temperature and humidity. Three cylinders of every mix underwent standard curing at 70°F and 100% humidity to allow the comparison of their FFRC moduli and compressive strengths with those of the reference mix at standard curing. Demolding of all specimens occurred 24-hours after casting.

### 3.2.3 Environmental Related Parameters

All tests were carried out in an environmental chamber where the humidity and temperature is controlled. Average daily humidity across Texas ranges from a high of nearly 80% on the Texas Gulf Coast to a low of about 40% around El Paso, Texas. Based on this information, the curing of specimens occurred at 80% and 40% nominal humidity levels at three different temperatures. The use of these two humidity levels allowed for a comparison of strength development near the extremes experienced in Texas.

The specimens were cured at three different nominal temperatures of 50°F, 70°F and 90°F. The 50°F temperature is above the minimum temperature restriction for placing concrete (TxDOT, 2014). The 90°F temperature served as the high-end temperature while 70°F was the medium range temperature. These three temperature ranges were used only with the reference mix at both 80% and 40% humidity.

### 3.2.4 Mix Related Parameters

The dolomite mix related parameters evaluated were the water-cement ratio, three chemical admixtures (accelerating agent, high-range water-reducer, and air entraining agent) and changes

to maximum coarse aggregate size and gradation. A discussion of each of these components and their individual impacts are presented below. Curing conditions for all mixes occurred at 70°F and 40% humidity. This correlates to the average temperature and humidity experienced in El Paso, Texas.

**Water-Cement Ratio**

The w/c ratio influences the strength development and the workability of fresh concrete. Higher w/c ratios generally indicate the need for increased workability, however strength generally decreases (as shown in Figure 3.5).
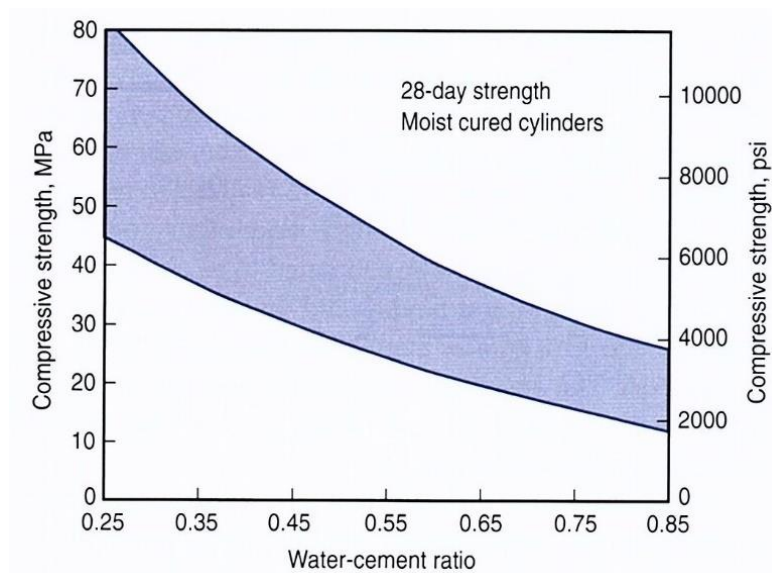


**Figure 3.5 Strength to Water-Cement Ratio Relationships (Kosmatka et al., 2002)**

To evaluate the impact of w/c ratio, the dolomite reference mix possessed w/c ratios of 0.45 and 0.40. A mix with higher w/c ratio than the reference was not considered since the reference mix contained a water reducer. In these experiments, the cement content was maintained constant while the water content varied for the two w/c ratios. Experiments with lower w/c ratio were also carried out for mixes with chemical admixtures. This is further discussed below.

**Chemical Admixtures**

According to ASTM C125 (2015), an admixture is defined as a material other than water, aggregates, cementitious material, or fiber reinforcement, and is used to modify setting, or hardened properties. These are added to the mix before or during mixing. The following details the use of the chemical admixtures for this research. Their intended use to modify specific properties is also discussed.

*Accelerating Agent*

The accelerating agent used in this research was Accelguard ACN 200 produced by Euclid Chemical. This agent was utilize to decrease the time to initial set. The low and high dosages used were 15 and 45 oz. per 100 lbs. of cementitious material. These doses are within the manufacturer recommended values.

*High-range Water-Reducer*

To evaluate the extent to which using a high-range water-reducer affects the early strength, a low and high dosage of 10 and 15 oz. per 100 lbs. of cementitious material of Eucon SP produced by Euclid Chemical were added to the mix. These ranges again fell within the manufacturer recommend range.

*Air Entraining Agent*

To evaluate the extent of the impact of air-entraining agent on the strength, two dosages within the prescribed range were selected. The evaluation occurred at dosages of 0.5 and 4 oz. per 100 lbs. of cementitious material of Eucon AEA-92 produced by Euclid Chemical.

**Coarse Aggregate**

Mixture variants of dolomite mix design were also evaluated. These variants exhibited changes to the coarse aggregate proportions. This was simulated by eliminating two of the coarse

aggregates used while maintaining a coarse to fine aggregate ratio of 60:40. This is shown in Figure 3.6.
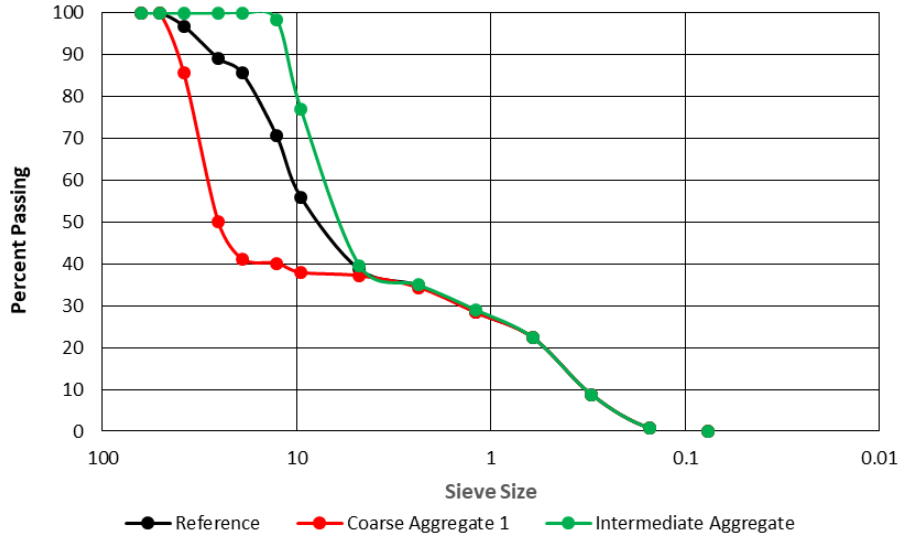


**Figure 3.6 Coarse Aggregate Gradation**

The overall reference mix is gap-graded with a maximum aggregate size of 1.5 in. Use of strictly Coarse Aggregate 1 results in a more extreme gap-graded mix with the same maximum aggregate size. Conversely, including just the intermediate aggregate yields a gap-graded mix as well, but with a maximum aggregate size of 0.5 in. TxDOT specifications classifies Coarse Aggregate 1 as a Grade 3; therefore, allowing both the reference mix and the intermediate mix with strictly this aggregate to meet the requirements for use in Class-S concrete (TxDOT, 2014). Use of the intermediate aggregate, Grade 6, meets requirements of Class-S concrete with a caveat. TxDOT specifications caveat states, "other grades of coarse aggregate maybe used in non-structural concrete classes when allowed by the Engineer".

## 3.3 Methods for Assessing Strength

Table 3.4 presents the destructive and nondestructive methods used in this research to assess the strength or stiffness of PCC. Destructive methods use techniques to assess the properties of a test specimen with damage occurring to the specimen. These methods provide a direct

measurement of the specimen strength. On the other hand, nondestructive methods obtain information about the internal conditions or properties of a test specimen without causing damage to the specimen.

**Table 3.4 Tests to Assess Concrete Properties**

| Method | Concrete Test | Test Standard |
|---|---|---|
| Set | Set by Penetration Test | ASTM C403 |
| Destructive | Compressive Strength Test | ASTM C39 |
| Nondestructive | Maturity Test | ASTM C1074 |
| | Seismic Test (FFRC) | ASTM C215 |

### 3.3.1 Compressive Strength Test

Performance of the standard compression test in accordance with ASTM C39 occurred on all 6-in. diameter by 12-in. length specimens. Testing occurred at one, three and seven-days for all mixes, with four specimens tested per day as outlined in ASTM C39. Tested specimens include three specimens at the prescribed testing temperature and humidity levels, with the fourth specimen under standard curing. An Instron universal testing machine allowed the cylindrical specimens to be loaded in uniaxial compression at a load rate of 30 psi/sec until failure (see Figure 3.7). This load rate conforms to the recommended load rate of 35 ± 7 psi/sec stated in ASTM C39.



**Figure 3.7 Compressive Strength Test**

### 3.3.2 Maturity Test

The internal temperatures of three separate specimens were continuously monitored for seven days using thermocouples. Data acquisition of time intervals and data point frequencies are shown in Table 3.5.

**Table 3.5 Recording Intervals**

| Time Intervals, hr. | Frequency, measurements per hour |
|---|---|
| 0-12 | 12 |
| 12-24 | 4 |
| 24-48 | 2 |
| 48-168 | 1 |

The method outlined in ASTM C1074 was used to convert the recorded temperature time histories into time-temperature factors (TTF). In addition to the standard method of calculating TTF, an alternative approach was tested in which the datum temperature used was the instantaneous ambient temperature of the environmental chamber. The rationale behind this approach was to delineate the heat of hydration from ambient temperature. The maturity values obtained with the new datum will be referred to as *Alternative TTF* for the remainder of this document. The alternative TTF and standard maturity procedures are compared and shown in Figure 3.8. This data comprises the seven-day monitoring period for the reference mixes cured at 70°F and 40% humidity. The alternative TTF (Figure 3.8) provides some insight in the original heat equilibrium between the specimen and ambient temperature followed by rapid increase in the alternative TTF during the setting period followed by a rapid decrease occurring at the time of mold removal and the eventual stabilization of the alternative TTF. A modification to the testing protocol was made for the gravel mix, where the thermocouple were calibrated to avoid the constant decrease (seen in the dolomite mix) after roughly 60 hours. This would essentially keep the temperatures in

equilibrium with minimal difference coming from the environmental chamber. This behavior will be discussed later in this report.
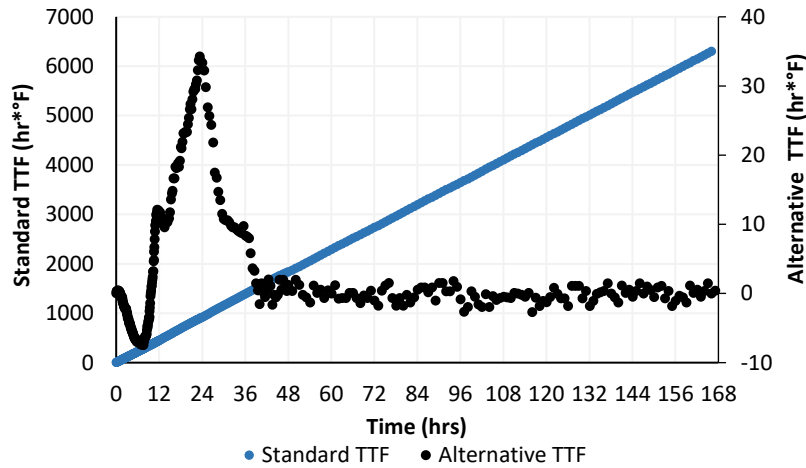
**Figure 3.8 Comparison of Maturity Calculation Approaches (Gravel mix 70ºF/40% Hum)**

### 3.3.3 Free-Free Resonant Column

Seismic moduli growth of specimens were monitored with a fully-automated free-free resonant column method that complied with ASTM C215 (2014). The seismic moduli were measured simultaneous, for three specimens' at-a-time, along with the internal temperatures over a seven-day period.

Based on difficulties found by Lara (2008) concerning transmission of seismic energy with an impact hammer on fresh concrete, accelerometers were attached to the head of a nail that was placed in the concrete offset from the point of impact. Additionally, point of impact occurred on large aggregates present on the surface of the specimen.

As a way to verify the seismic modulus from the automated system, a manual (traditional) FFRC test was carried out on each specimen prior to the one, three, and seven day compressive strength testing. The manually-obtained moduli and the automated-acquired moduli were within 3% for the dolomite mix, and within 2% for the gravel mix.

## 3.4    Infrared Imaging

The infrared imaging was utilized to produce a thermal profile of the specimens at distinct points. This was performed in the initial 48-hours after production, and was only performed on dolomite mixes. Although there are ASTM test methods for use of infrared imaging systems, there is not a particular procedure that applies towards to the early-age phase. Rather, the methods are applicable towards other applications, such as detecting delamination in bridge decks (ASTM D4788-03) and inspecting insulation (ASTM C1060-11a). A trial-and-error approach was followed to establish a consistent method. An *Infrared Cameras Inc.* model *T2I* system was used to collect thermal images of the specimen; the set placed at a distance of approximately 5-ft. The specimens were spaced about 1 in. apart to obtain concurrent images of the three specimens with limited background interference (as seen in Figure 3.9). The device was calibrated prior to the start of data collection for every mix and curing condition. Data collection occurred at five-minute intervals for a 48-hour period. It was difficult to isolate the thermal images from each individual specimen beyond 24-hours, given that the specimen temperatures met equilibrium with the ambient temperature.



**Figure 3.9 Set-up for Thermal Imaging of Cylinders**

Figure 3.10 displays a sample of a raw image collected during testing. A rectangular frame was placed around each of the three cylinders. The digital temperature data for each vertical and horizontal pixel of each specimen was exported into a data reduction worksheet that was developed for this purpose. The ambient temperature was first subtracted from the temperature measured at each pixel. This data was then visualized based on the criteria displayed in Table 3.6. Images captured at the start of curing, initial set, final set, 24, 36, and 48-hours after curing were of particular interest since they provided a better understanding of how the heat of hydration dissipated at critical points. As sample thermal profile is displayed in Figure 3.11.
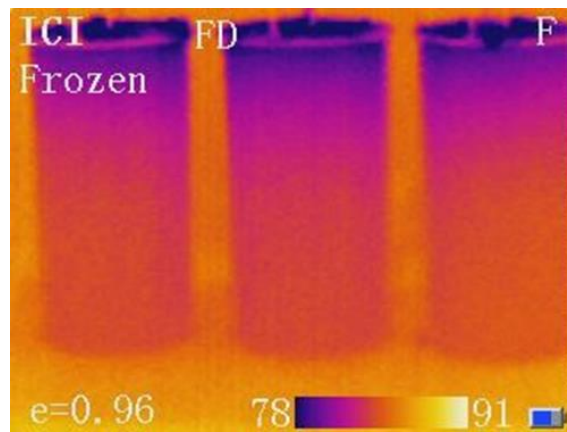


**Figure 3.10 Thermal Image of Cylinders**

**Table 3.6 Infrared Imaging Value and Color Assignment**

| Normalized Temperature | Assigned Value | Meaning | Color |
|---|---|---|---|
| > 10° above ambient | 2 | Hot | Red |
| 4<ambient<10 | 1 | Warm | Yellow |
| -4<ambient<4 | 0 | Neutral | White |
| < -4° below ambient | -1 | Cold | Blue |
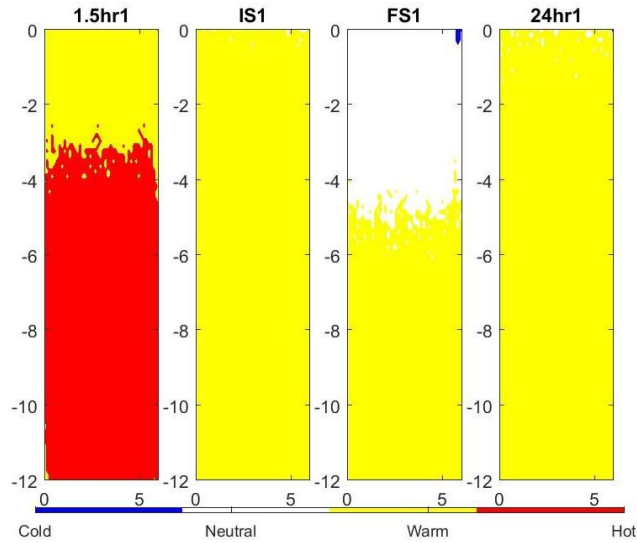
**Figure 3.11 Example Thermal Profile of Single Cylinder**

## 3.5    Determination of Set

The initial and final sets for each mix were estimated as per ASTM C403through use of a Humboldt ACME Penetrometer (Figure 3.12). Rather than sieving the concrete mix, the mortar mix was prepared to exclude the coarse aggregates. The reasoning behind this was to limit the amount of material wasted. Mortar specimens underwent identical curing conditions as the specimens in the environmental chamber. This data, paired with thermal profiles, yielded a comprehensive view into observing the heat of hydration.



**Figure 3.12 Humboldt ACME Penetrometer**

48

## 3.6    Modulus Based Approach for Determining Setting Times

Observing the inflection points in the seismic modulus growth curve, throughout the curing process of the specimens, may allow the identification of the dormant, setting, and hardening stages of concrete. For demonstration, Figure 3.13a displays the seismic modulus growth with time for an evaluated dolomite data set at 70°F and 40% humidity. This data was obtained from the developed system for automated FFRC. Figure 3.13b displays this seismic modulus data plotted with maturity. The three different phases: dormant, setting and hardening can clearly distinguished on a time-based or maturity-based series. As displayed in the figures, regression functions were fit to the data points.  The regression curves are based on the initial 72-hours of recorded data. This will be further discussed in the following sections.
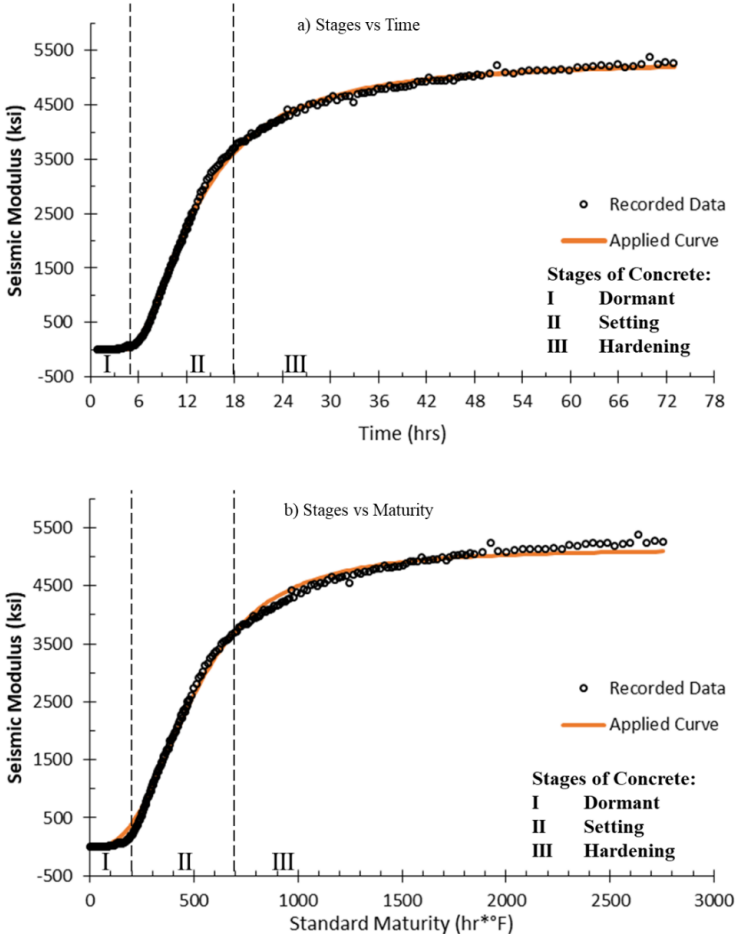


**Figure 3.13 Basic Stages of Concrete Hydration**

### 3.6.1 Determining Set from a Time-Based Modulus Growth

The equation that best represents the modulus growth over time was found to be:

$$modulus = e^{\left(a - \left(\frac{b}{(time)^2}\right)\right)}$$

EQN 3.1

where $a$ and $b$ are regression coefficients. Variable $a$ related to the long-term modulus. Variable $b$ controls the rate at which the moduli becomes asymptotic to the long-term modulus. Table 3.7 details interpretation of the three hydration stages observed in the modulus growth curve.

**Table 3.7 Stages of Hydration from Variation in Modulus with Time**

| Stage | Model Name | Description |
|---|---|---|
| Dormant | $y_1$ | Near horizontal model, early-age |
| Setting | $y_2$ | Steep gain model |
| Hardening | $y_3$ | Near horizontal model, long-term |

Figure 3.14a displays how the modulus growth curves can be further approximated through applying three, separate linear regression functions. The intersections between the two adjacent linear functions are considered as alternative definitions for times of initial set (IS) and final set (FS). The intersection of models $y_1$ and $y_2$ defines the initial set time (Figure 3.14 demonstrates IS = 5.8 hrs.). While the intersection of models $y_2$ and $y_3$ defines the final set time (Figure 3.14 demonstrates FS = 18.0 hrs.). For the evaluated mixtures, this modulus-based initial set time was found to be within 15 minutes of the set time determined through standard penetration resistance procedure. The final sets between both approaches differed by around 60-minutes. The differences between the standard and modulus-based approach can be attributed to several factors. A main justification being that the standard penetration resistance method bases the set time on what is essentially the mortar component of the mix, while the modulus-based approach takes into account the entirety of the mixture. Figure 3.14b displays the three stages of the concrete. In this case, the initial set is at a standard maturity of 156 hr.\*°F or approximately 5.1 hours; while the final set occurs at a standard maturity of 748 hr.\*°F or approximately 19.1 hours.
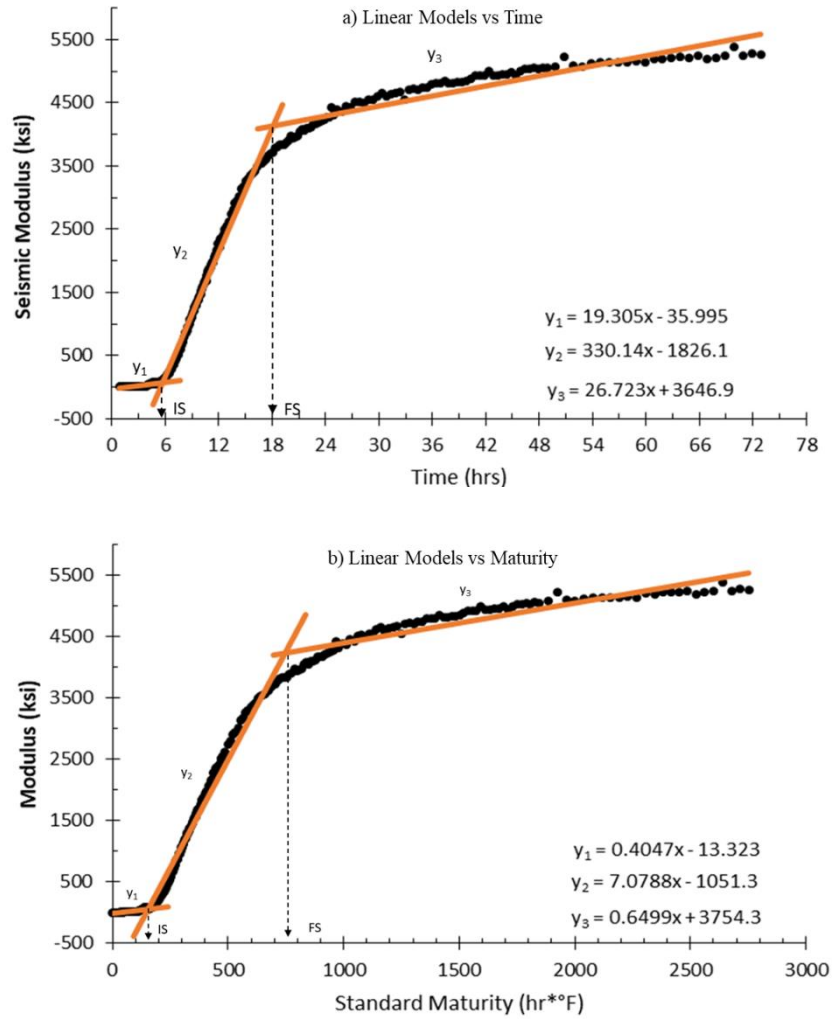
**Figure 3.14 Linear Functions Used to Determine Alternative Initial and Final Sets**

### 3.6.2   Determining Set from a Standard Maturity-Based Modulus Growth

Viewing the modulus growth and curvature on a basis of maturity (i.e. maturity as the x-axis) does not vary differently from a time-based series. This can be observed when comparing Figures 3.13a and 3.13b. However, the regression function does exhibit significant, fundamental differences that are largely attributed to the difference in scale. Due to this scale change, a function with more than two-coefficients is required to model the modulus behavior. In this case, the most appropriate equation found is:

$$modulus = \frac{c}{1 + \left(\frac{d}{TTF}\right)^f} \qquad \text{EQN 3.2}$$

where *c* corresponds to the long-term modulus, d is indicative of the early-age modulus, and *f* is indicative of the growth. As seen in Figure 3.13b, this generalized equation well represents the experimental data up to a standard maturity of 2,000 hr.*°F.

## 3.7    Summary

This chapter outlines the methodology for evaluating early age behavior of portland cement concrete. An experiment design to study the effects of both environmental conditions and mix-related parameters on the strength and modulus development of both mixes was developed. Six environmental variations that are based on the average high and low temperatures and humidity were considered to model the extreme weather conditions in Texas. Mix-related parameters were adjusted (for only the dolomite mix) and included reduction of w/c ratio, addition of admixtures approved for use by TxDOT, and change in maximum aggregate size and gradation. The admixture quantity was taken at the high and low range of manufacturer recommended dosages.

The continuous monitoring of specimens on a developed data acquisition system allows for observing the modulus growth with time and maturity. These data enables data analyses and comparisons that provide the opportunity to identify trends that may be useful in observing hydration and the overall curing process. The potential for considering an alternate datum for calculating the concrete maturity is also studied; this metric is identified as the *Alternative TTF*. This method of visualizing heat production duration provides a more clear and practical metric for delineating the hydration process.

Even though the penetration resistance procedure to determine set has been effectively used for decades, it does not consider the concrete mix as a whole. Instead, this standard method considers, what is essentially, the mortar component of the mixture. A method to determine the initial and final set based on modulus development is discussed. This is performed through

observing modulus growth on both a time-based and maturity-based series. This proposed method enables the ability to assess initial and final set times on the concrete mix in its entirety, as opposed to just the mortar component.

# Chapter 4: Results and Analysis

## 4.1     Introduction

As discussed in Chapter 3, experimental testing of the dolomite and gravel mixes yielded times of initial and final set, time records of internal temperature, compression wave frequency with time, shear wave frequency with time, and compressive strength readings at 1-day, 3-days and 7-days of curing. In addition, dolomite mix underwent infrared imaging over the first 48-hours. From this information, the time-temperature factors (i.e., standard maturity and alternative TTF), seismic moduli, Poisson's ratios, and thermal profiles were obtained. Analyses of this data considering the impacts of the environmental-related and mix-related parameters on curing, stiffness and strength development are presented.

Figure 4.1[2] contains a visual comparison of the seismic moduli obtained from the automated FFRC system with manual FFRC tests. Overall, the results from the two tests are closely aligned.  Given that these data sets are so closely aligned, a focus on the automated FFRC results will be displayed for the remainder of this document. In addition to approximate unity with the manual FFRC test, the automated system also yielded similar output results when considering the three test replicates (i.e. a single data set composed of three replicates) in the developed test system. Across the twenty-four mixes, the average standard deviation of the recorded moduli among the three specimens was less than 270-ksi.

---

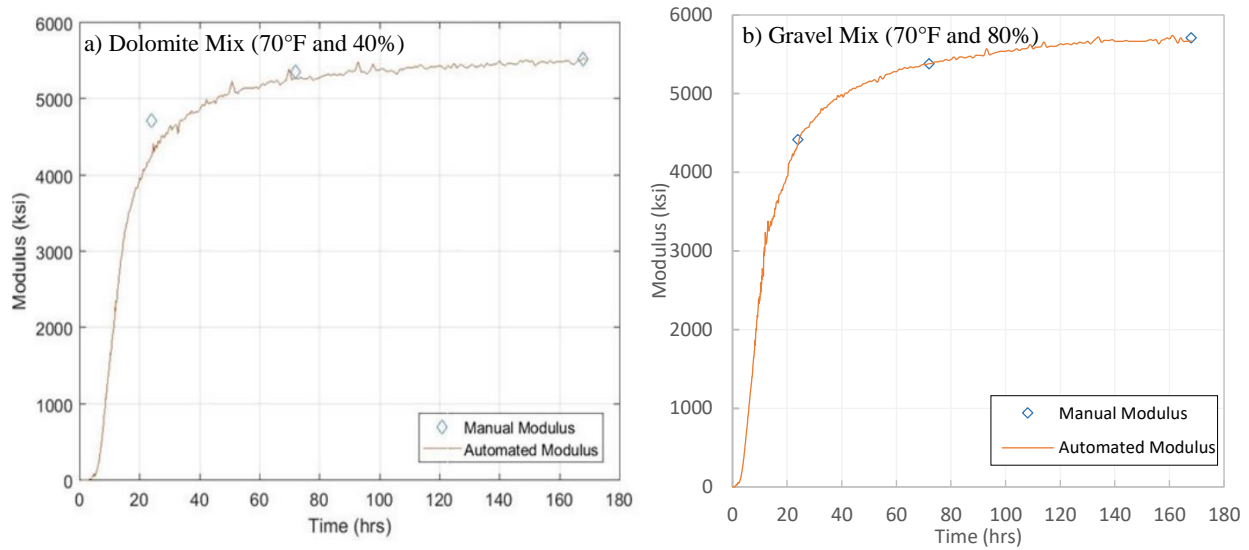[2] Data shown represents average modulus data considering three replicates.

**Figure 4.1 Comparison of Seismic Moduli from Automatic and Manual FFRC Tests**

Figure 4.2 displays the time-series of internal temperatures[3] for the data sets at the different, ambient curing temperatures. For demonstration, the plots are shown at 40% humidity. Figure 4a details these temperature series for the dolomite mix and Figure 4.2b displays the data for the gravel mix. Figure 4.2a shows that for the first four to six hours, the internal temperatures are either increasing or decreasing toward the ambient temperature (this is dependent on the ambient setting and conditions that the specimens were prepared in). After the specimens met equilibrium with the ambient air temperature, the internal temperatures are shown to increase to a maximum, typically occurring between 12 and 18 hours in the curing process. Similarly, Figure 4.2b displays this same general behavior for the gravel mix. As, previously mentioned, the gravel mixing conditions were controlled at room temperature (70°F); therefore, at 70°F the specimens were in equilibrium with ambient air temperature at the start of testing. Likewise, the internal temperature is shown to increase during curing until reaching a maximum between ten and fourteen hours.

---

[3] Data shown represents average internal temperature data considering three replicates.
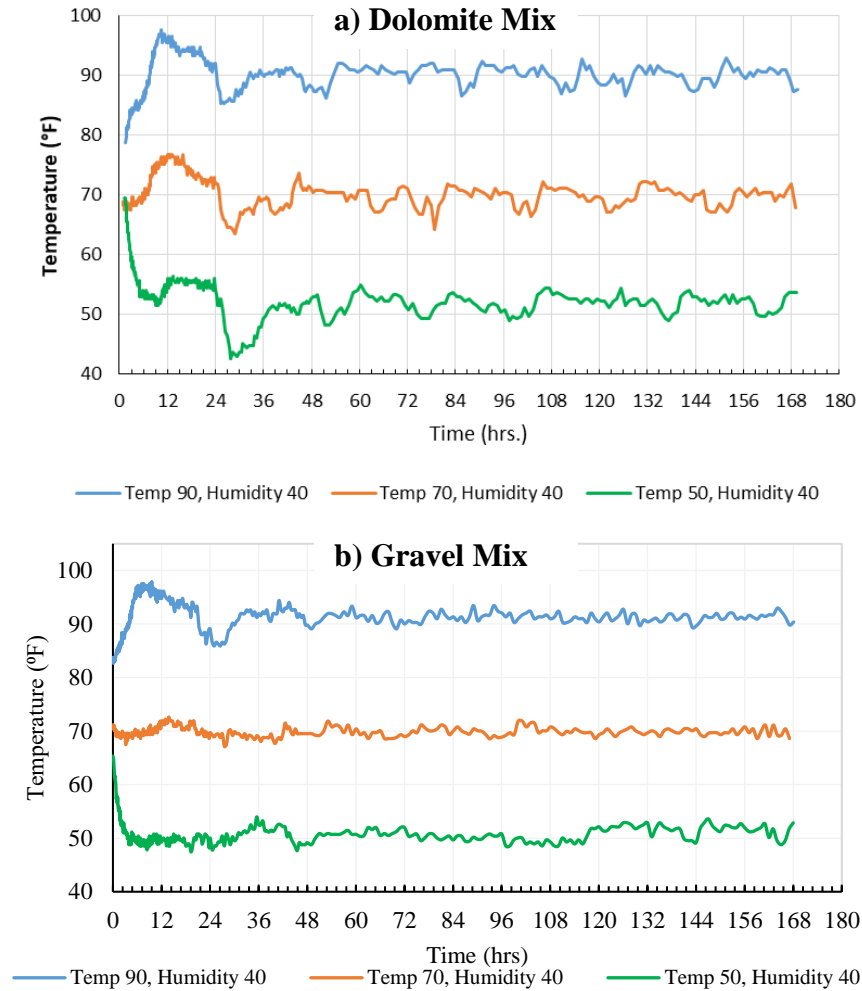
55

**Figure 4.2 Recorded Time-Series of Internal Temperature**

An observation was the similarity between the timing of the peaks and valleys of the generalized hydration plots reported by Neville (1996) and Mindess et al. (2003) in Chapter 2. Within a few hours of one another, all dolomite mixes went through an approximate nine-hour period without heat production; starting from when the mix is between 25 and 28 hours. The gravel mixes had a smaller period of roughly four-hours from 26 to 30-hours. These points correspond to the period where hydration changes from C3S to C3A. After that period, the specimens generally revert equilibrium with the ambient temperature.

The variation in internal temperature as compared to alternative TTF is shown with time in Figure 4.3. While standard maturity employs a datum temperature, commonly taken as 14°F or

32°F, the integration of the temperature-time curve usually yields a piece-wise type of linear function, with a change in slope at points where the internal temperature of the specimen attains equilibrium with the ambient air temperature, and additional changes in slope corresponding to variations in internal temperature. While standard maturity has traditionally held useful utility in assessing heat production during the hydration process, this data visualization method presents limitations in interpretation of the piece-wise linear functions. The subtle change in slopes can be difficult to interpret in a graphical method, for practical purposes. Alternative maturity employs the ambient air temperature as the datum temperature, as opposed to the constant datum temperature associated with standard maturity. This metrics provide a clearer mode for delineating heat generation during concrete hydration, considering the influence from ambient air temperature and humidity.
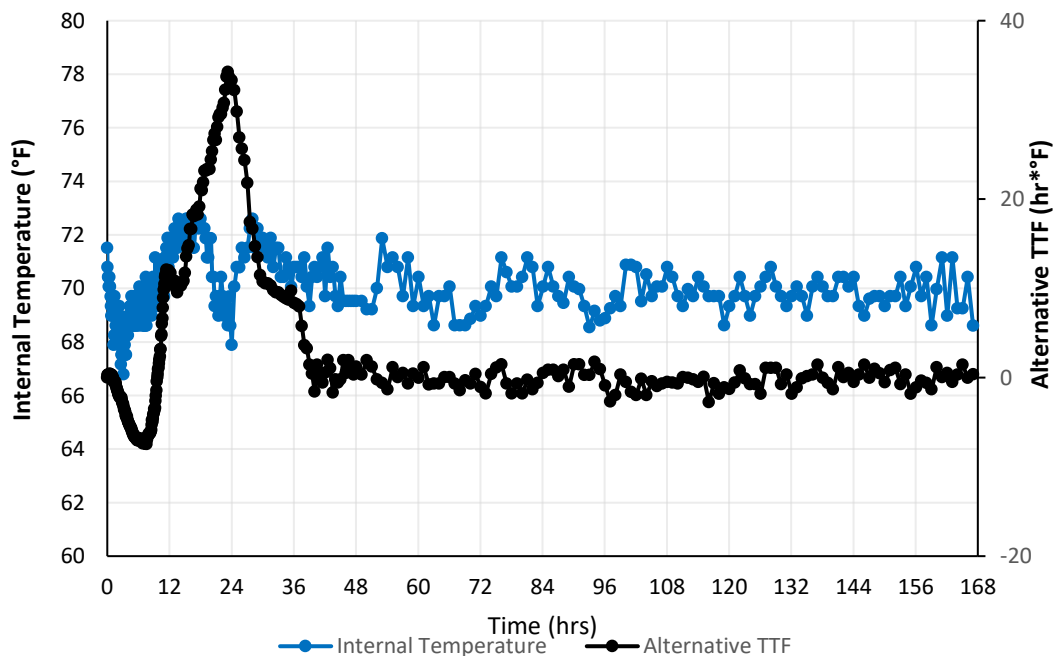


**Figure 4.3 Internal Temperature and Alternative TTF (Gravel mix 70°F/40% Hum)**

Figure 4.4 depicts the variations of the alternative TTF for the dolomite and gravel mixes at the tested environmental conditions: controlled temperatures (50 °F, 70 °F, 90 °F) and 40%

humidity level. Heat production duration can be observed as the time period from a) when the concrete specimen equilibrates with the ambient air temperature of the experiment to- b) the end of primary concrete hydration. This primary stage of concrete hydration, as referred to in this report, is interpreted as the instances where the internal temperature of the concrete is exceeding the surrounding ambient air temperature. This method of visualizing heat production duration provides a more clear and practical mode for delineating the hydration process. As primary hydration concludes, the concrete internal temperature again equilibrates with the ambient air temperature; effectively concluding this distinct duration of heat production. As a consistent measure to this study, the concrete specimens are demolded at 24-hrs; where the internal temperature of the concrete drops below the ambient air temperature for a period of time.
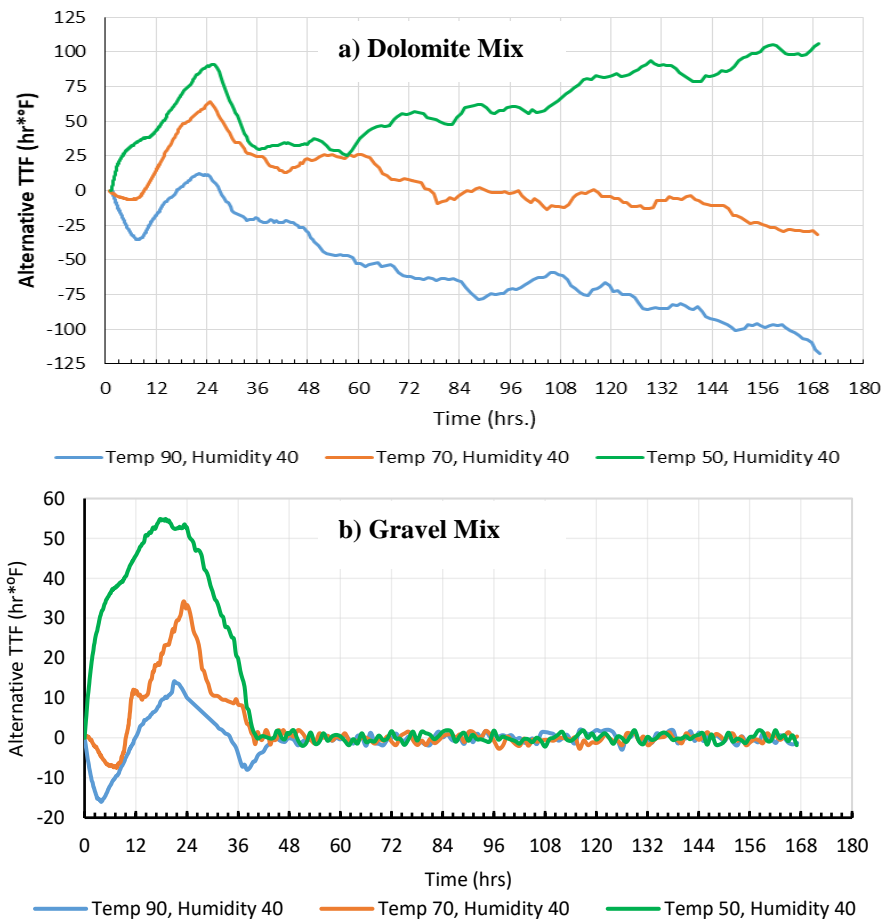


**Figure 4.4 Corresponding Alternative TTF Trends**

## 4.2    Modulus-Strength Relationships

As discussed in Nazarian et al. (2006), the continuous seismic moduli can then be leveraged to obtain empirical relationships between the modulus and concrete compressive strength. The unconfined compressive strengths taken at 1-day, 3-day, and 7-day ages can be plotted with the respective seismic modulus. For demonstration, Figure 4.5 displays such analysis being performed on the gravel and dolomite concrete mixtures taken at 70°F and 40% humidity. The equation that best explains the modulus-strength relationship was an exponential equation of the basic form of

$$strength = je^{k*modulus}$$    EQN 4.1

where *j* and *k* are the coefficients defining the intercept and shape of the curve.
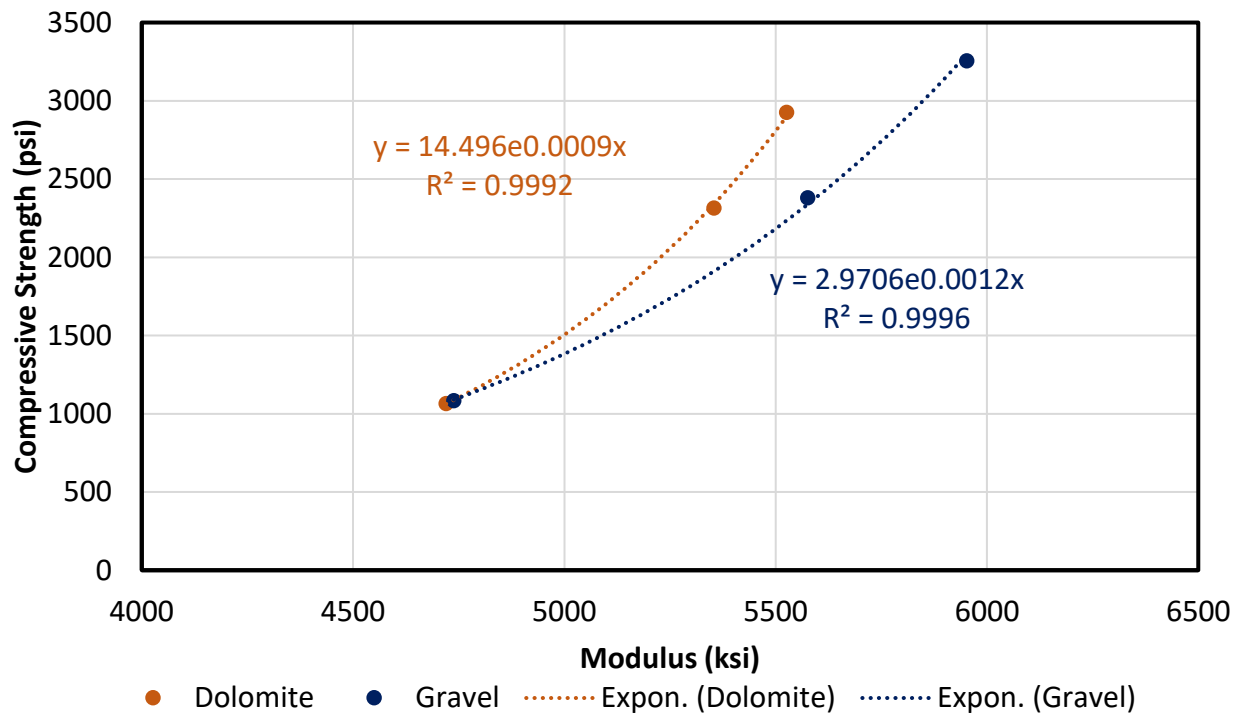


**Figure 4.5 Modulus-Strength Relationship of Mixes at 70°F/40% Hum**

Table 4.1 and Table 4.2 summarizes the modulus-strength relationship for each mix tested (Note: gravel mixes were only tested to assess environmental impact, and not mix-related parameters). A larger variance was observed in the *j*-coefficients, while the *k*-coefficients exhibited

less variance. The dolomite average value for the *k*-coefficients was $8.7 \times 10^{-4}$, with a standard deviation of $2.3 \times 10^{-4}$. The gravel average *k*-coefficients was $8.8 \times 10^{-4}$ and $2.5 \times 10^{-4}$ in standard deviation. These shape parameters suggest that the strength develops in a fairly uniform manner, as modulus increases during the first seven-days. Overall, a high confidence was found for each mix as observed with the $R^2$ values (0.86-1.00). The lower-end $R^2$ values generally occurred for mixes that experienced little gain in strength between three and seven days.

**Table 4.1 Modulus-Strength Relationship Coefficients and $R^2$ Values (Dolomite and Gravel) Obtained from Evaluation for Environmental Impacts**

| Controlled Humidity | Curing Temperature | Dolomite | | | Gravel | | |
|---|---|---|---|---|---|---|---|
| | | *j* | *k* | $R^2$ | *j* | *k* | $R^2$ |
| 40% | 50°F | 5.5 | 0.0011 | 0.99 | 31.7 | 0.0009 | 0.99 |
| | 70°F | 3.0 | 0.0012 | 0.99 | 6.0 | 0.0011 | 0.99 |
| | 90°F | 2.8 | 0.0012 | 0.99 | 2.9 | 0.0013 | 0.99 |
| 80% | 50°F | 20.7 | 0.0009 | 0.99 | 42.0 | 0.0008 | 0.99 |
| | 70°F | 76.4 | 0.0006 | 0.92 | 78.3 | 0.0006 | 0.97 |
| | 90°F | 74.3 | 0.0006 | 0.87 | 76.3 | 0.0006 | 0.90 |

**Table 4.2 Modulus-Strength Relationship Coefficients and $R^2$ Values (Dolomite) Obtained from Evaluation for Mix-related Parameters**

| Controlled Humidity | Curing Temperature | Mix-Related Parameters | Dolomite | | |
|---|---|---|---|---|---|
| | | | *j* | *k* | $R^2$ |
| 40% | 70°F | 0.40 w-c | 85.0 | 0.0006 | 0.96 |
| | | 15 oz. AA | 34.3 | 0.0008 | 0.97 |
| | | 45 oz. AA | 10.3 | 0.0011 | 1.00 |
| | | 45 oz. AA; 0.40 w/c | 20.3 | 0.0009 | 0.99 |
| | | 10 oz. HRWR | 13.1 | 0.0009 | 0.94 |
| | | 15 oz. HRWR | 15.4 | 0.0009 | 0.99 |
| | | 10 oz. HRWR; 0.40 w/c | 41.5 | 0.0007 | 1.00 |
| | | 0.5 oz. AE | 27.3 | 0.0009 | 0.99 |
| | | 4 oz. AE | 16.1 | 0.0013 | 0.95 |
| | | 0.5 oz. AE; 0.40 w/c | 103.0 | 0.0005 | 0.86 |
| | | Large Agg. | 45.2 | 0.0007 | 0.99 |
| | | Small Agg. | 40.3 | 0.0008 | 1.00 |

No significant trends are observed amongst the *j* or *k*-coefficients with regard to environmental conditions or mix changes. The dolomite mix changes that saw the greatest similarities in both

coefficients involved the addition of a high-range water reducer and the aggregate change. The 0.5 oz. AE; 0.40 w/c mix resulted with the largest *j*-coefficient and lower *k*-coefficient compared to all other mixes with the lowest confidence.

## 4.3    Standard Maturity-Strength Relationships

The compressive strength of the concrete can also be observed with standard maturity. For demonstration, this procedure is displayed in Figure 4.6 for the reference mixes cured at 70F and 40% humidity. A logarithmic equation was found to be the best model for a standard maturity-strength relationship. The equation takes the basic form of:

$$strength = \text{m} \ln(TTF) - n \qquad \qquad \text{EQN 4.2}$$

where *m* and *n* serve as coefficients controlling the rate of growth and y-intercept, respectively.
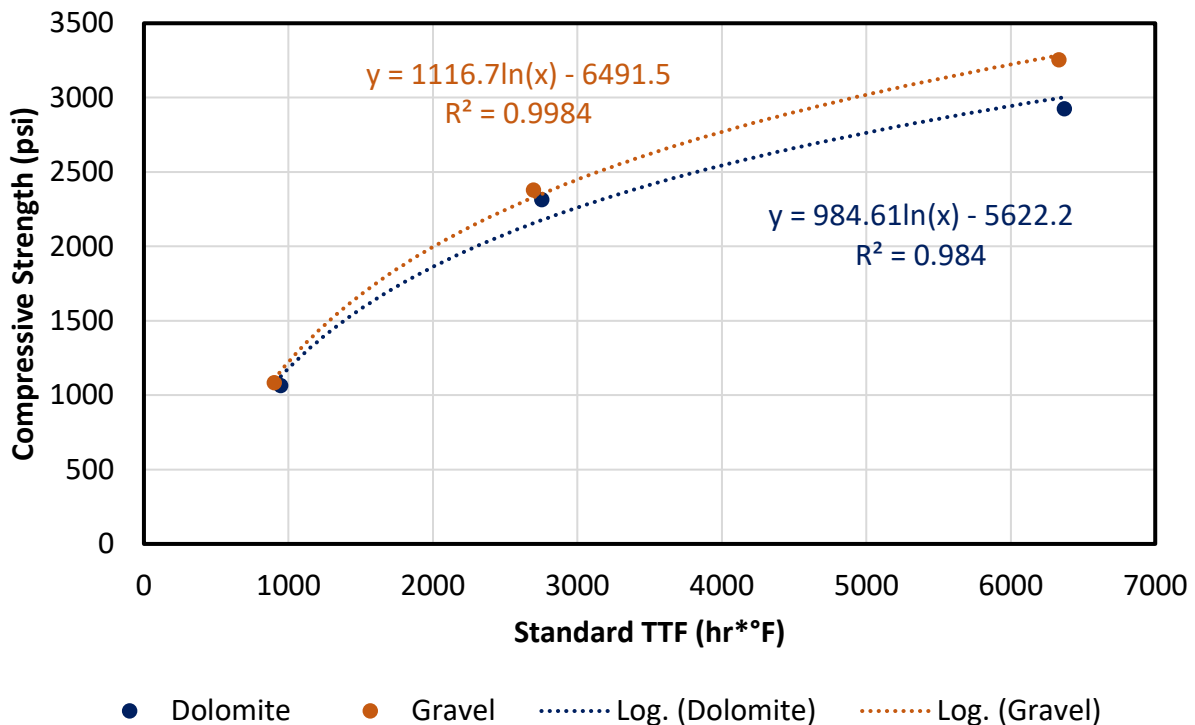


**Figure 4.6 Standard Maturity-Strength Relationship for Mixes at 70°F/40% Hum**

61

Table 4.3 and Table 4.4 lists the standard maturity-strength relationship regression coefficients and the associated $R^2$ value for the test variants. Most mixes show a good relationship between standard maturity and strength. The growth factor (*m*-coefficient) observed for dolomite are generally greater than 1,100 for low temperature (50°F) curing, and less than 650 for high temperature (90°F) curing. This growth factor is shown to be in between those two ranges for 70°F curing. The gravel exhibited growth factor coefficients around 530-560 for high temperatures (90°F). These growth coefficients at 50°F and 70°F ranged from 950 to 1320. The coefficient of determinations ($R^{2)}$ are shown to range 0.66-1.00. The mixes with i) reduced water-cement ratio, ii) accelerating agent, and iii) large coarse aggregates generally exhibited lower *m*-coefficients. The two mixes with the lowest *m*-coefficients were those with the high dosage of air entraining admixture, and those with low dosage of air entertainer admixture combined with a low-water cement ratio. These mixes also had the low $R^2$ value.

**Table 4.3 Standard Maturity-Strength Relationship Coefficients and $R^2$ Values (Dolomite and Gravel) Obtained from Evaluation for Environmental Impacts**

| Controlled Humidity | Curing Temperature | Dolomite | | | Gravel | | |
|---|---|---|---|---|---|---|---|
| | | *m* | *n* | $R^2$ | *m* | *n* | $R^2$ |
| 40% | 50°F | 1188.3 | 7266.4 | 1.00 | 966.3 | 5301.4 | 1.00 |
| | 70°F | 984.6 | 5622.2 | 0.98 | 1116.7 | 6491.5 | 1.00 |
| | 90°F | 619.6 | 2782.9 | 0.99 | 557.6 | 2367.6 | 0.94 |
| 80% | 50°F | 1230.7 | 7178.2 | 1.00 | 1316.2 | 7950.6 | 1.00 |
| | 70°F | 1008.7 | 5821.7 | 1.00 | 951.5 | 5208.5 | 1.00 |
| | 90°F | 590.7 | 2554 | 0.81 | 537.7 | 2063.8 | 0.80 |

**Table 4.4 Standard Maturity-Strength Relationship Coefficients and $R^2$ Values (Dolomite) Obtained from Evaluation for Mix-related Parameters**

| Controlled Humidity | Curing Temperature | Mix-Related Parameters | Dolomite | | |
|---|---|---|---|---|---|
| | | | *m* | *n* | $R^2$ |
| | | 0.40 w-c | 719.0 | 3448.9 | 0.87 |
| | | 15 oz. AA | 892.6 | 4945.5 | 0.97 |
| | | 45 oz. AA | 903.9 | 5204.8 | 0.93 |
| | | 45 oz. AA; 0.40 w/c | 830.7 | 4366.9 | 0.85 |
| | | 10 oz. HRWR | 1155.8 | 6859.2 | 0.96 |
| | | 15 oz. HRWR | 907.0 | 5318.4 | 0.94 |
| 40% | 70°F | 10 oz. HRWR; 0.40 w/c | 901.0 | 4640.6 | 0.94 |
| | | 0.5 oz. AE | 1005.1 | 5880.3 | 0.91 |
| | | 4 oz. AE | 375.9 | 2194.6 | 0.81 |
| | | 0.5 oz. AE; 0.40 w/c | 638.5 | 2868 | 0.66 |
| | | Large Agg. | 718.3 | 3689.5 | 0.95 |
| | | Small Agg. | 1136.1 | 6483.5 | 0.95 |

## 4.4     Impact of Environmental Parameters

The reference mix was tested under variable curing conditions at controlled temperatures (50 °F, 70 °F, 90 °F) and humidity levels (40% and 80%) to assess their effects on the concrete times of set and strength and modulus development. Additionally, the impact from mold removal at various times was briefly investigated to assess influence.

### 4.4.1   Impact of Temperature

The variations in penetration-based times of set, while considering the variable environmental conditions, are shown in Figure 4.7[4]. Regardless of the level of humidity, times of set occurred earlier at higher temperatures for dolomite and gravel mixes. The longer setting times between initial and final set were observed when curing at 50°F; approximately twice as long when compared to curing at 70°F and 90°F.

---

[4] Data shown represents average setting time data considering three replicates.

## a) Dolomite Mix



## b) Gravel Mix
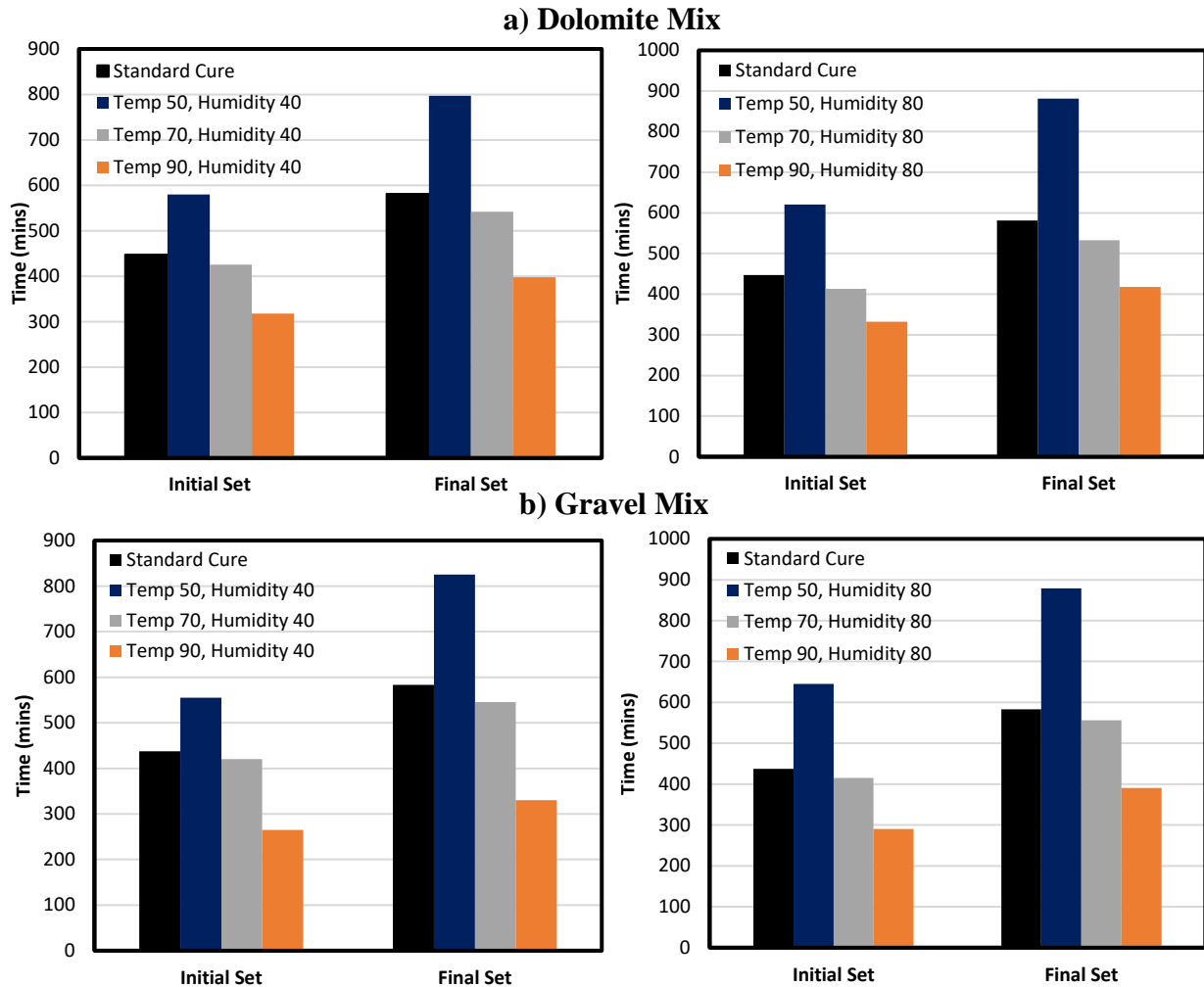


**Figure 4.7 Temperature Impact on Set at High and Low Humidity**

Figure 4.8[5] summarizes the variations in modulus with time for the low and high humidity curing conditions. For each humidity level, it seems the moduli appear to converge to a common value. Due to this, it is likely that the mixes would yield similar 28-day modulus results. Increasing the curing temperature seem to increase the rate of modulus growth, while a lower temperature yield a slower rate of growth. The specimens exposed to the high and mid-range curing temperatures seemed to become asymptotic of their long-term moduli between 40 and 60 hours; whereas the specimens cured at 50°F required approximately 80-hours to achieve to that level.

---

[5] Data shown represents average modulus data considering three replicates.

**a) Dolomite Mix**

Modulus Development of Low Humidity

Modulus Development of High Humidity

**b) Gravel Mix**

Modulus Development of Low Humidity

Modulus Development of High Humidity
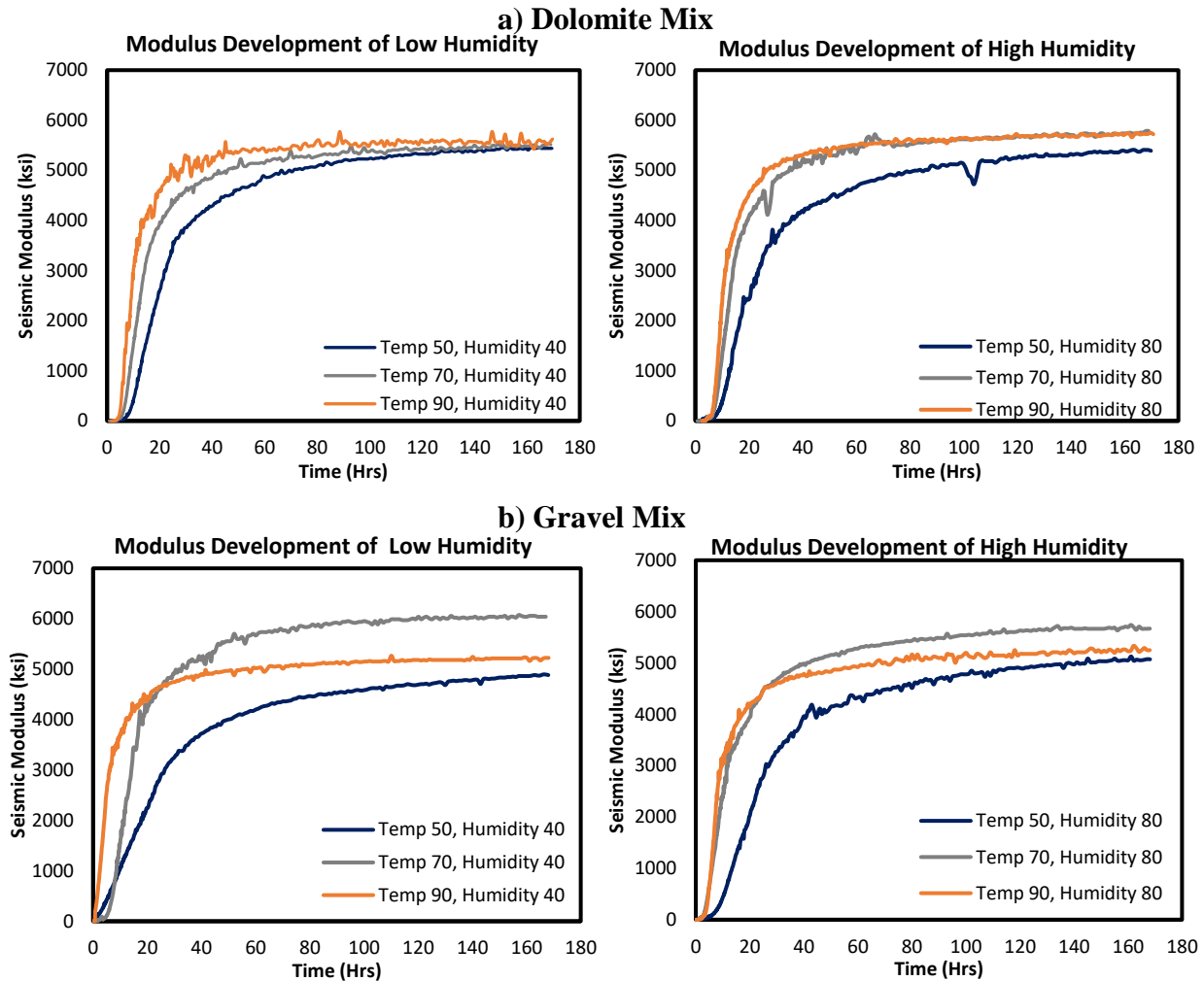
**Figure 4.8 Temperature Impact on Modulus Development at High and Low Humidity**

Figure 4.9[6] shows the variations in compressive strength with time. The results obtained are consistent with the previous research reviewed in Chapter 2. Changing the curing temperature from 70°F to 90°F yielded more proportional changes in the properties than observed when the curing temperature was changed from 70°F to 50°F. High temperature curing resulted in a high one-day strength following by a less than 50% gain at three-days. By seven days, there was little strength gain recorded; indicating a rapid initial strength gain that rapidly decreases beyond three days. Low temperature curing resulted in a very low one-day strength followed by rapid gain to

---

[6] Data shown represents average compressive strength data considering three replicates.

the achieved three-day strength. Although the strength gain from three-to seven days was less rapid, it was still a larger rate of growth than observed at high temperature curing. Unlike the early growth seen at 90°F, the low temperature curing went through an initial slower rate of growth followed by a consistent rate of growth to reach the three- and seven-day strengths.
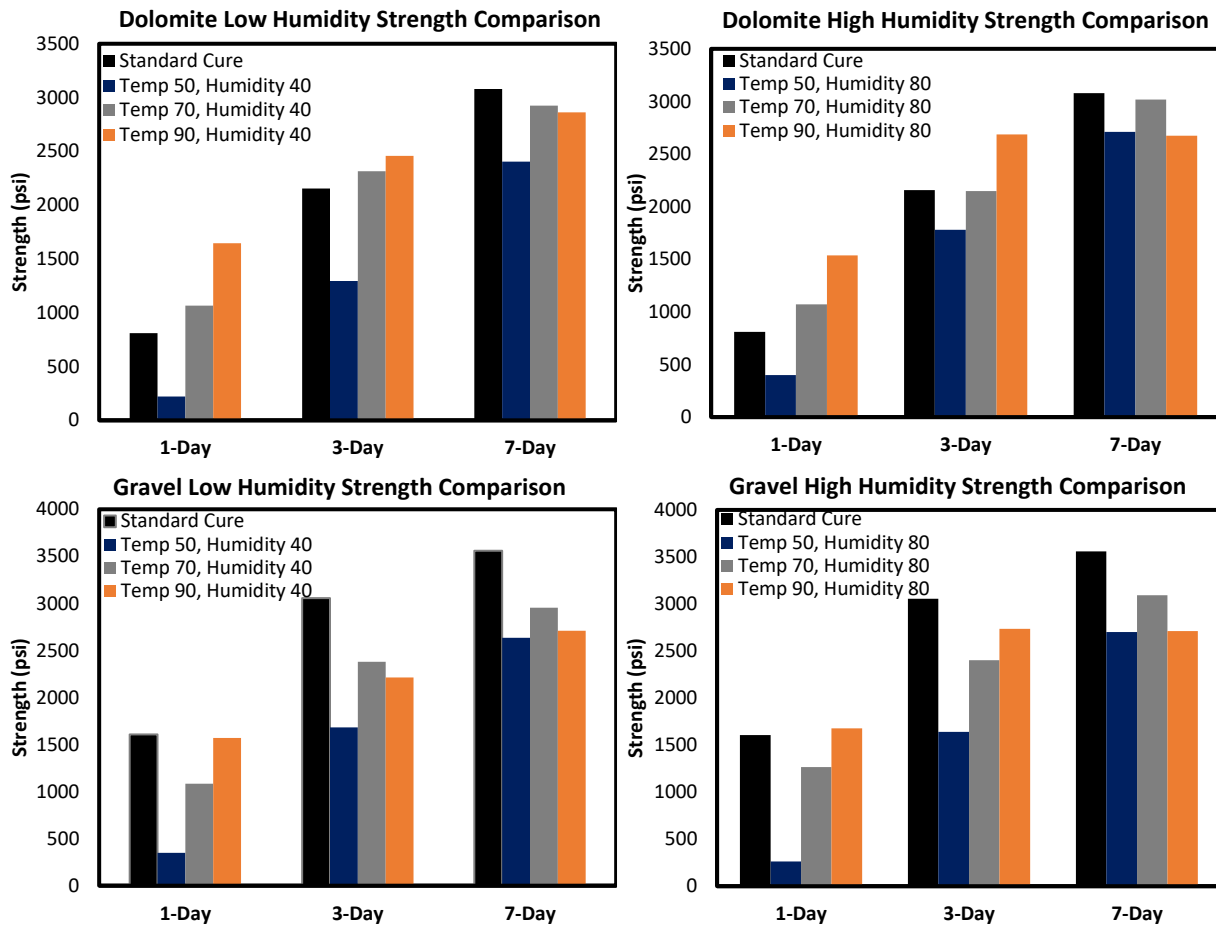


**Figure 4.9 Temperature Impact on Strength at High and Low Humidity**

### 4.4.2 Impact of Humidity

The impact of humidity was analyzed across the curing temperatures (50 °F, 70 °F, 90 °F). Results indicated there is still an impact from humidity on set, strength, and modulus; however this impact is not as great as that caused by temperature. Referring back to Figure 4.7, the low humidity specimens show lower times of initial and final set when compare to the high humidity

specimens cured at the same temperature. At 70°F and 90°F curing, initial and final set times where within 20 minutes of each other at both humidity conditions. The low temperature curing; however, reached initial set almost 45-minutes faster at low humidity, and over an hour faster for final set.

Figure 4.10[7] shows the variations in the internal temperature of the specimens cured at the same temperature, but at different levels of humidity. The impact of the humidity on the internal temperature is rather small, as compared to the impact of curing temperature discussed in the previous section. However, the impact of the humidity on the strength (and to lesser extent on modulus) is more pronounced. At demolding (24 hrs.), a decrease in temperature, or cooling, can be observed from one to two hours. This cooling period was observed to last between two to four-hrs. By roughly 36 hours, the internal temperatures revert to equilibrium with the ambient temperature. This indicates that minimal heat is generated from the concrete and temperature changes primarily result from changes in the environment. Further findings are discussed below to expand on humidity impacts at each tested temperature.

---

[7] Data shown represents average internal temperature data considering three replicates.

**Dolomite Mixes**  **Gravel Mixes**
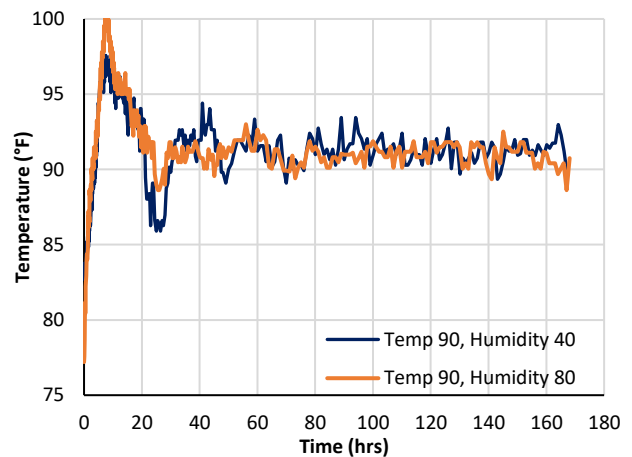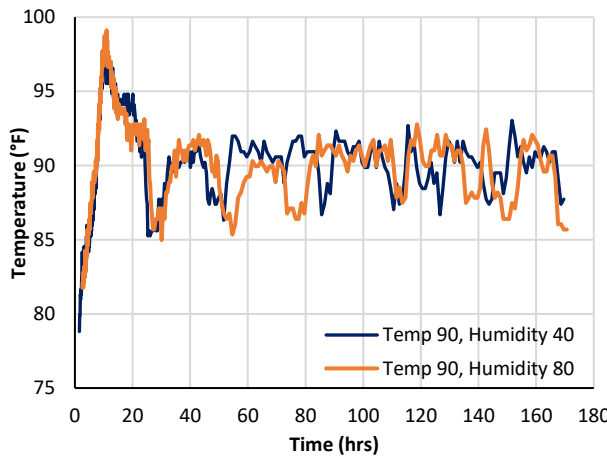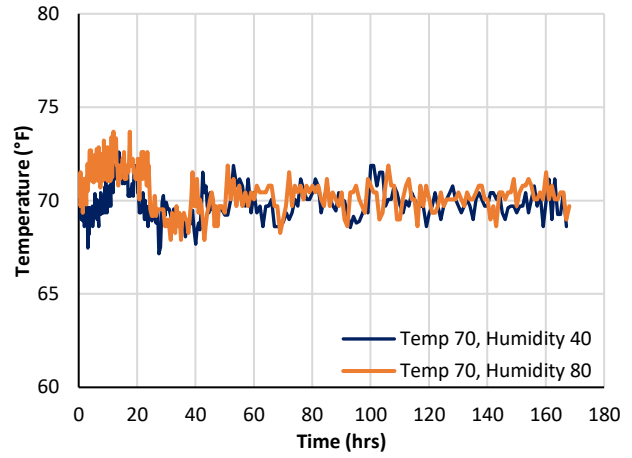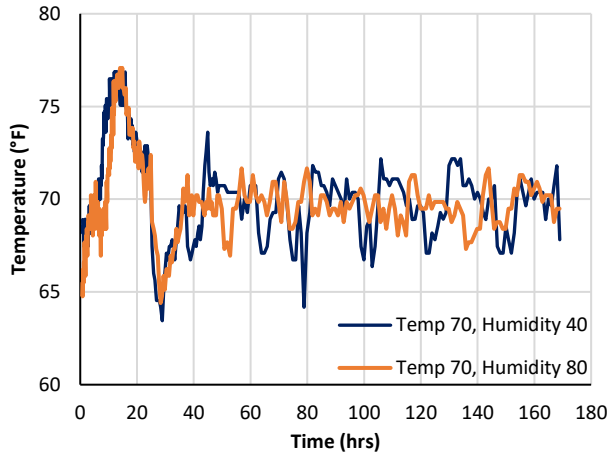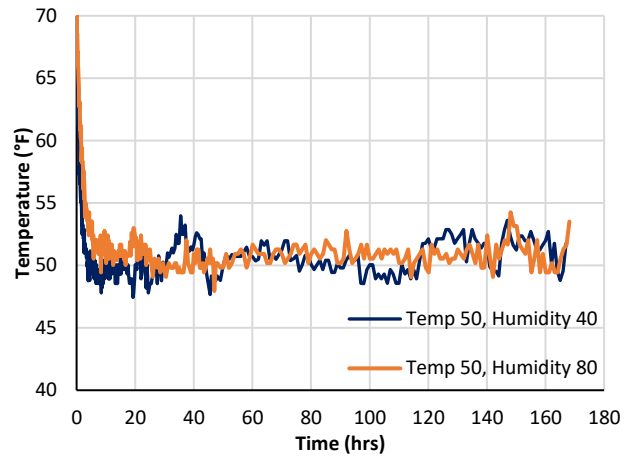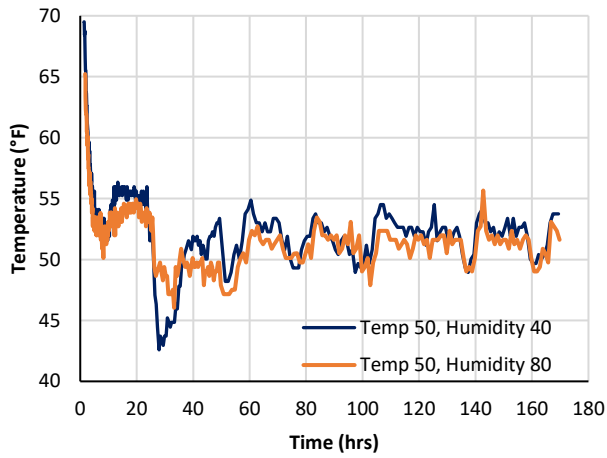


**Figure 4.10 Internal Temperature Comparisons**

Figure 4.11 displays the variations in strength and modulus with time (1-day, 3-day, 7-day) for the specimens cured at 50°F and 40% and 80% humidity. The dolomite specimens cured at 40% humidity yield lower compressive strengths as compared to the specimens cured at 80% humidity. However, the increase in modulus with time seems to be almost independent of the humidity. Reviewing the times of initial and final set previously depicted in Figure 4.7, the low humidity curing conditions saw both initial and final set occur nearly an hour earlier than the high humidity curing.
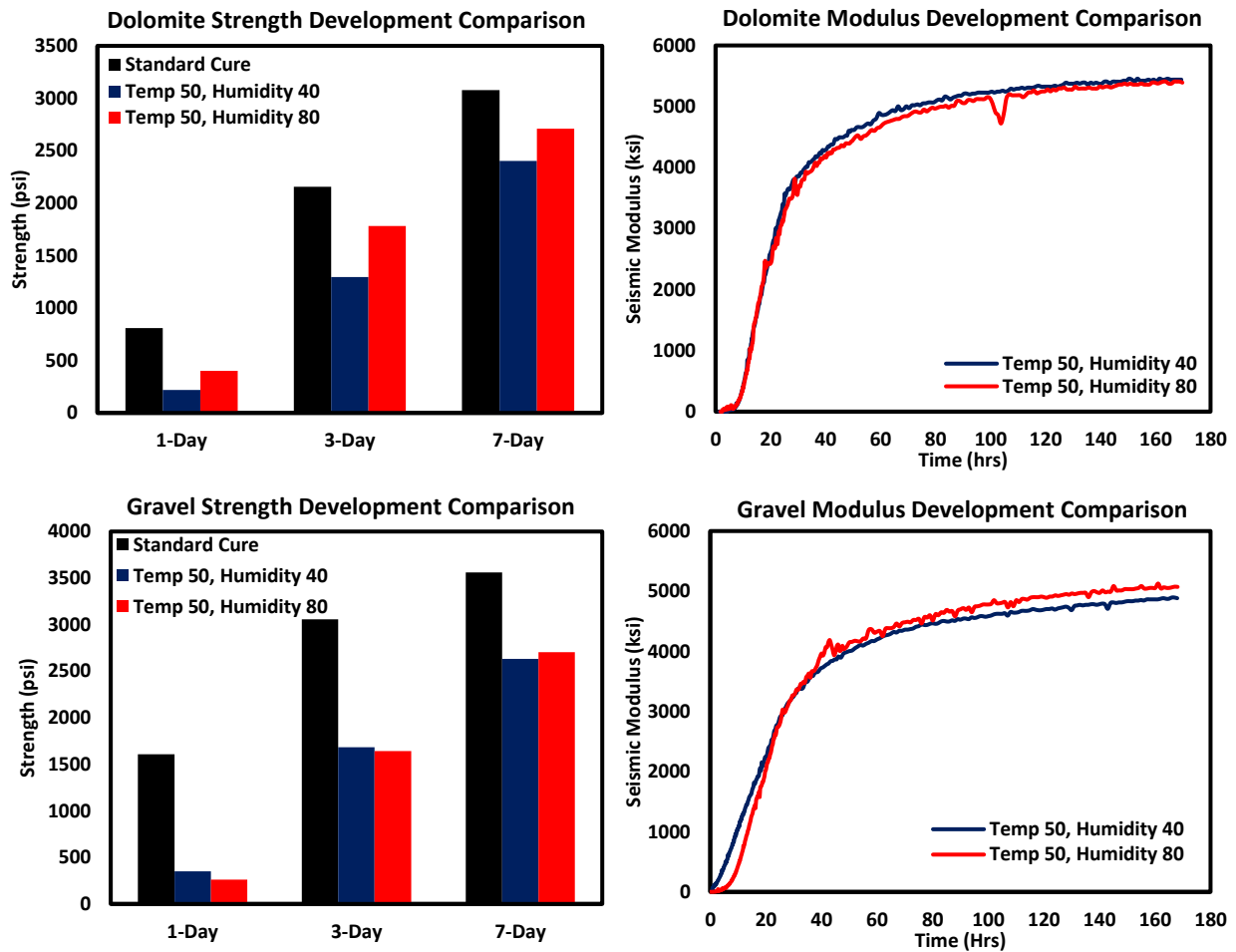


**Figure 4.11 Strength and Modulus Development at 50°F Curing**

As shown in Figure 4.12, the dolomite and gravel specimens cured at 70°F exhibited similar strength and modulus development at 1-day, 3-day and 7-days. The results show the

strength and modulus gain to be independent of the 40% and 80% humidity level. As shown in Figure 4.7, the initial and final sets across the three humidity conditions were within 60 minutes of one another, with the specimens cured at 40% and 80% humidity exhibiting sets that are 15 minutes of each other.
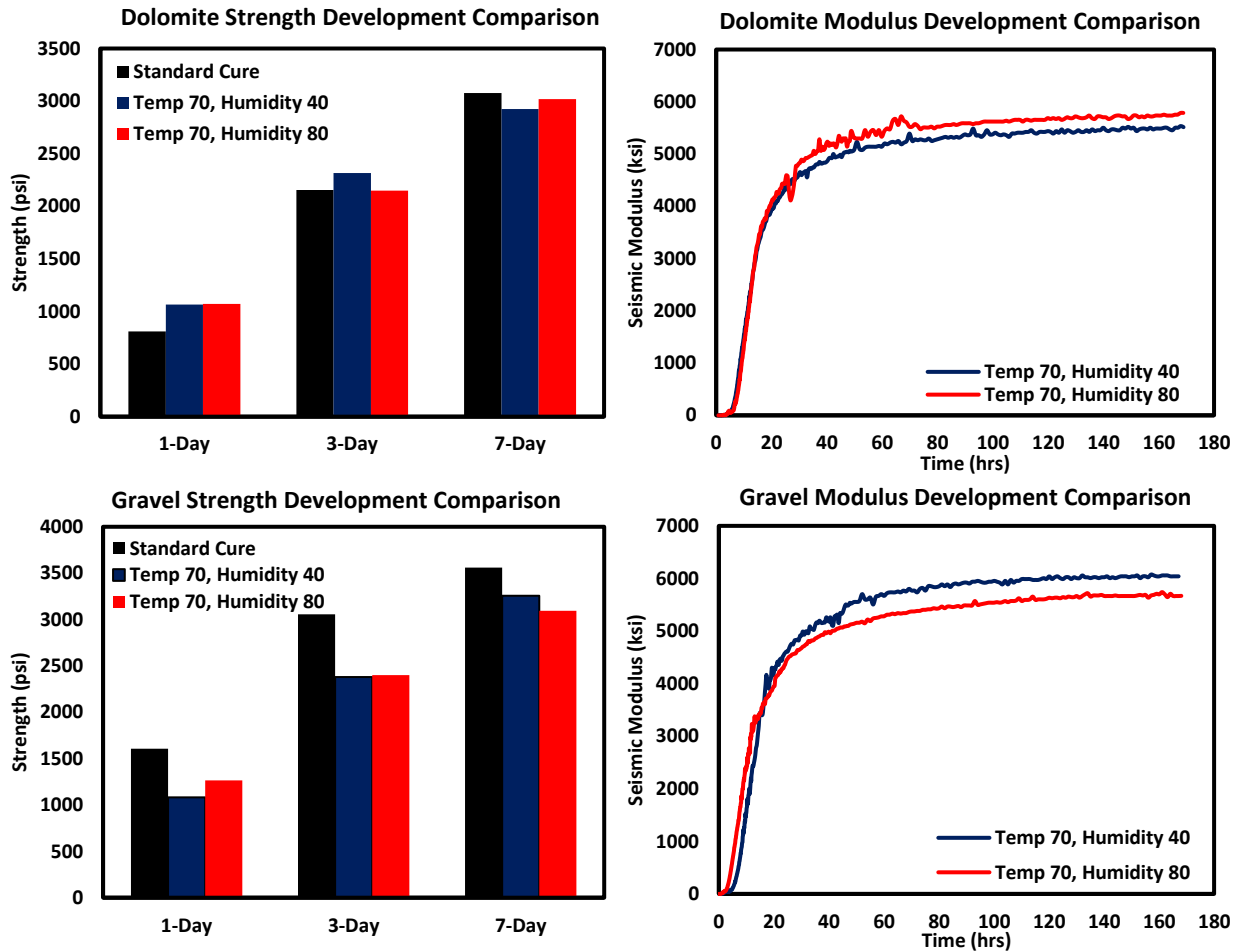


**Figure 4.12 Strength and Modulus Development at 70°F Curing**

Observing Figure 4.13, the setting, strength and modulus developments are shown to be independent of the humidity levels (40% versus 80%) when the specimens were cured at 90°F. As shown in Figure 4.7, the times of set were mostly within 20 minutes of one-another. The gravel mix did see a 60-min between initial and final set at 80% humidity. One significant finding is the significant gain in strength and modulus for the specimens cured at $90^{\circ}$F relative to those cured

under standard curing conditions of 70°F and 100% humidity. This trend reverses after 7 days when the strength and modulus of the standard cured specimens are greater than those cured at higher temperature. Additionally, the setting times regardless of mix were the lowest under this curing condition.
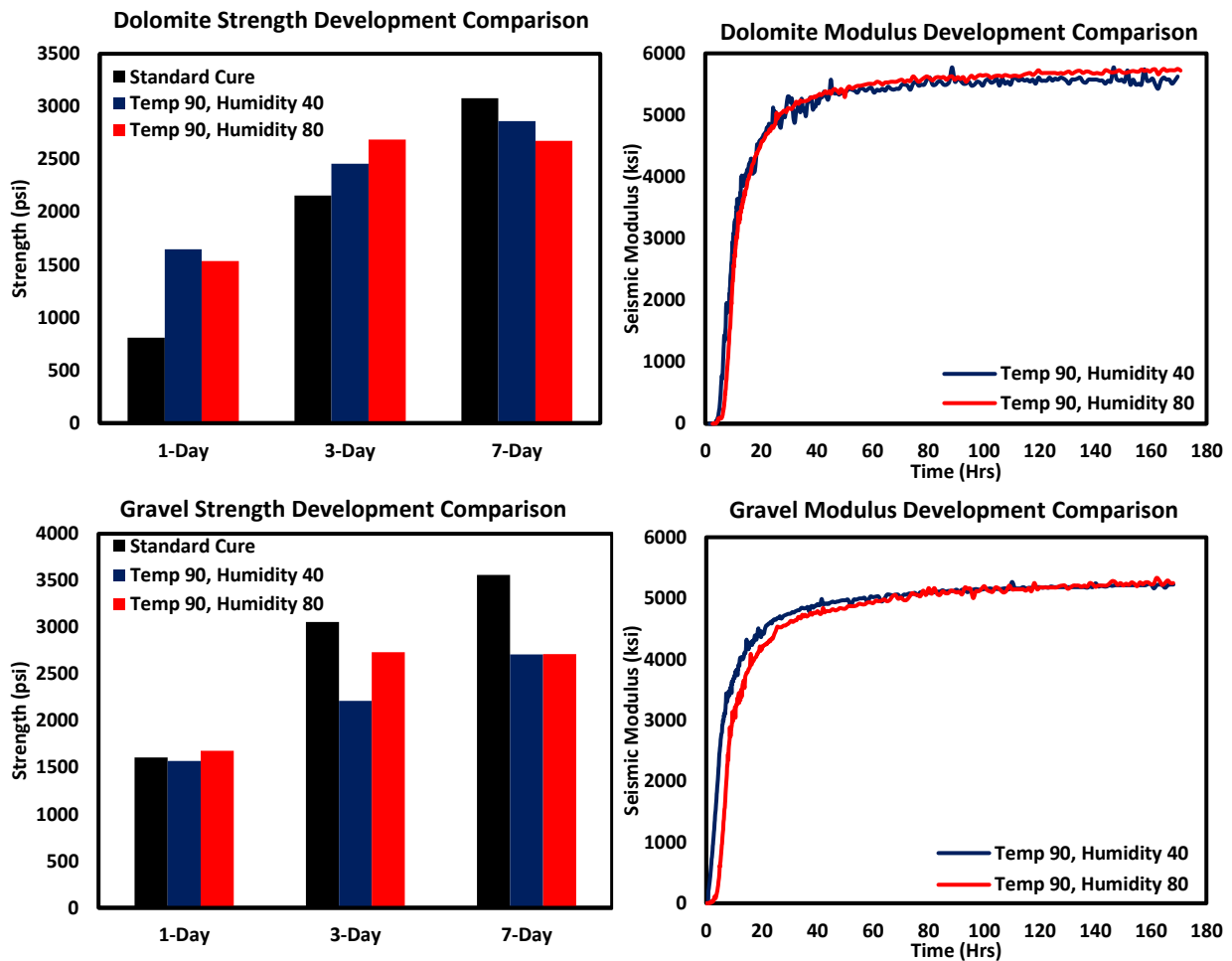


**Figure 4.13 Strength and Modulus Development at 90°F Curing**

In summary, the one-day strengths for the specimens cured at high humidity were essentially the same or slightly greater than the strengths at the lower humidity. This pattern was not seen at the low temperature scenarios due to the ambient temperature slowing the hydration process. Therefore, the impact of humidity plays a larger role at lower curing temperatures, but still not to the same extent as curing temperature.

71

### 4.4.3 Mold Removal

The remainder of Chapter 4 discusses a data analysis of impact of mold removal and influence of various mix-related parameters on early strength and stiffness development. As discussed previously, this testing and ensuing analyses was only performed for the dolomite mix.

A brief investigation was carried out to observe the impact of the removal of the mold (after 24 hrs.) on the properties of the concrete. The variations in the internal temperatures of two specimens (one demolded after 24 hrs. and the other maintained in the mold for seven days) from the reference mix and under the same curing conditions are shown in Figure 4.14. The internal temperatures change rapidly during the first 6-hours towards reaching ambient temperature. The temperature patterns from the two specimens are similar when observing between 6 hrs. and 24 hrs. At the nominal time of 24 hrs. the demolded specimen experiences a drastic drop of the temperature, despite the specimens being demolded in the environmental chamber. This pattern was observed for all the demolded specimens, as previously shown in Figure 4.10. When the mold is removed, the entire surface area of the specimen is able to transfer heat and moisture. This results in the cooling of the specimen beyond the ambient temperature.
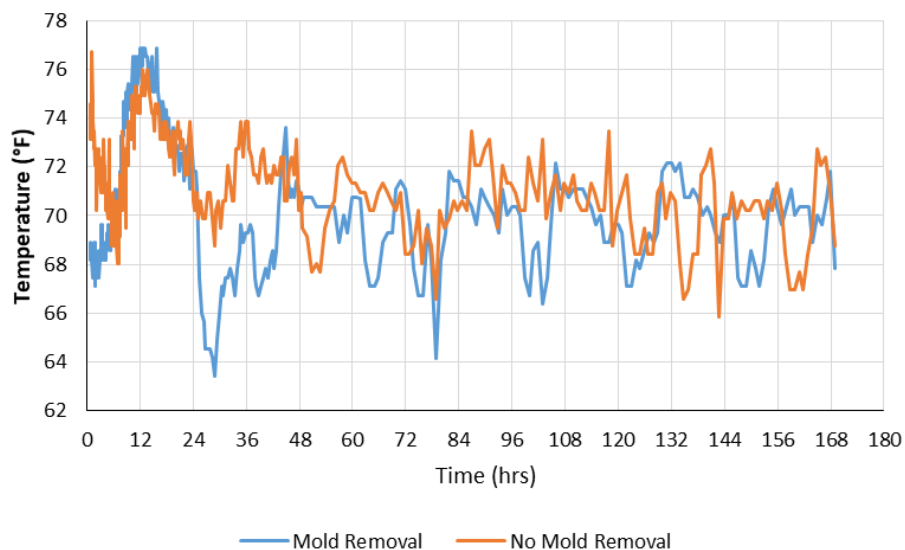


**Figure 4.14 Impact of Mold on Internal Temperature (Dolomite mix 70⁰F/40 Hum)**

This loss of heat and moisture slows the hydration process; resulting in lower strength and seismic modulus at seven days. Removal of the mold yielded an average seven-day strength of 2,925 psi, while keeping the mold on for the full seven days resulted in an average strength of 3,370 psi. Figure 4.15 displays the modulus development for both conditions. Modulus development is similar for the first 20 hrs. of monitoring, however distinction in modulus development is evident between both conditions. The specimens with "no mold removal" clearly achieve a higher stiffness.
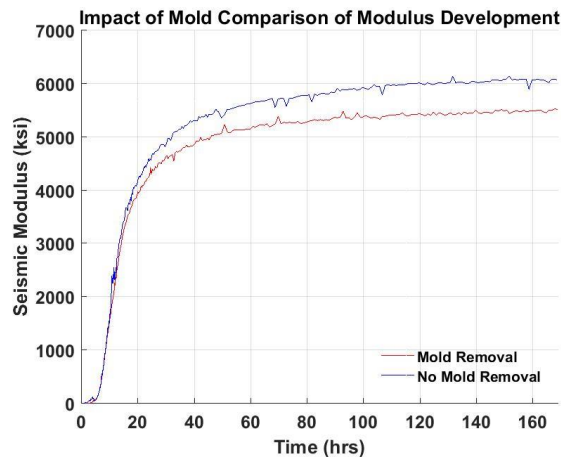


**Figure 4.15 Impact of Mold on Modulus Development (Dolomite mix 70$^0$F/40 Hum)**

## 4.5    Mix Related Parameters

The following sections discuss the early age effects of perturbing the water-cement ratio, accelerating agent, high-range water reducer, air entraining agent, and gradation of the coarse aggregate. Since all mixes were cured at 70°F and 40% humidity, their characteristics were compared to the reference mix that was cured under the same conditions. In addition to the cylinders cured under those environmental conditions, three cylinders from each mix were prepared and cured under the standard curing conditions for comparison purposes.

Appendix A contains detailed information about the variation in internal temperature with time. The trends observed for different mixes are similar to the trends observed for the reference

mix cured at 70°F as discussed in the previous section. For that reason no further discussion on that topic is included.

### 4.5.1 Impact of w/c Ratio

As shown in Figure 4.16, reducing the water-to-cement ratio from the reference value of 0.45 to 0.40 reduced the time of initial set from 7.1 hrs. to 6.2 hrs. while the time to final set decreased from 9.0 hrs. to 8.1 hrs.
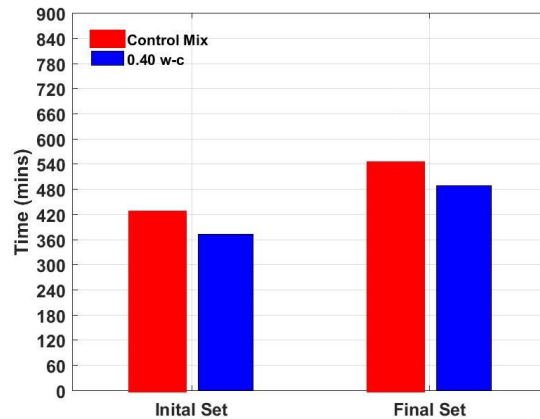


**Figure 4.16 Impact of Set Caused by Change in Water-Cement Ratio**

The changes in strength and modulus with time caused by reducing the water-cement ratio are shown in Figure 4.17. As compared to the standard mix, the mix with less water exhibited higher strength for the first three days, and slightly lower strength after seven days. Reduced water yielded an average one-day strength approximately 300 psi greater than the reference mix, and an average three-day strength nearly 250 psi greater. However, the modulus of the reference mix was consistently less than the modulus of the mix with less water throughout the seven days of testing.
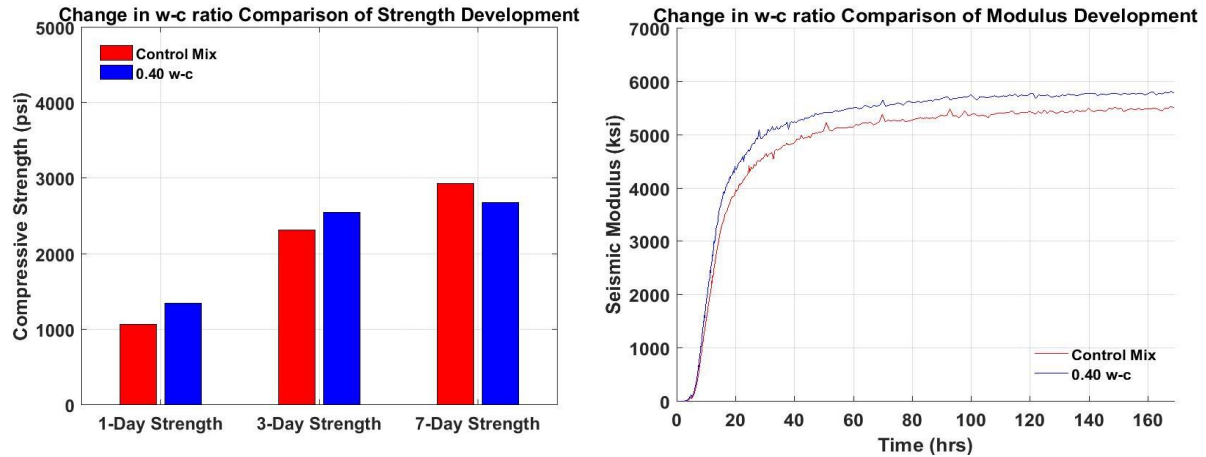
**Figure 4.17 Strength and Modulus Development for Change in Water-Cement Ratio**

As seen in Figure 4.18, consistent increase in strength and modulus due to decrease in water-to-cement ratio was observed for specimens cured under standard curing. One-day strength was almost 500 psi greater, while three- and seven-days specimens were 1,700 psi to 1,800 psi stronger than the reference mix. Similarly, the modulus determined from the FFRC tests on the specimens with lower water-cement ratio was i) 1,000 ksi greater than those from the standard mix after one and three days and ii) 700 ksi after seven days.
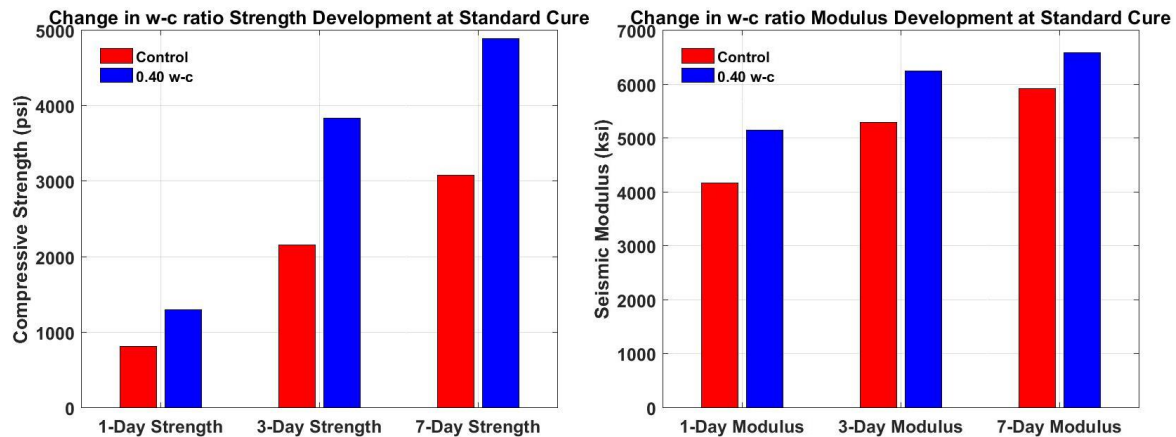


**Figure 4.18 Strength and Modulus under Standard Curing with Reduced w-c Ratio**

## 4.5.2   Impact of Accelerating Agent

The impact of an accelerating agent on the early-age behavior of concrete was evaluated with the use of Accelguard ACN 200. The effect of this admixture was studied by preparing and

testing specimens near the recommended low dosage (15 fl oz. per 100 lbs. of cement), and high dosage (45 fl oz. per 100 lbs. of cement). In addition, another test variant with a high dosage of accelerating agent (45 fl oz. per 100 lbs. of cement) and a reduced water-to-cement ratio of 0.40 was evaluated.

As shown in Figure 4.19, the presence of the accelerating agent resulted in a faster set. However, the evaluated dosages of accelerating agent used had little impact on the times of set. Using the penetrometer, the initial sets were largely shown to be within six minutes of one-another. The final sets were shown to be within 30 minutes of one another. Based on these results, the high dosage of accelerating agent in the mix may result in a slightly faster set compared to the low dosage mix.

As shown in Figure 4.20, the strengths and moduli of the mixes with accelerating agent were nearly the same or lower than those of the reference mix, through-out the 7-day period. The mix with the high dosage of accelerating agent actually exhibited lower strengths and moduli than the mix with the low dosage of accelerating agent.
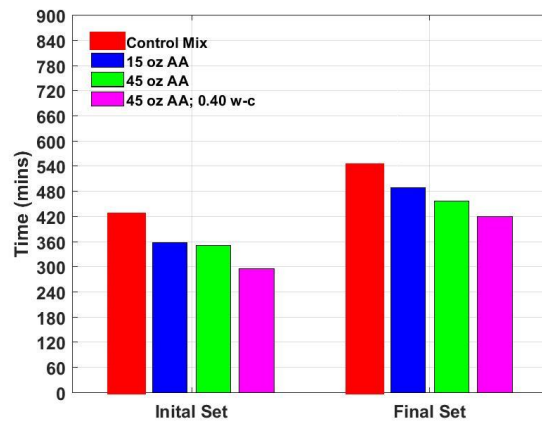


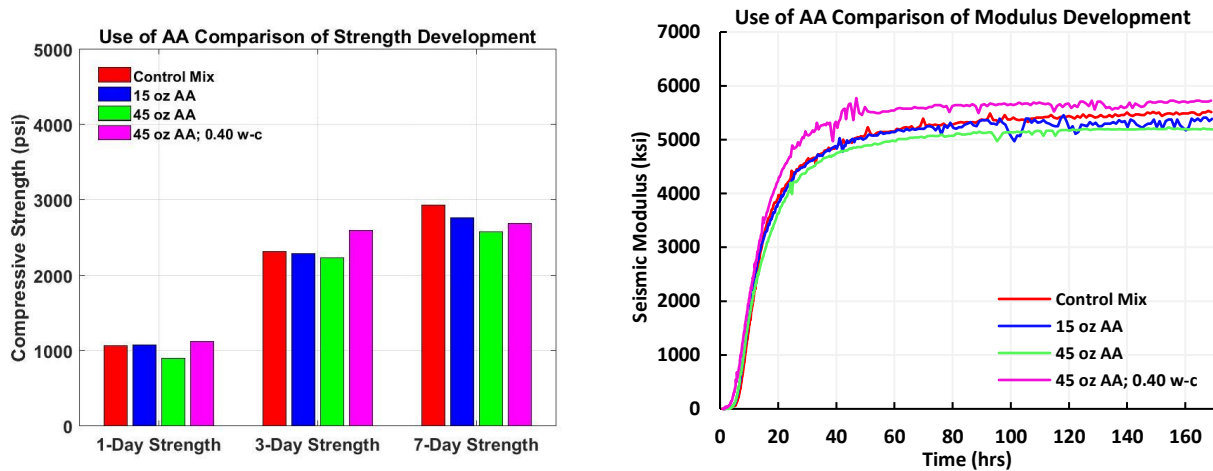**Figure 4.19 Impact of Set Caused by Addition of Accelerating Agent**

**Figure 4.20 Strength and Modulus Development for Addition of Accelerating Agent**

The mix with the combination of accelerating agent and lower water-cement ratio further reduced the times to the initial set and final set relative to the mix with the high dosage of accelerating agent. That mix exhibited a lower initial set (about 1-hr less) than the mix with the high dose of accelerating agent. This mix also achieved initial set about two hours faster than the reference mix. The mix with the reduced water-cement ratio also achieved a faster set and higher strengths at 1- and 3-day relative to the mix with the high dose of accelerating agent. However, when compared to the mix with the low dose of accelerating agent, the one-day strengths were within 50 psi of each other. The variations in the modulus with time exhibit the same pattern as strength development (i.e., higher moduli achieved throughout the seven-day testing for the mix with the high dose of accelerating agent and reduced water).

Figure 4.21 displays the variations of strength and modulus with time for the specimens that were cured under the standard curing conditions. Under standard curing, all three mixes with the accelerating agent achieved higher strengths than the reference mix. Similar to the specimens cured at the humidity of 40% (shown in Figure 4.19), the two mixes with the low and high dose of the accelerating agent exhibited similar strengths. The moduli of the three mixes were essentially

77

the same for all three mixes with the accelerating agent. These were typically marginally or significantly greater than the corresponding moduli from the reference mix.

Strengths recorded under standard curing were 500 psi higher than the low humidity curing at one-day, and over 1,000 psi greater at seven days. This was observed regardless of mix. Similarly, results were observed for the seismic modulus. This shows the advantage of adding accelerating agent are more apparent under standard curing than at 40% humidity. Regardless of curing conditions, the change in quantity of admixture yields limited benefit.
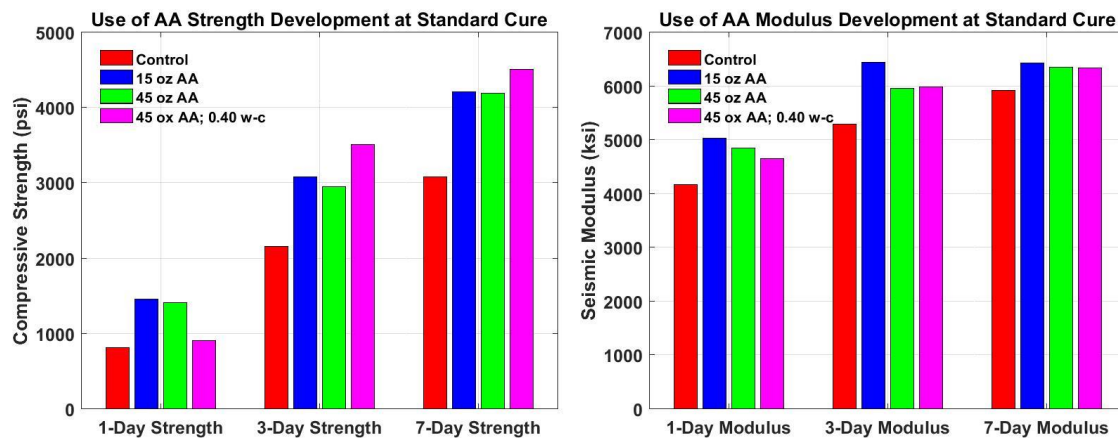


**Figure 4.21 Strength and Modulus under Standard Curing with Accelerating Agent**

### 4.5.3    Impact of High Range Water Reducer

A high-range water reducer (HRWR), Eucon SP, was used to evaluate its impact on the early-age characteristics of concrete. Two mixes near the recommended low dosage (10 fl oz. per 100 lbs. of cement) and high dosage (15 fl oz. per 100 lbs. of cement) were used for this purpose. Once again, a third mix with the low dosage of HRWR (10 fl oz. per 100 lbs. of cement) with the water-to-cement ratio with of 0.40 was also evaluated.

For all three mixes, the times of set were slower than the reference mix (as shown in Figure 4.22). The mix with the low dose of HRWR exhibited an initial and final set that was about 2 hours later than the reference mix, and one hour earlier than the mix with the high dose of HRWR. The

mix with the low dose of HRWR and reduced water-cement ratio reached initial set about 30 minutes after the reference mix. Considering that the purpose of HRWR is to increase the workability with less water, it makes sense that these sets were slower than those of the reference mix.
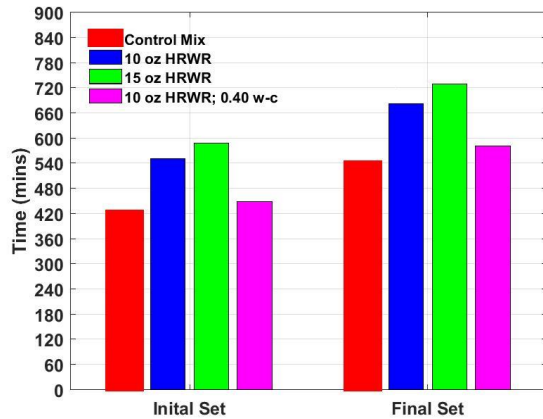


**Figure 4.22 Impact of Set Caused by Addition of High-Range Water Reducer**

The variations in the strength and modulus with time for the three mixes with HRWR are shown in Figure 4.23. The mix with the low dose of HRWR achieved greater strength than the mix with high dose of HRWR at each day of testing. This mix also exhibited higher strengths than that of reference mix (with the exception of the one-day test). On the other hand, the mix with the high dose of HRWR recorded lower strengths and modulus than the reference mix during all three days of testing. Modulus development began slightly sooner than the mixes with HRWR, but also approached the long-term modulus sooner. The mix with the high dosage of HRWR had a similar long-term modulus but went through a faster initial growth due to the delayed start. A similar initial growth was seen by the low dose mix, but this mix saw a longer growth which resulted in a nearly 500 ksi higher modulus than the high dose mix at seven days.
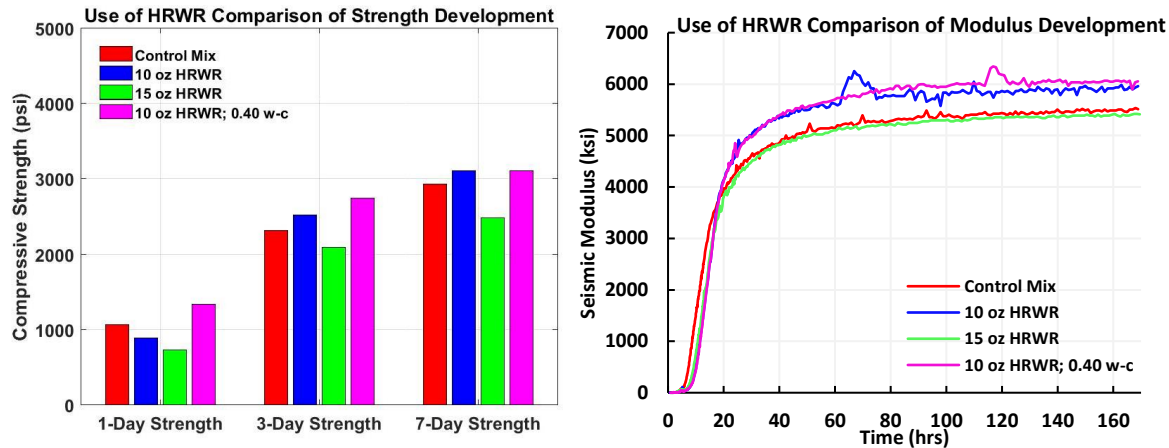
**Figure 4.23 Strength and Modulus Development for Addition of HRWR**

Comparing the characteristics of the mix with the low dose of HRWR with that of the low dose of HRWR/reduced water-cement ratio shows the advantage of reducing water. The strengths were consistently higher for the mix of low dose of HRWR/reduced water-cement ratio. The variations in the modulus with time for the first 40 hours are similar until the mix with the reduced water exhibits a slightly higher modulus than the mix with just HRWR.

Similar to the use of the accelerating agent, the mixes containing HRWR cured under standard curing showed greater as seen in Figure 4.24. Under these conditions, the mix with the low dose of HRWR exhibited a similar strength to the standard mix after 1 day, and nearly 1,000 psi higher strength at three- and seven-days. The mix with the low dose of HRWR and reduced water experienced a further 1,000 psi strength than the mix with the low dose of HRWR at three and seven-days. The mix with the high dose of HRWR achieved a lower strength than the mix with the low dose of HRWR, but higher strength than the reference mix. The moduli measured after standard curing were more consistent between the mixes with the low and high dose of HRWR. The mix with the low dose of HRWR and reduced water-cement ratio exhibited the highest strengths among the four mixes. The differences in the moduli among the mixes diminishes as the specimens cure longer.
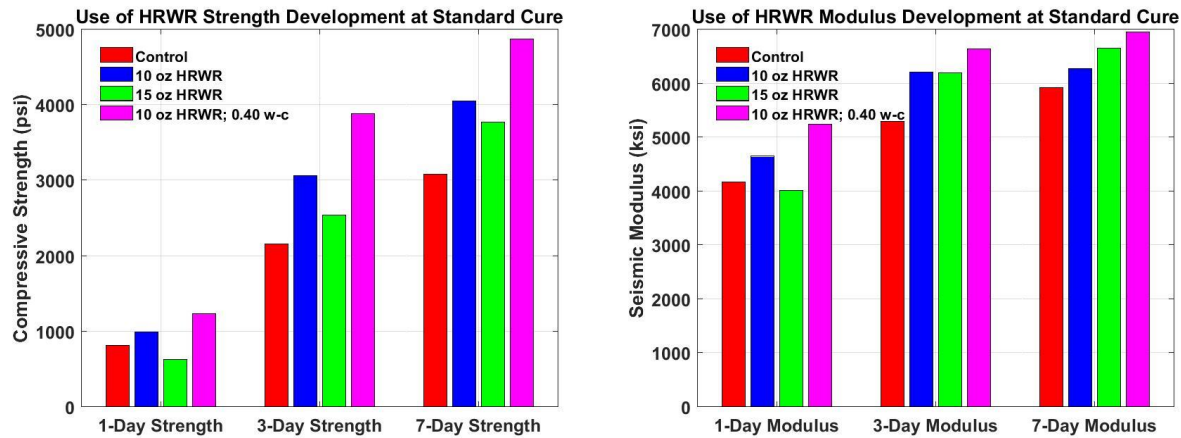
80

**Figure 4.24 Strength and Modulus under Standard Curing with HRWR**

### 4.5.4    Impact of Air Entraining Agent

The impact of an air entraining agent (AEA) on early-age behavior was evaluated using Eucon AEA-92. The impact of the dosage of this admixture was carried out at two levels of the recommended low dosage (0.5 fl oz. per 100 lbs. of cement) and high dosage (4 fl oz. per 100 lbs. of cement). Again the effect of the combination of adding a low dosage of AEA (0.5 fl oz. per 100 lbs. of cement with the reduced water-cement ratio of 0.40) was studied.

Figure 4.25 provides a comparison of times of set among the mixes. The mix with the low dose of AEA achieved times of initial and final set nearly the same as the reference mix, while the mix with the high dose of AEA was nearly an hour slower at reaching the set. The initial set of the mix with the low dose of AEA and reduced water was reached about 30 minutes faster than the mix with the low dose of AEA. Final set was closer to that of the mix with the high dose of AEA.

As shown in Figure 4.26, the strengths and moduli for the mixes with the high and low doses of AEA are very different. The mix with the low dose of AEA yielded strengths that were comparable to the strengths from the reference mix after 3 days of low-humidity curing. The variations in the modulus with time are even more similar for these two mixes (especially after 24 hours).
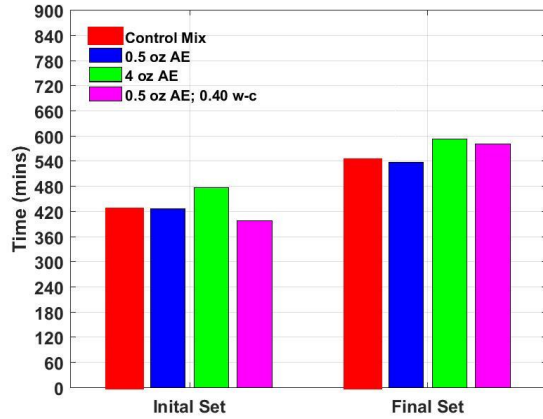
**Figure 4.25 Impact of Set Caused by Addition of an Air Entraining Agent**
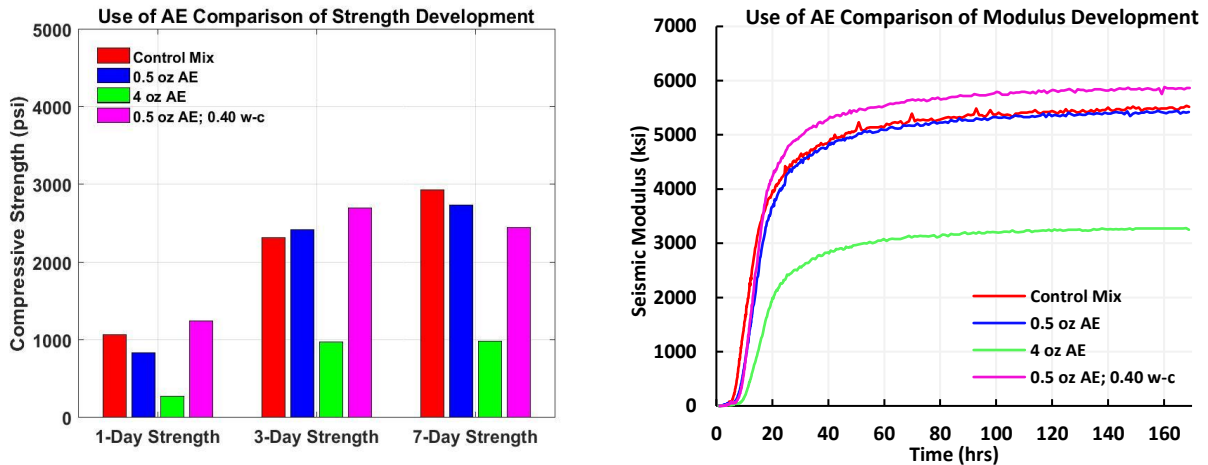


**Figure 4.26 Strength and Modulus Development for Addition of Air Entraining Agent**

Using the high dosage of air entraining agent had a negative impact on both the strength and modulus of the mix. At a high dosage, the strengths of specimens remain below 1,000 psi, even after seven days. Similarly, the modulus development for that mix was severely impaired.

Even under standard curing conditions, the mix with the high dose of AEA was negatively impacted with a seven-day strength of about 1,000 psi and modulus of about 4000 ksi. The mix with the low dose of AEA showed a strength advantage under these conditions, with a slightly lower modulus advantage as compared to the reference mix (see Figure 4.27).
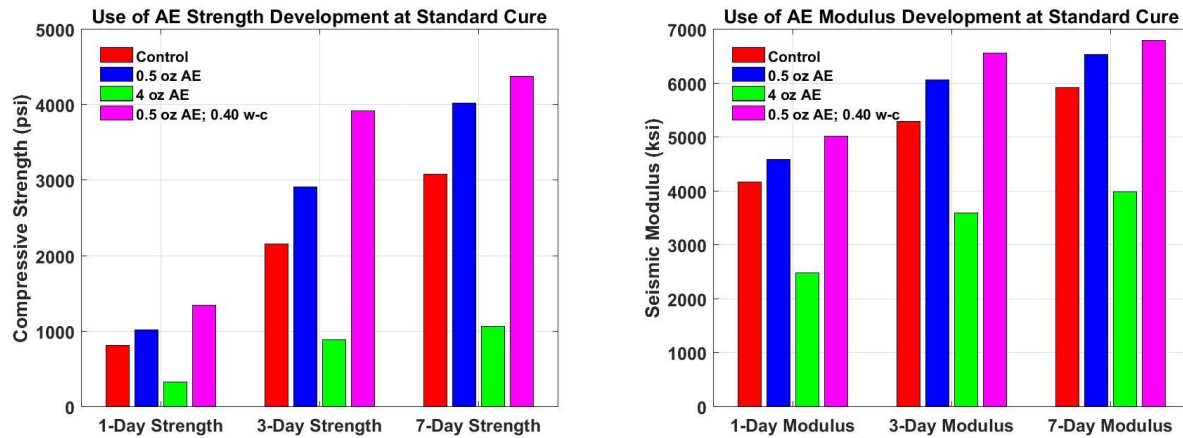
**Figure 4.27 Strength and Modulus under Standard Curing with Air Entraining Agent**

Similar to the other admixtures use, reducing the water-cement ratio was advantageous. The mix with the low dose of AEA and reduced water-cement ratio yielded higher strengths than both the reference mix and the mix with the high dose of AEA during all testing days. Under the low humidity curing, that mix showed a higher modulus that was greater than the mix with the low dose of AEA after 24 hours of curing. Under standard curing conditions, the mix with the high dose of AEA and reduced water-cement ratio exhibited nearly 1,000 ksi higher modulus than the reference mix.

### 4.5.5    Impact of Coarse Aggregate Size and Gradation

To gain an understanding on the impact of the aggregate gradation, two mixes were tested that used just one coarse aggregate in a 60:40 ratio of coarse to fine aggregate. Figure 3.6 displays the change in coarse aggregate gradation of the reference mix and the two single coarse aggregate mixes. Using just the largest coarse aggregate; resulted in a mix with the crushed stone being larger than 0.5 in. The intermediate aggregate contained crushed stone that was between 0.5 and 0.05 in.

As shown in Figure 4.28, as expected, there are no significant impacts on the times of initial or final set due to changes in coarse aggregates. The reason for this is that the mortar mixes used for checking the set using the penetrometer were similar.
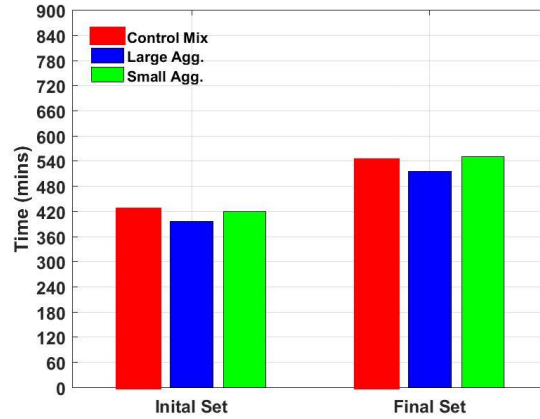
**Figure 4.28 Impact of Set Caused by Change in Coarse Aggregate**

Despite a minimal impact on the measured sets, the strengths and moduli were significantly impacted (as shown in Figure 4.29) at low humidity curing. The mix with the smaller coarse aggregates generally exhibited a higher strength, while the mix with the coarser large aggregates exhibited a higher modulus. The one-day strengths for specimens were very similar for the three mixes. At three and seven days, the reference mix had recorded strengths greater than the large aggregate mix. Modulus development of the three mixes began at approximately the same time, but the large aggregate mix had a longer period of development resulting in over 500 ksi higher modulus at seven days. Results of higher strengths from the small aggregate is the result of fewer voids remaining; thus allowing greater bonding with the cement and increasing interaction amongst aggregates.
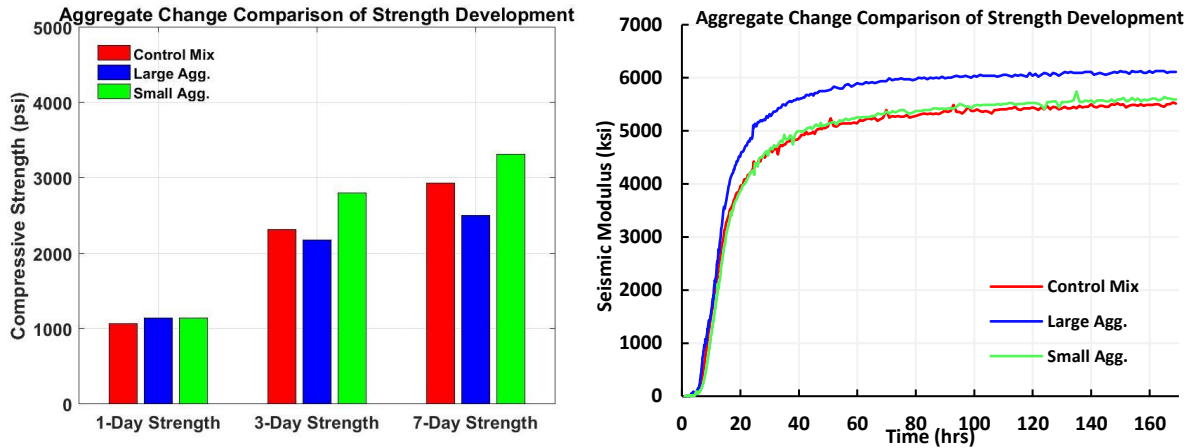
**Figure 4.29 Strength and Modulus Development for Change in Coarse Aggregate**

When cured under standard curing conditions, similar results were observed as seen in Figure 4.30. However, under standard curing the large aggregate mix achieved a higher seven-day strength than both the reference and small aggregate mix. Also observed is the similarity in three-day strengths of the large and small aggregated mixes; these were within 100 psi of each other. This differs from the nearly 1,000 psi, as seen under low humidity curing. Modulus development occurred in much the same manner at low humidity curing. The large aggregate mix was over 500 ksi higher than the small aggregate mix at all three testing days. One difference in modulus development was that the small aggregate mix showed a slightly higher modulus development than seen at low humidity curing. Lower confidence occurs in these observations since only single cylinders were tested under standard curing.
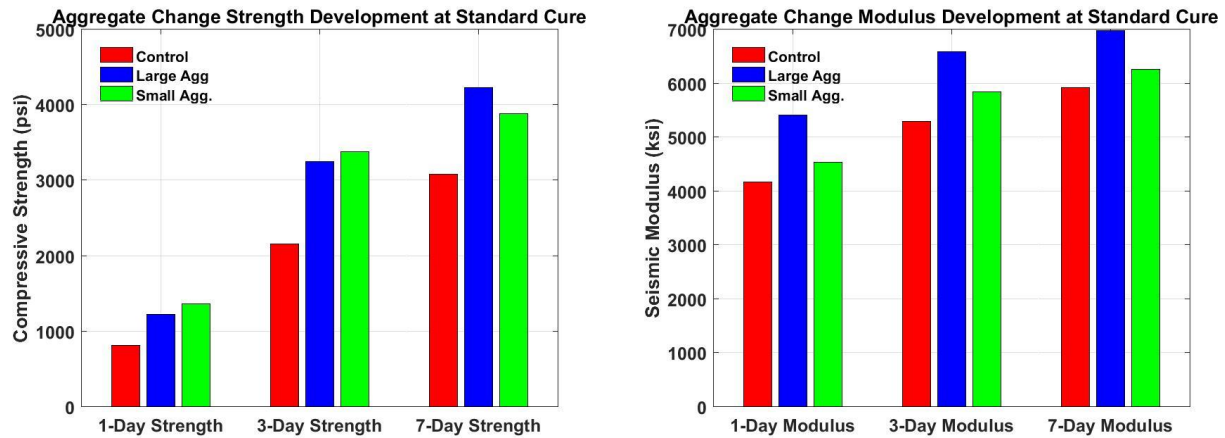
**Figure 4.30 Strength and Modulus under Standard Curing with Aggregate Change**

## 4.6 Comments and Conclusions

Use of the developed testing apparatus yielded reliable seismic modulus readings which were closely in-line with modulus readings obtained using the traditional FFRC method. Both methods showed to be within 11% of another for dolomite and 6% for gravel mix. In addition to this, the modulus-strength relationships for all mixes had similar *k*-coefficient values. The standard maturity-strength relationship on the other hand, showed *m*-coefficients within a certain range based on the curing temperature.

Results obtained from the environmental testing confirmed that curing temperature has a more significant impact on times of set and one-day strength than the humidity. As expected, the higher temperatures caused faster times of initial and final set and also yield higher strength. Regardless of curing temperature, the seismic modulus was shown to approach a similar seven-day value with higher temperatures having a faster development. The impact of humidity was most evident in the low temperature curing. At low temperatures, the penetration resistance showed longer times to reaching either setting conditions. Conversely, the lower humidity had strengths consistently lower by several hundred pounds per square inch.

Mix parameter changes showed that a reduction in water-cement ratio was the only consistent parameter that provided benefits in terms of faster sets, as well as higher strengths and moduli. This was seen when solely the ratio was reduced, and also when implemented in combination with a chemical admixture. Addition of an accelerating agent, only, improved the time of set, with little or no benefit to strength or modulus under the low humidity. This was shown to be independent of the used dosage. Only at standard curing was there a benefit in three- and seven-day strengths, with the greatest occurring when the low dosage was used. Similarly, the greatest benefit on set, strength, and modulus was achieved when the low dosage of HRWR was added under both the standard curing and low-humidity curing. Addition of an air-entraining agent had essentially no impact on set, strength or modulus when used at low dosage, but a severe negative impact on modulus and strength when used at the recommended high dose. Low dosage of this chemical admixture was beneficial to strength under standard curing, but was shown to be detrimental at high dosage. In general, the low quantities of the tested chemical admixtures were more beneficial than a high dosage with benefits being greater under standard curing conditions.

A change in the aggregate gradation and size showed a higher magnitude of modulus growth than when a larger aggregate was used. A higher strength was seen with the small aggregate at low humidity, while similar strengths were observed at standard curing. The small aggregate exhibited very similar modulus development as the reference mix. Smaller aggregates allowed for increased bonding with the cement paste, as well as increased interaction with each other due to smaller voids.

# Chapter 5: Developed Methods

## 5.1    Introduction

This chapter highlights the results of three developed methods. The first item discussed is set determination through a predictive approach based on standard penetration and modulus development. The second item discussed provides a detailed analysis of alternative maturity. The last item discuss the use of thermal profiles as obtained through a thermal camera.

## 5.2    Set Determination

The primary approach to determine times of set of concrete is based on standard penetration resistance method (ASTM C403). Although that method has served the engineering community well, it has some drawbacks. For example, that method determines the set based on using only the mortar mix rather than the actual concrete mix. Aside from being a tedious and time consuming process, the impact of coarse aggregates on the workability of concrete is neglected. An alternative, more objective method for the determination of times of set are described in Chapter 3. The method is based on the continuous monitoring of modulus development of concrete from the onset of pouring to 3 days. The proposed methodology is evaluated in this chapter.

### 5.2.1   Prediction from Penetration Resistance

Determination of set using the penetration resistance method was performed for every mix. Since this method requires a mortar mix, all mortar mixes across the testing matrix remained the same. Figure 5.1 displays the times of initial and final set of the reference mix, large aggregate mix, and small aggregate mix cured at 70°F and 40% humidity. The initial sets for all five tests were within one hour, while the final sets were within 75 minutes of each other. The variability in the sets demonstrates the uncertainty associated with using the penetration method since all mortar mixes were essentially the same.
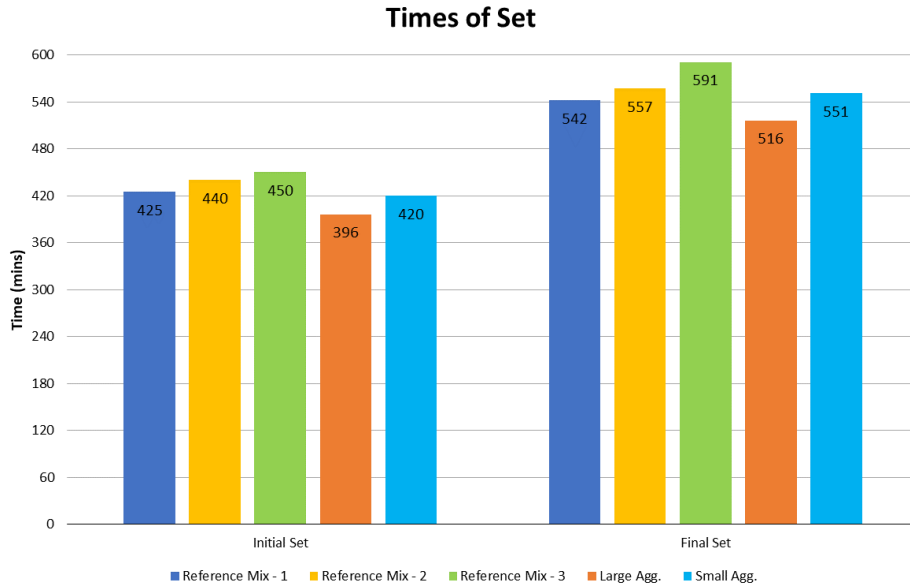
**Figure 5.1 Ranges of Sets based on Penetration Resistance on Similar Mortar Mix**

Referring back to Figure 4.7, which displays the times of set of the six environmental test as well as standard curing, a nearly proportional change was noticed based on changes in temperature and humidity. Using the 70°F curing as the reference, it took about 50% longer for the specimens cured in 50°F temperature to reach their initial and final sets. It took around 25% less time for the specimens in 90°F temperature to achieve these sets. Similarly, slight reduction of times of set were noticed as the humidity decreased while being cured at 70°F. These observations led to the parameters indicated in Table 5.1. These parameters can be multiplied by the initial or final set measured at standard curing condition of 70°F and100% humidity to predict the set under other curing conditions. This is shown in equation 5.1.

$$set_{exp} = set_{SC} * t * h \qquad \text{EQN 5.1}$$

where $set_{SC}$ is the penetration resistance determined time of either initial or final set and $set_{exp}$.is the time of set under the expected curing temperature and humidity. Parameter t, is the value used based on the expected curing temperature while parameter h is used to adjust for the expected humidity conditions.

**Table 5.1 Penetration Resistance Adjustment Factors to Predict Set**

| Temperature (°F) | Parameter *t* | Humidity | Parameter *h* |
|---|---|---|---|
| 90 | 0.75 | 100% | 1 |
| 70 | 1 | 80% | 0.98 |
| 50 | 1.5 | 40% | 0.94 |

Figures 5.2 provides a comparison of the predicted and measured initial sets, while Figure 5.3 compares the final sets. Overall, this approach resulted in predicted sets within 4% of the measured for both environmental changes and mix changes. The greatest differences occurred at 50°F curing, as well as when high-range water reducer added. The use of accelerating agent decreased the times of set, while the high-range water reducer increased the set to times closer to that of the low temperature curing test. The use of an air entraining agent also increased the time of set from the reference mix, but to a lesser degree. Regardless of the type of chemical admixture added, a reduction in the water-cement ratio generally reduced the times of set as compared to the same mix with the higher water content.

Although this predictive approach looks promising a few shortfalls are still present. Aside from neglecting the impact of the coarse aggregates and the level of uncertainty of the measurements, these factors were only verified at curing conditions of 70°F and 40% humidity.
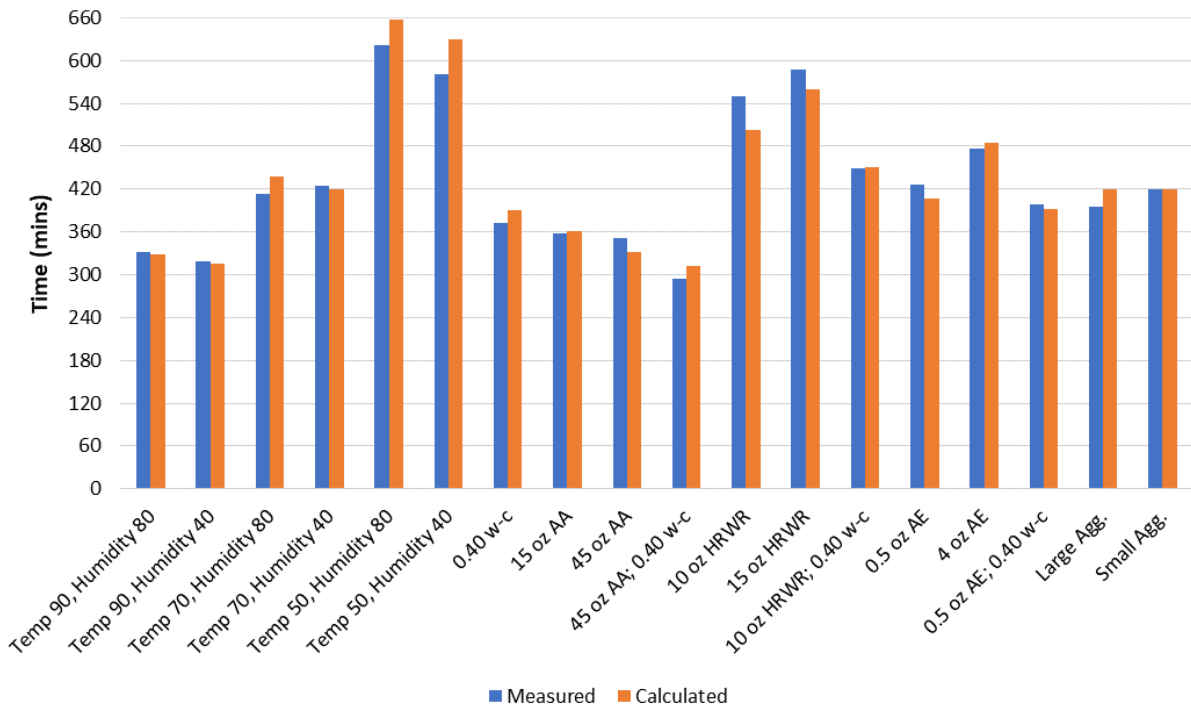
**Figure 5.2 Comparison of Penetration Resistance Predicted Initial Set**
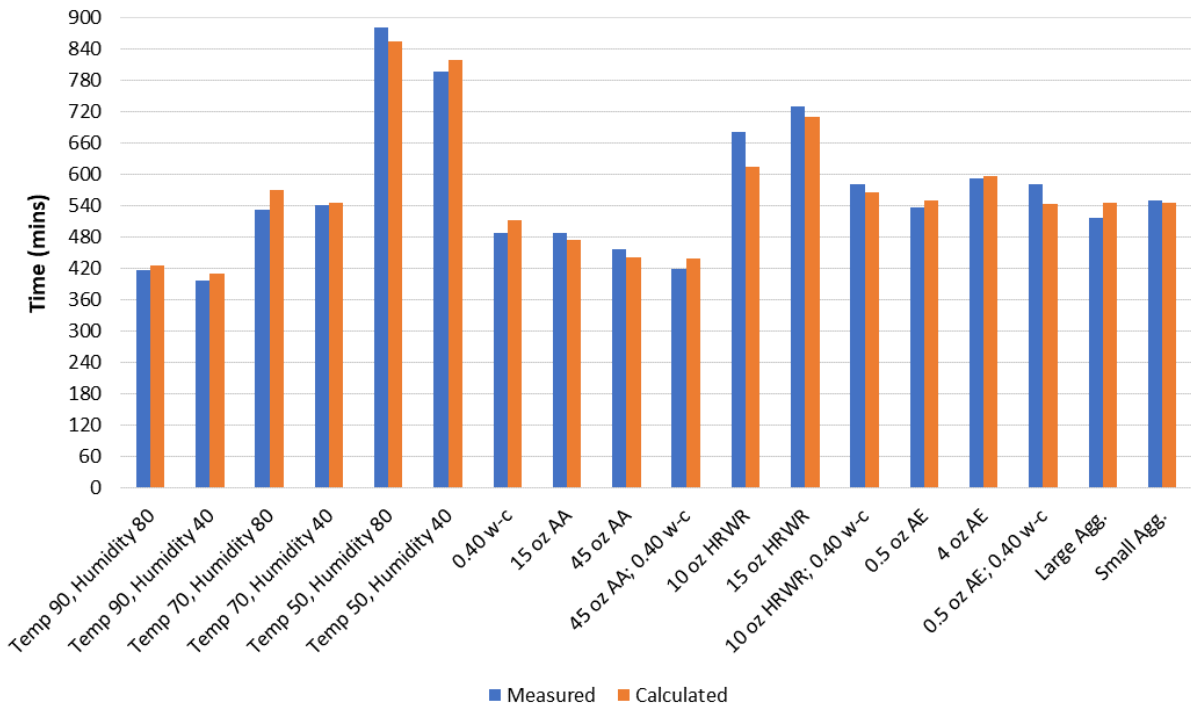


**Figure 5.3 Comparison of Penetration Resistance Predicted Final Set**

91

Figure 5.4 shows the calculated strengths of the reference mix cured at 70°F and 40% humidity using both the modulus-strength relationship and standard maturity-strength relationship (as discussed in Chapter 4). The times of initial and final sets based on penetration resistance are also marked in the figure. The demonstrated case displays the strength calculated from the modulus strength-relationship to initiate rapid growth around the final set, while the strength calculated from the standard maturity-strength relationship initiates at final set. This period of rapid growth at, or after final set, was seen for every mix. This characteristic of the strength value initiating at final set through use the standard maturity-strength relationship was observed in over half of the mixes tested. The mixes that did not follow that trend include: i) the mixes subjected to the high temperature curing, ii) most of the mixes with reduced water-cement ratio, and iii) the mix that used just the large aggregate. Based on these results, the definition that *the final set is the point that the concrete can sustain a load*, is questionable. The calculated strengths from both relationships are under 90 psi at the final set, as determined from the penetration resistance.
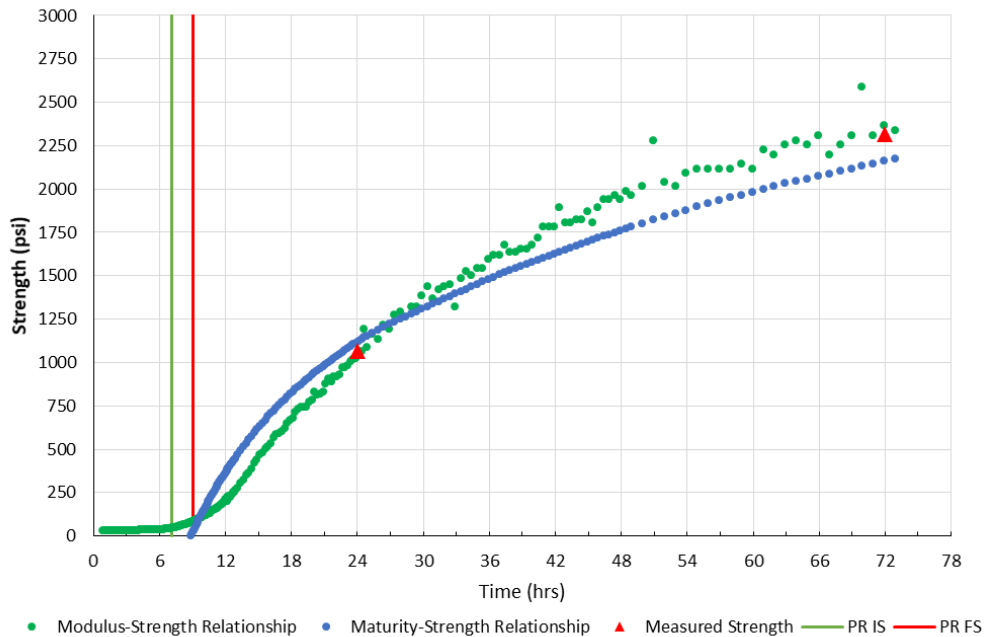


**Figure 5.4 Calculated Strength Compared to Penetration Determined Set**

### 5.2.2 Modulus Approach

The process of estimating the times of initial and final set based on the modulus development was discussed in Section 3.6.1. The modulus growth curve reflects three distinct segments indicating the dormant, setting, and hardening of the specimen.

Table 5.2 displays shape parameters for each of the seismic modulus growth development functions. The shape parameters were summarized in order to obtain coefficients that are representative of the collective data used in equation 3.1.

**Table 5.2 Coefficients and $R^2$ Values from Modulus over Time Equation**

| Material | Mix | *a* | *b* | $R^2$ |
|---|---|---|---|---|
| Gravel | Temp 50 Humidity 40 | 8.4 | 331 | 1.00 |
| | Temp 50 Humidity 80 | 8.5 | 350 | 1.00 |
| | Temp 70 Humidity 40 | 8.7 | 163 | 1.00 |
| | Temp 70 Humidity 80 | 8.7 | 129 | 1.00 |
| | Temp 90 Humidity 40 | 8.6 | 60 | 1.00 |
| | Temp 90 Humidity 80 | 8.6 | 72 | 1.00 |
| Dolomite | Temp 50 Humidity 40 | 8.5 | 257 | 1.00 |
| | Temp 50 Humidity 80 | 8.5 | 229 | 1.00 |
| | Temp 70 Humidity 40 | 8.6 | 124 | 1.00 |
| | Temp 70 Humidity 80 | 8.6 | 139 | 1.00 |
| | Temp 90 Humidity 40 | 8.6 | 65 | 1.00 |
| | Temp 90 Humidity 80 | 8.6 | 88 | 0.99 |
| | 0.40 w-c | 8.7 | 110 | 1.00 |
| | 15 oz. AA | 8.6 | 111 | 1.00 |
| | 45 oz. AA | 8.5 | 113 | 1.00 |
| | 45 oz. AA; 0.40 w-c | 8.6 | 93 | 0.99 |
| | 10 oz. HRWR | 8.7 | 198 | 0.99 |
| | 15 oz. HRWR | 8.6 | 173 | 1.00 |
| | 10 oz. HRWR; 0.40 w-c | 8.7 | 199 | 0.99 |
| | 0.5 oz. AE | 8.6 | 178 | 1.00 |
| | 4 oz. AE | 8.1 | 240 | 1.00 |
| | 0.5 oz. AE; 0.40 w-c | 8.7 | 174 | 0.99 |
| | Large Agg. | 8.7 | 122 | 1.00 |
| | Small Agg. | 8.6 | 151 | 1.00 |

Variable *a,* which is related to the long-term modulus of the mix, is a parameter of high sensitivity. Eq. 5.2 displays the generalized prediction function. Parameter *b* controls the rate of change of modulus development. Variable *b,* related to the rate of modulus development, is indicative of time of set. As *b* increases, the set times increase. It was observed, that as the curing temperature increases, parameter *b* decreases. This translates to a shorter time to reach the long-term modulus.

$$modulus = e^{\left(a-\left(\frac{b}{(time)^2}\right)\right)}$$
EQN 5.2

Trends and consistency were identified for the b-coefficient at various temperatures. The b-coefficient was therefore summarized as representative values of temperature for each evaluated material. The resulting coefficients are listed in Table 5.3.

**Table 5.3 Primary *b*-Coefficients for Modulus Approach**

| Gravel | | Dolomite | |
|---|---|---|---|
| Temperature (°F) | *b*-Coefficient | Temperature (°F) | *b*-Coefficient |
| 50 | 340 | 50 | 243 |
| 70 | 146 | 70 | 131 |
| 90 | 66 | 90 | 76 |

Table 5.4 contains relative changes in parameter *b* due to changes in the mix parameters, where the relative change is defined as the parameter *b* for a given mix divided by coefficient *b* from the standard mix. Since a number less than unity indicates a faster gain in modulus, reducing water-cement ratio, adding accelerating agent will result in a faster set. On the other hand, adding HRWR, air entraining agent retards the set.

**Table 5.4 Parameter *b* and Relative Change due to Mix Changes for Modulus Approach**

| Mix change | Parameter *b* | Relative Change |
|---|---|---|
| Control Mix at 70°F | 131 | 1.00 |
| Reduce w-c ratio from 0.45 to 0.40 | 110 | 0.84 |
| Add low dosage Accelerating Agent | 111 | 0.85 |
| Add high dosage Accelerating Agent | 113 | 0.86 |
| Add accelerating agent and reduce w-c ratio | 93 | 0.71 |
| Add low dosage of HRWR | 198 | 1.51 |
| Add high dosage of HRWR | 173 | 1.32 |
| Add low dosage of HRWR and reduce w-c ratio | 199 | 1.52 |
| Add low dosage of air entraining agent | 177 | 1.35 |
| Add high dosage of air entraining agent | 240 | 1.83 |
| Add low dosage of air entrain agent and reduce w-c ratio | 173 | 1.32 |
| Use large aggregate | 122 | 0.93 |
| Use small aggregate | 151 | 1.15 |

### 5.2.3   Hybrid Maturity-Modulus Approach

Using the equation discussed in section 3.6.2 and a similar methodology as the time-based modulus approach, sets were determined using the standard maturity-based modulus. However, this approach provided points of initial and final set as the standard time-temperature factor. By reviewing the collected raw data for these points the approximate time of sets could be determined. Table 5.5 contains the three coefficients needed to model the recorded data using equation 3.2.

**Table 5.5 Coefficients and $R^2$ Values from Modulus over Standard Maturity Equation**

| Mix | c | d | f | $R^2$ |
|---|---|---|---|---|
| Temp 50 Humidity 40 | 5002.39 | 421.97 | 3.12 | 1.00 |
| Temp 50 Humidity 80 | 4856.59 | 391.74 | 2.86 | 1.00 |
| Temp 70 Humidity 40 | 5135.38 | 492.11 | 2.76 | 1.00 |
| Temp 70 Humidity 80 | 5365.61 | 500.87 | 2.94 | 0.99 |
| Temp 90 Humidity 40 | 5330.41 | 450.89 | 2.39 | 0.99 |
| Temp 90 Humidity 80 | 5377.71 | 491.42 | 2.60 | 1.00 |
| 0.40 w-c | 5425.56 | 450.17 | 2.84 | 1.00 |
| 15 oz. AA | 5134.93 | 473.59 | 2.54 | 1.00 |
| 45 oz. AA | 5091.94 | 529.98 | 2.43 | 1.00 |
| 45 oz. AA; 0.40 w-c | 5769.15 | 449.13 | 2.14 | 1.00 |
| 10 oz. HRWR | 5608.22 | 565.80 | 3.83 | 1.00 |
| 15 oz. HRWR | 5023.15 | 521.43 | 3.31 | 1.00 |
| 10 oz. HRWR; 0.40 w-c | 5565.65 | 538.66 | 3.82 | 1.00 |
| 0.5 oz. AE | 5047.52 | 563.17 | 3.29 | 1.00 |
| 4 oz. AE | 3012.00 | 641.07 | 3.75 | 1.00 |
| 0.5 oz. AE; 0.40 w-c | 5425.13 | 503.52 | 3.63 | 1.00 |
| Large Agg. | 5867.83 | 474.28 | 2.76 | 1.00 |
| Small Agg. | 5188.18 | 524.38 | 3.06 | 1.00 |

Using the standard maturity-based modulus approach as a predictive model to determine set required a similar approach as the time-based method. The original equation used to model the recorded data had three unique coefficients for each mix. However, the $f$ coefficient turned out to be within a narrow range of values; thus enabling its replacement with a constant of 3.1:

$$modulus = \frac{c}{1+(d/_{TTF})^{3.1}} \qquad \text{EQN 5.3}$$

Like above, the primary $c$- and $d$-coefficients were based on curing temperature and are shown in Table 5.6. As temperature increased, the value of each coefficient increased, however not in proportional increments. Larger increases occurred from 50°F to 70°F than from 70°F to 90°F. A unique adjustment factor was needed for each coefficient to obtain values similar to the recorded coefficients. This factors were not consistently increasing or decreasing the values of the primary coefficients, as can be seen in Table 5.7.

**Table 5.6 Primary *c*- and *d*-Coefficients for Hybrid Maturity-Modulus Approach**

| Temperature (°F) | *c*-Coefficient | *d*-Coefficient |
|---|---|---|
| 50 | 4930 | 405 |
| 70 | 5250 | 495 |
| 90 | 5350 | 500 |

Table 5.7 displays the relative changes in both the *c* and *d* parameters due to adjustments in the mix parameters. The relative change is defined in the same manner as discussed for Table 5.4. A relative change of the *c* parameter indicates a higher modulus. This is verified when reviewing results from the previous chapter, where it was observed that every mix that had a lower water-cement ratio also possessed a higher modulus. Though not as definitive as the modulus approach, a relative change in *d* parameter less than unity generally indicates a faster gain in modulus and indicates a faster set. Reducing water-cement ratio, adding accelerating agent, and the large aggregate mix showed faster initial sets in this scenario. However, final set of these same mixes was not always faster. The reason for less definitive conclusions concerning the unity of the *d* parameter is the result of reducing the two coefficients affecting the modulus growth to a constant and a parameter.

**Table 5.7 Parameters and Relative Change due to Mix Changes for Hybrid Maturity-Modulus Approach**

| Mix change | Parameter $c$ | Relative Change | Parameter $d$ | Relative Change |
|---|---|---|---|---|
| Control Mix at 70°F | 5250 | 1.00 | 495 | 1.00 |
| Reduce w-c ratio from 0.45 to 0.40 | 5407.5 | 1.03 | 450.45 | 0.91 |
| Add low dosage Accelerating Agent | 5145.0 | 0.98 | 475.20 | 0.96 |
| Add high dosage Accelerating Agent | 5092.5 | 0.97 | 534.6 | 1.08 |
| Add accelerating agent and reduce w-c ratio | 5775.0 | 1.1 | 450.45 | 0.91 |
| Add low dosage of HRWR | 5617.5 | 1.07 | 564.30 | 1.14 |
| Add high dosage of HRWR | 5040.0 | 0.96 | 5193.75 | 1.05 |
| Add low dosage of HRWR and reduce w-c ratio | 5565.0 | 1.06 | 539.55 | 1.09 |
| Add low dosage of air entraining agent | 5040.0 | 0.96 | 564.30 | 1.14 |
| Add high dosage of air entraining agent | 2992.5 | 0.57 | 643.50 | 1.3 |
| Add low dosage of air entrain agent and reduce w-c ratio | 5407.5 | 1.03 | 504.90 | 1.02 |
| Use large aggregate | 5880.0 | 1.12 | 475.20 | 0.96 |
| Use small aggregate | 5197.5 | 0.99 | 527.70 | 1.06 |

By defining the hybrid maturity-modulus sets as time, instead of standard TTF, a comparison can be made with the modulus method.

### 5.2.4 Comparison of Approaches

The times of initial set found from the standard method, time-based method, and hybrid method are compared in Figure 5.8 for environmental changes and Figure 5.9 for mix changes. The variance was generally within 3 hours depending on the method and mix being tested. Low temperature testing, mixes with high-range water reducer, and the high quantity of air entraining agent showed the greatest variance. A large variance in the mix with the high dose of air entraining agent was expected because of the significantly lower modulus achieved. Comparing just the modulus defined approaches showed even greater similarity with the time-based approach; indicating a slower initial set. The standard maturity method generally indicated quicker times of initial set, while the penetration resistance method indicated longer set times. Mixes with air

entraining agent added, and mixes with HRWR and a reduced water-cement ratio where the only

mixes that the standard method indicated a faster initial set than both modulus-based methods.
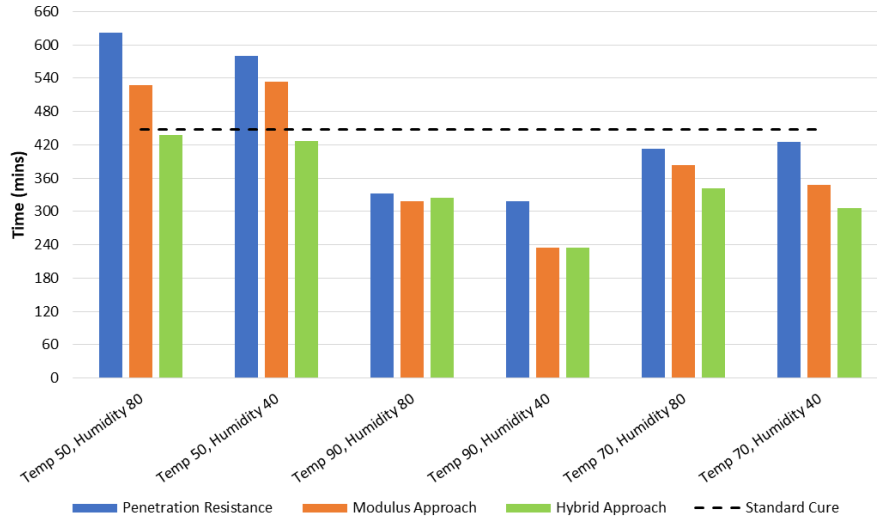


**Figure 5.8 Comparison of Initial Set across Environmental Changes**
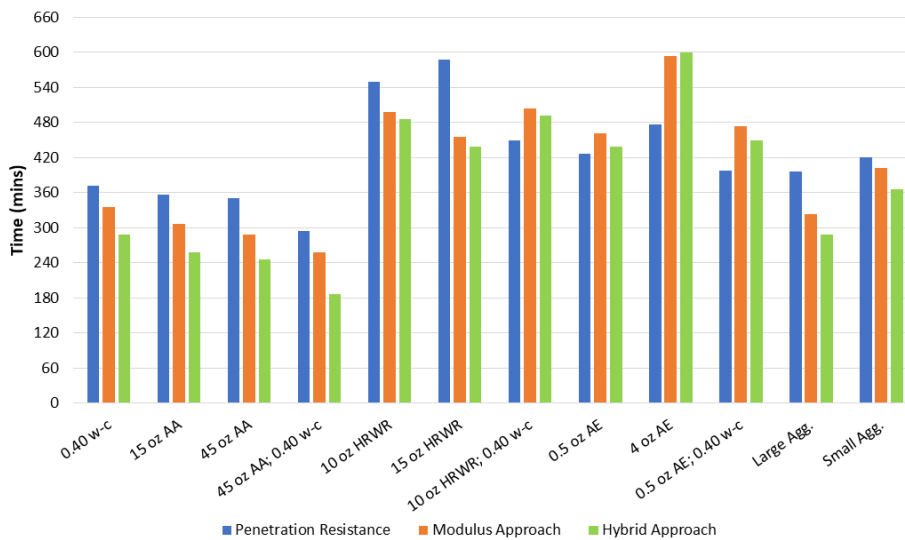


**Figure 5.9 Comparison of Initial Set across Mix Changes**

The final set comparisons considering the environmental variants are shown in Figure 5.10.

Figure 5.11 displays final set comparisons considering the mix-related parameter variants. Final

set between the two modulus defined methods, though significantly different from the standard

method, yielded times within two-hours of each other. The penetration resistance method times of

final set generally occurred in half the time as the two modulus-based methods. The modulus method showed final set was attained faster than the hybrid method for every mix, except those cured at 90°F. The similarity in the determined initial set, as well as final set, using the two modulus-based methods provides further evidence that defining set based on the modulus of concrete is a feasible non-destructive method.
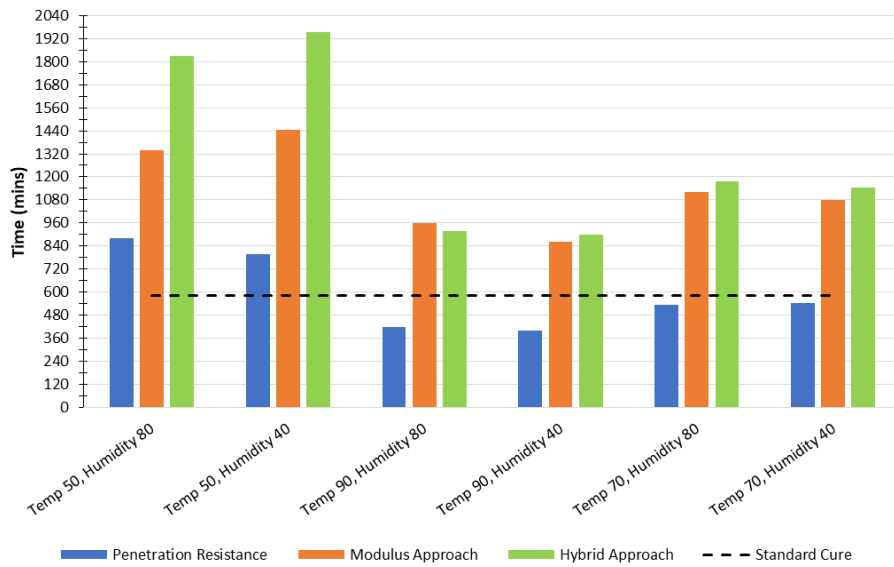


**Figure 5.10 Comparison of Final Set across Environmental Changes**
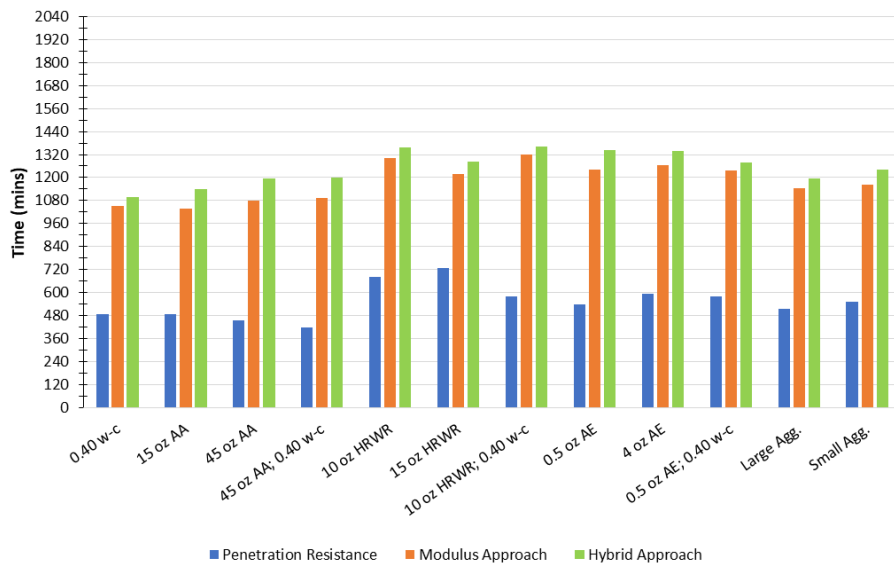


**Figure 5.11 Comparison of Final Set across Mix Changes**

The need to redefine final set so it is based on a measured concrete property is seen in Figure 5.12. Strengths calculated from the recorded data, using the modulus-strength and standard maturity-strength relationships are shown as similarly expressed in Figure 5.4. However, the time of final set is shown based on both the modulus and hybrid methods, rather than penetration determined final set. In this figure, both methods show calculated strengths closer to 750 psi, compared to less than 100 psi seen in Figure 5.4. This is a more reasonable strength for final set, as per definition.
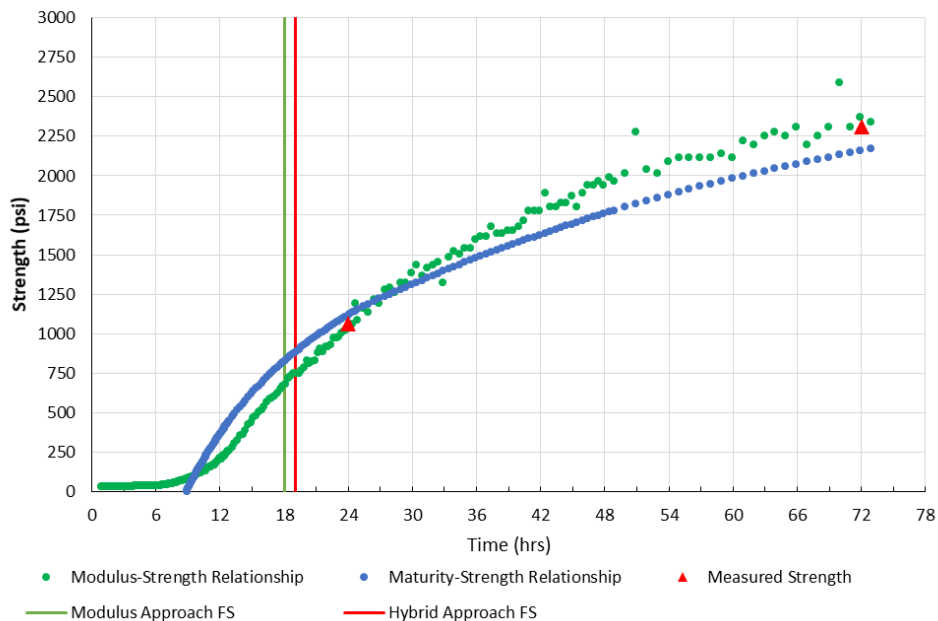


**Figure 5.12 Calculated Strength Compared to Modulus Determined Set**

This supports the need to define initial set as the point of rapid modulus development; corresponding to stiffening of the cement paste and loss of workability. Whereas the definition of final set could be the point of cessation of modulus growth caused by culmination of primary hydration.

### 5.3 Alternative Maturity

The conventional method for quantifying heat production during the concrete hydration and curing process is to develop and assess standard maturity plots. Standard maturity is performed in a controlled laboratory setting. While standard maturity employs a datum temperature, commonly taken as 14°F or 32°F, the integration of the time-temperature curve usually yields a piece-wise type of linear function, with changes in slope corresponding to significant variations in internal temperature. While standard maturity has traditionally held useful utility in assessing heat production during the hydration process, this data visualization method presents limitations in interpretation. The subtle change in slopes can be difficult to interpret in a graphical method, for practical purposes. Alternative maturity employs the ambient air temperature as the datum temperature, as opposed to the constant datum temperature associated with standard maturity. As discussed, alternative maturity method was described in Chapter 3. For further demonstration, the alternative maturity visualization method is displayed in Figure 5.13.
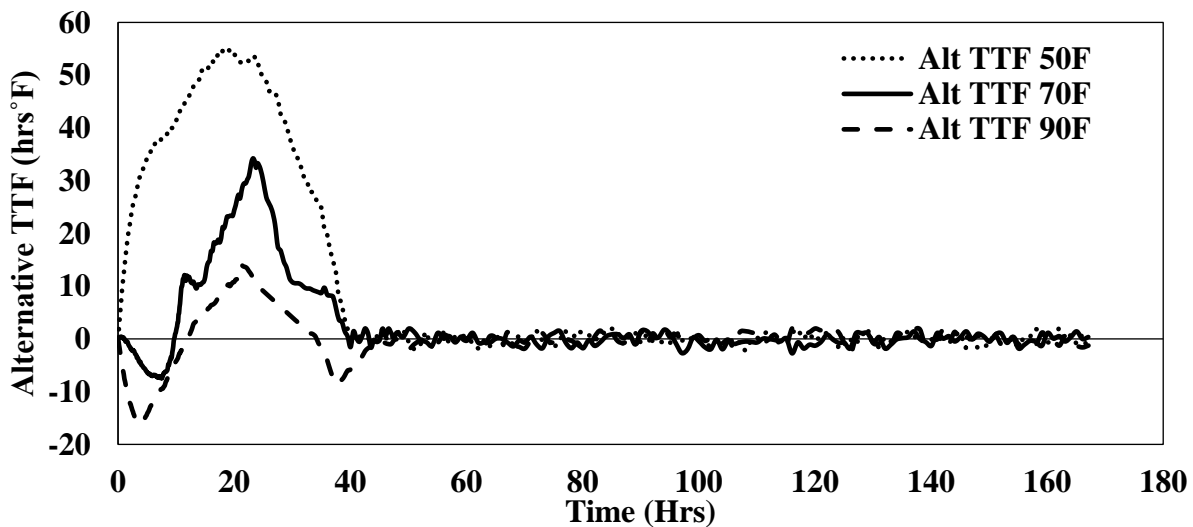


**Figure 5.13 Alternative Maturity of Concrete Concept (40% Humidity, Gravel Mix)**

To expand the discussion to the temperatures significantly warmer or cooler than 70°F, the alternative TTF curves from these two temperatures are expanded up to a time of 60 hours in

Figure 5.14. The corresponding times of initial and final sets as determined using the modulus approach are also included in the figure. For the specimen cured in a higher ambient temperature, the time of initial set is about 3 hrs. before the minima of the alternative TTF curve, while the final set is roughly half way to the maxima of the alternative TTF curve. The initial set for the specimen cured at a cooler ambient temperature occurs around the transition point of the alternative TTF curve. This trend also shows the final set occurring closer to the maximum peak. Since by definition, the modulus-based initial set corresponds to the time when the specimen starts to transition from liquid to solid, the arrows associated with the initial sets may point to the time when the generation of the heat of hydration becomes significant. Before the modulus-based initial set, the alternative TTF is primarily dominated by the heat transfer between the specimen and ambient temperatures.
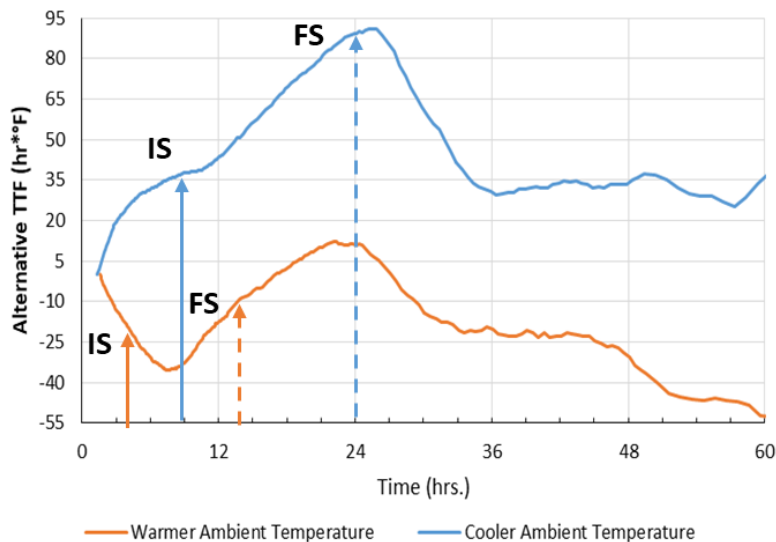


**Figure 5.14 Alternative TTF Trends and Times of Set**

Based on the discussion above, it would be desirable to subtract the heat transfer between the specimen and ambient condition, to better relate the gain in strength to the heat of hydration. From Figure 5.14, the specimen cured in the warmer ambient temperature was cured at 90°F. Not only there was a temperature difference between the mixing and curing, there was also an

approximate 1.5 hr. gap from start of mixing until start of testing, which recorded the specimen temperature at about 79°F. Likewise, the specimen cured in the cooler ambient temperature was cured at 50°F, but prepared at 70°F and had a 1.3 hr. gap until the first specimen temperature reading of 69°F. By removing the heat transfer between the specimens and curing environment, the heat of hydration can be isolated and will theoretically indicate time of initial set.

Previous studies on early-age heat in concrete either focused on the heat evolution with regard to cracking or as a way to model heat of hydration based on equivalent age maturity (Ballim and Graham 2004; Schindler and Folliard 2005). Schindler and Folliard (2005) determined that the heat of hydration is affected by the composition of cement, amount of cement, and water to cement ratio and that the specific heat capacity of the concrete changes over time. Further, Khan (2002), showed the difference in thermal conductivity of the aggregates based on type and moisture content. Other studies (e.g., Bentz 2008; Lee et al. 2009; Guo et al. 2011) have found that thermal conductivity and heat transfer coefficients change throughout the hydration process and are affected by wind velocity, curing conditions, and evaporation. Generally, thermal conductivity is affected to a greater extent by concrete constituent properties, while heat transfer variations primarily occurred due to the environmental curing conditions. As such, the precise determination of heat transfer becomes more difficult, since these parameters are not normally measured. Despite these complications, a simple heat transfer model was developed assuming representative values for the thermal conductivity, $k$, and heat transfer coefficient, $h$ of the concrete mix.

A simple steady-state heat transfer model was developed to determine the heat energy usage, $s_{rxn}$, at each time step. Expressed as BTU/hr., the heat energy use per hour was found using;

$$s_{rxn} = \frac{T_{cyl} - T_{amb}}{\frac{r^2}{4k} + \frac{r}{2h}} * V_{cyl} \qquad\qquad \text{EQN 4.5}$$

where $T_{cyl}$ = temperature of cylinder in °F, $T_{amb}$ = ambient temperature in °F, $V_{cyl}$ =volume of the cylinder and $r$ = radius of the specimen. A value of 0.35 BTU/hr./(ft.*°F) was used for the thermal conductivity, ("Thermal Conductivity of Common Materials and Gases" 2003), while 3.5 BTU/hr./(ft$^2$*°F) was used for the heat transfer coefficient (Lee et al. 2009). Since both properties vary based on numerous factors, the selected values were selected based on conditions that closely represented the testing process used in this research

The heat energy time history was estimated by calculating the heat energy usage at each time step, as depicted in Figure 5.15. The heat energy and internal temperature trends shown in Figure 4.2 are similar. For the specimen cured in a warmer ambient temperature, the local minima corresponds closely to a neutral heat energy as seen in Figure 5.15. This neutral heat energy also corresponds to the transitions point of the specimen cured at a cooler ambient temperature.
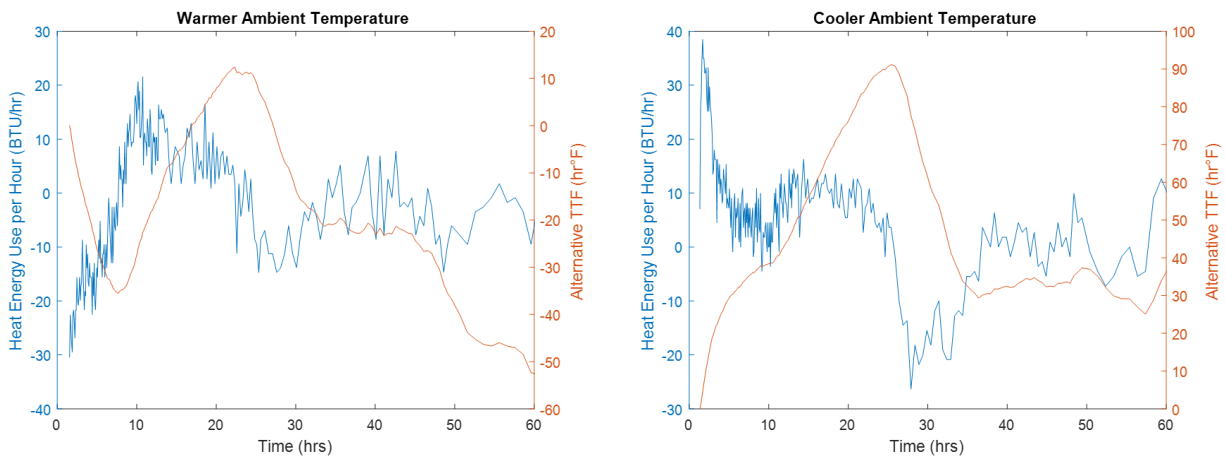


**Figure 5.15 Heat Energy Use and Alternative TTF Trends**

The numerical integration of the heat energy time histories in Figure 5.15 are compared with the corresponding alternative TTF curves in Figure 5.16. The two curves follow similar trends but shifted by a factor of approximately two for the specimen subjected to the warmer curing and approximately 2.5 for the specimen subjected to cooler curing. This similarity indicates that the

alternative TTF is the equivalent of a quasi-steady state heat transfer analysis, assuming the rate of heat production is constant.
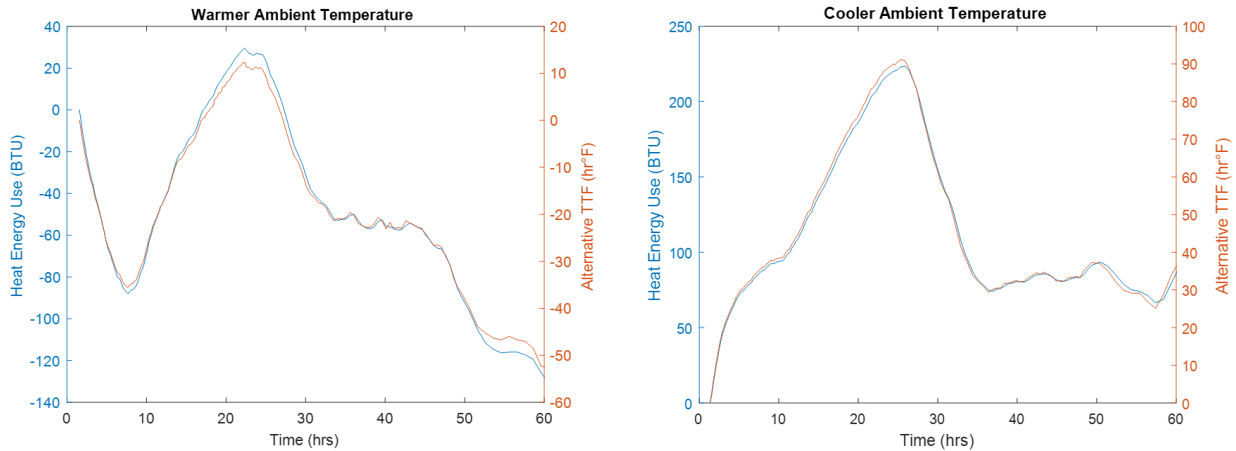


**Figure 5.16 Heat Energy Use and Alternative TTF Trends**

Figure 5.17 depicts a theorized alternative TTF for the two ambient temperatures based on two assumptions. First, it assumes that no heat transfer occurs and a temperature difference only begins once hydration starts. This assumption is based on the corresponding times of neutral heat energy usage corresponding to the transition point and local minima indicted in Figure 5.15. No heat production occurring past 36 hours, resulting in the specimen having the same temperature as the ambient, is the second assumption made. As depicted, the alternative TTF for both curing conditions become normalized with the growth indicating the start of hydration and initial set. The positive slope would indicate the rate of hydration while the negative slope would indicate the rate of equilibrating to the ambient temperature once hydration ceases. Additionally, the similarity in maximum alternative TTF is expected in this normalized model since maximum internal temperatures were consistently around 110% of the curing temperature as noted in Section 4.1.
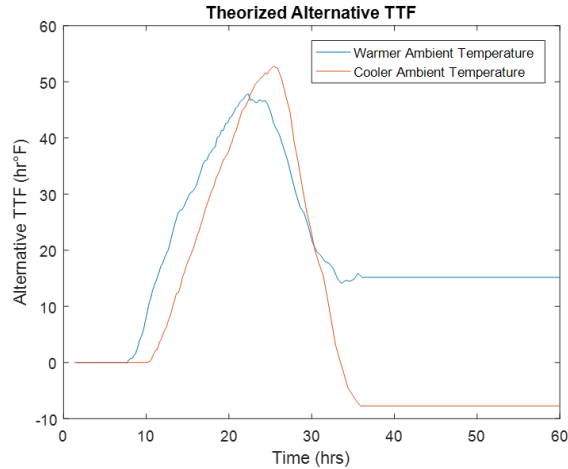
**Figure 5.17 Theorized Alternative TTF Trends**

The use of this alternative TTF provides the potential to monitor hydration of concrete regardless of curing temperature and determine the time of initial set using minimal equipment. It can also be used as a method to conduct a rudimentary heat transfer analysis. A more precise model would be possible if heat transfer and heat of hydration can be isolated.

## 5.4    Thermal Profile

As discussed in Section 3.4, a thermal camera was used to obtain simultaneous images of the triplicate specimens. For the most part, the full area of each cylinder was imaged, except in some occasions when small parts of the outer cylinders were cut off. Similar to the seismic and maturity methods, all three cylinders yielded similar profiles as seen in Figure 5.18, using the color codes discussed in section 3.4.

(a) Cylinder 1

(b) Cylinder 2

(c) Cylinder 3
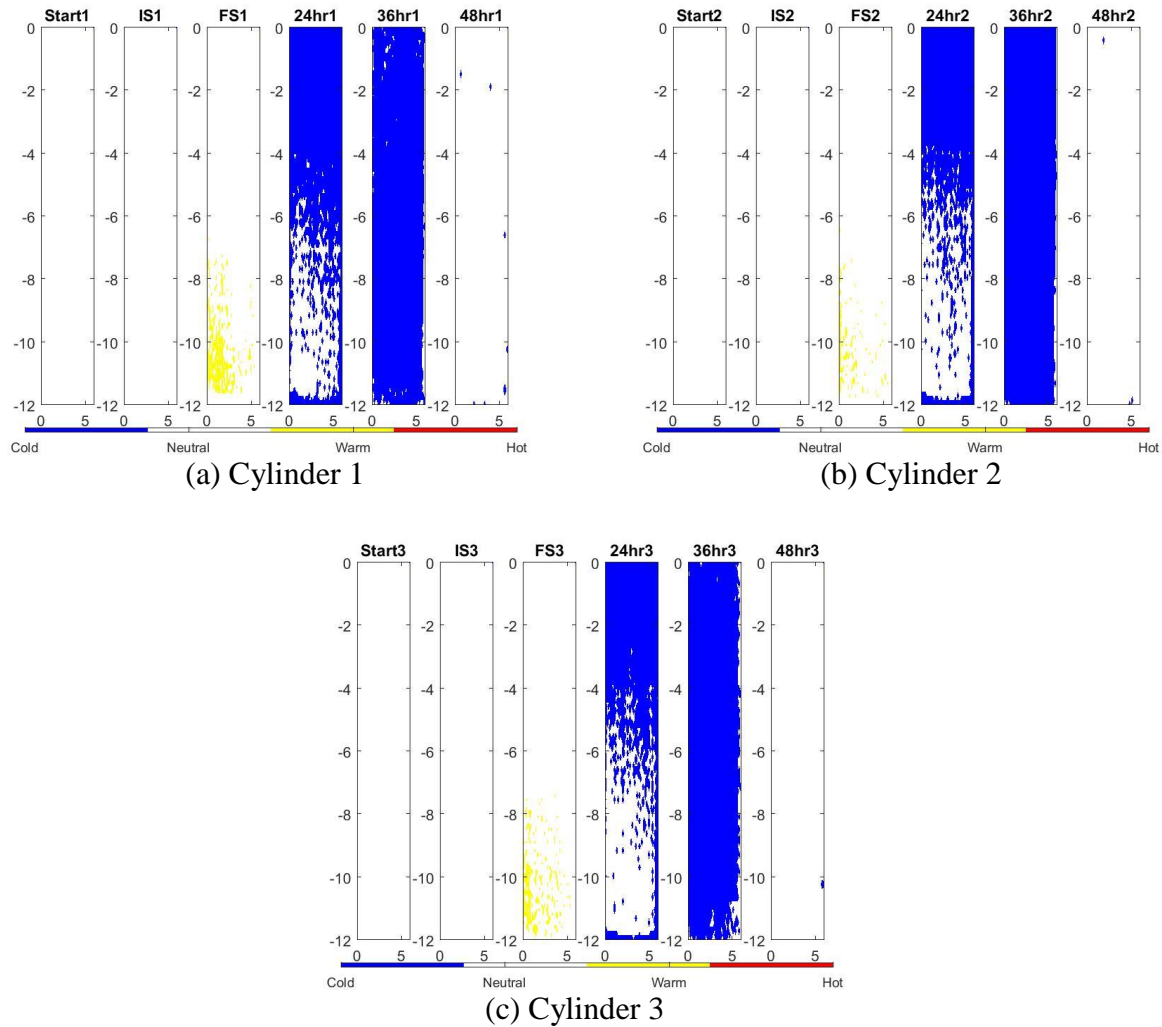
**Figure 5.18 Thermal Profile for Reference Mix at 70°F and 40% Humidity**

The header above each profile indicates the time when the image was captured. Start corresponds to the first image captured, IS corresponds to the image at the initial set and FS corresponds to the image at the final set using the traditional method. The last three images correspond to the temperature profile at 24 hrs., 36 hrs., and 48 hrs. from the initial water-cement contact. The images from the center cylinder for each mix are shown in Appendix C. Generally, the modulus approach yielded warmer images at IS and FS as compared to the standard approach. The hybrid approach profiles are not shown because of the similarities with the modulus-based

results. Generally, the images at 36 hrs. and 48 hrs. ages are close to or cooler than the ambient temperature.

Figure 5.19 compares the variations in the internal temperature recorded with the thermocouple with the minimum, maximum, and average temperature of the surface of the specimen captured with the thermal camera of a specimen cured at 70°F and 40% humidity without the mold removed. The internal temperatures are typically within 3°F of the average temperature recorded by the camera with both having the same general trend. From approximately 9 hrs. to 18 hrs. age, the average surface temperature readings show the greatest difference from the internal temperatures. This time period corresponds with the time that the specimen is in the setting phase and indicates that heat generation is more prominent at the center.

Referring back to Figure 4.14, a temperature drop commonly seen around 24 hrs. was not as large in the specimen that did not have the mold removed. A similar effect is seen in Figures 5.20 and 5.21. This data displays the thermal profiles of the reference mix cured at 70°F and 40% humidity with the mold removed after one day, as well as without the mold removal. The specimen retained in the mold has a consistent profile at 24 hrs., 36 hrs., and 48 hrs. The temperature profiles of the specimen demolded undergoes a drop in temperature at 24 hrs. and 36-hrs. Review of the raw data recorded by the thermal camera showed that the average temperature of the demolded specimen is about 65°F at 24 hrs. and 36 hrs., while the average temperature of the specimen retained in the mold are around 68°F at 24 hrs. and 72°F at 36 hrs. Comparison of these profiles, internal temperature readings, and alternative maturity indicate that the mold acts as a barrier that holds heat and moisture within the system. Maintaining the heat and moisture in the system encourages accelerated hydration that results in higher strength and modulus (as discussed in

Section 4.4.3). Once the mold was removed, the evaporation of moisture causes a reduction in the internal and surface temperatures of the specimen, resulting in a reduced rate of hydration.
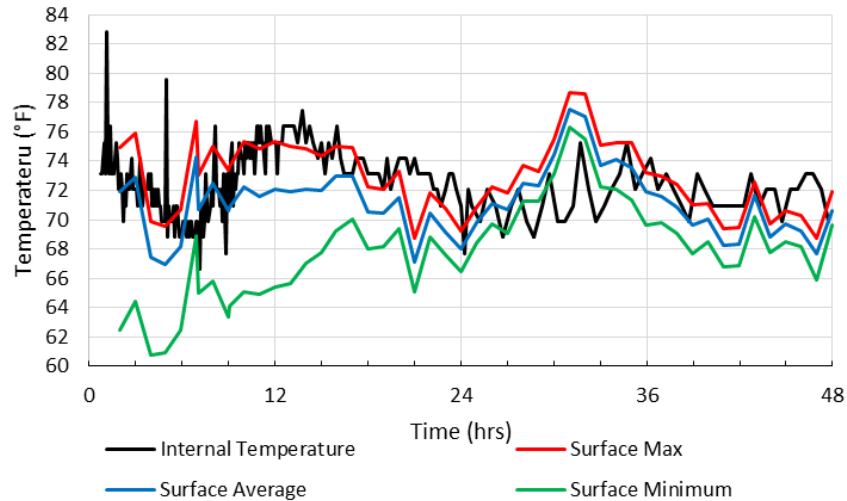


**Figure 5.19 Comparison of Internal and Surface Temperatures of Specimen without the Mold Removed**

The infrared camera showed that specimens from the same mix and under the same curing conditions undergo similar heat dissipation. Additionally, the surface temperatures recorded by the camera were similar to the internal temperature recorded by the thermocouple. The temperature profiles indicate that initially the bottom of the specimen is warmer and that heat dissipates. Additionally, the Start, IS, and FS profiles generally appear cooler at the top. This is expected since the mold does not cover the top, thus allowing unimpeded heat transfer out of the system. From all of the mixes monitored, there was no noticeable profile or behavior indicating initial or final set.
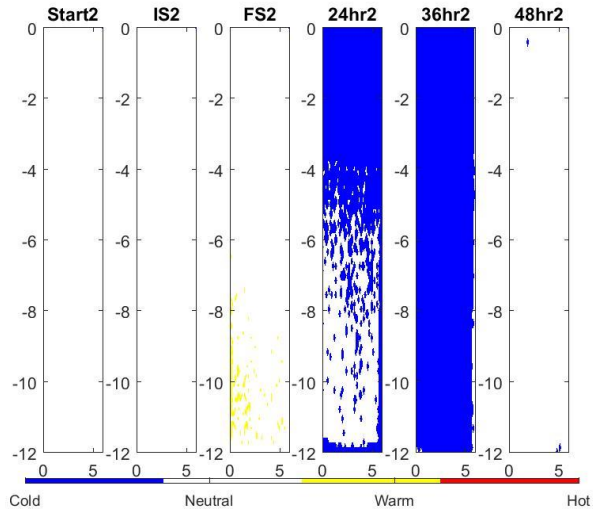
**Figure 5.20 Thermal Profile with Mold Removed After 24 Hours**
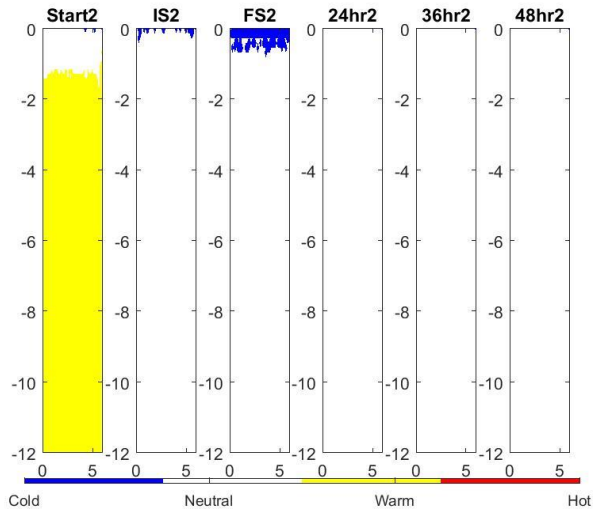


**Figure 5.21 Thermal Profile without the Mold Removed**

## 5.5    Comments and Conclusions

Applying some adjustment factors to the set measured at standard cured, times of set of the same mix were predicted under other curing conditions. Good confidence was seen across the six environmental conditions as well as the 12 mix changes. Although this is method provided predictions of set with good confidence, it still has the shortfalls of only using a mortar mix to determine set, completely ignoring the coarse aggregates.

Dividing the modulus growth into dormant, setting, and hardening segments provided a method to determine set in terms of either time or standard TTF based off the entire concrete mix. The first approach used the modulus growth over time while the hybrid method used the modulus over standard maturity to determine the standard TTF at times of initial and final set. Results from both approaches showed similar times of initial set compared to the standard method. The hybrid method generally determined an earlier initial set and later final set compared to the modulus approach. The difference between the methods was generally within two hours. When extrapolating the specimen strengths using the determined strength relationships these approaches indicated strengths at final set of over 600 psi versus the penetration resistance method which indicated strengths of under 100 psi, indicating the need for redefinition of set.

The introduction of an alternative method to measure maturity in terms of a time-temperature factor provided a unique trend when plotted over time versus a linear trend seen with the standard TTF over time. This approach changed the datum temperature from a constant temperature to the instantaneous ambient temperature to provide an indication of the effect of ambient temperature on the maturity of the concrete. Continued focus on this method may provide another method to determine set based on curve changes identified in the plots. This method may also provide a way to track the heat transfer in the cylinder to pin-point the time that hydration begins to generate heat.

Thermal imaging provided a means to create a thermal profile of a concrete specimen at distinct times during curing. Results indicated essentially no heat generation beyond 36 hours as well as similar trends between internal and surface temperatures. Although it was thought that a unique profile would be evident at time of initial or final set no such indication was seen. It did show a profile at final set that was generally warmer compared to the penetration method.

# Chapter 6: Conclusions and Recommendations

## 6.1     Review of Testing Approach

The goals of this study consist of i) modelling the early age strength and modulus development of concrete more accurately and ii) determining the initial and final setting times in more systematic manner. There are some shortfalls associated with using the traditional penetration resistance for defining the set. For example, that approach does not account for the coarse aggregate effect on the set. On the other hand, concrete set defined based on modulus provides several advantages. First, it takes into account the inclusion of large aggregates. Another advantage is the ability to not only develop a systematic process to predict times of set, but also to develop a relationship between the strength and modulus for more mechanistic approach to estimating the time for saw cutting and premature cracking of the concrete.

This research project developed a nondestructive method for observing the early-age strength and modulus development of concrete mixes over seven days in a controlled, laboratory setting. An apparatus was designed and built for continuous acquisition of seismic modulus data (using free-free resonant column) and heat of hydration/ maturity information (derived from ambient air temperature and specimen internal temperature). The free-free resonant column (FFRC) tests provides a convenient way to nondestructively monitor the increase in the modulus of the concrete which can potentially lead to a more objective way of determining the initial and final set. Acquisition of maturity provides for a complementary approach for the determination of set and strength with time. Once the specimens were monitored for seven days, their compressive strength can be determined for relating modulus and maturity to strength.

A thermal camera was also used to model the dissipation of heat from the concrete specimens over the course of the first 48 hours as they cured. This was performed to gain further insight on the impact of the ambient temperature and humidity on the curing of the concrete.

## 6.2    Limitations of Research

Although a robust number of cylinders were tested during this research, several limitations related to this study should be enumerated. Most limitations dealt with the limited number of perturbations of the parameters due to the time limitations. The continuous monitoring of the reference mix under standard curing (100% humidity and $70^{\circ}$F) as a "true reference" was not possible because of the prototype nature of the system developed. Further, no monitoring of internal humidity occurred, which could potentially further model the termination of hydration.

Since concrete mixes are usually designed based on compressive strength, neither the tensile strength nor flexural strength of the concrete was studied due to time constraints and limited space in the temperature control chamber. Another limitation in the process is that direct correlation to standard maturity and seismic modulus to strength development were only obtained for the specimens tested after seven days of curing.

## 6.3    Recommendations for Future Research

Of the limitations just discussed, there is great potential for future work to fill research gaps. Areas of focus would be a reference mix comprised of only Portland cement with no SCMs or admixtures and comprising of a single Coarse Aggregate. From this mix, it is recommended to add different chemical admixtures in five quantities to yield further, comprehensive understanding of the effects. This will also identify a point of diminishing returns for the ideal amount of chemical admixture to use for the desired results. Additionally, changes in the aggregate types and gradation

will verify if similar trends continue to appear and allow identification of any potential correlations.

To obtain a more comprehensive modeling approach, it is recommended to expand the study to a 28-day and/or 56-day analysis period. This will also provide a wider testing window to observe maturity and strength and stiffness development. Based on initial observations of the modulus-strength and standard maturity-strength relationships, the potential exist to determine base coefficients and adjustment factors for application towards variable, mix-related parameters and environmental conditions.

Another recommendation, is to expand the environmental testing conditions to account for additional temperatures and humidity levels. This can more comprehensively represent the varying climate zones in Texas. In addition, all approaches discussed could be further refined to account for additional mix-related parameters, variants and testing conditions.

The alternative TTF approach provides an additional method to visualize and interpret the maturity process. Additional test variants (representing a wider range of environmental and mix-related parameters) would provide for an opportunity to expand on the interpretation and development of alternative TTF analysis metrics. From this, improvement to data analysis visualization of the complete curing process can be improved for implementation towards practical application.

Other future research can utilize this test procedure and apply the process to field testing. Results from the field testing can confirm that the effects of admixtures fall within the range determined in lab testing. This can provide better understanding to contractors and agencies. Additionally, this can provide a more precise method that can be leveraged in determining when to make saw cuts and remove formwork.

# References

Alexander, K. M. (1972). "The Relationship Between Strength and the Composition and Fineness of Cement." *Cement and Concrete Research*, 2, 663–680.

Ashraf, W.B. and Noor, M.A., 2011. Performance-evaluation of concrete properties for different combined aggregate gradation approaches. *Procedia engineering*, *14*, pp.2627-2634.

ASTM C1074. (2017). "Estimating Concrete Strength by the Maturity Method." *American Society for Testing and Materials*.

ASTM C125. (2019). "Standard Terminology Relating to Concrete and Concrete Aggregates." *American Society for Testing and Materials*.

ASTM C191. (2019). "Standard Test Methods for Time of Setting of Hydraulic Cement by Vicat Needle." *American Society for Testing and Materials*.

ASTM C215. (2014). "Standard Test Method for Fundamental Transverse , Longitudinal , and Torsional Resonant Frequencies of Concrete Specimens." *American Society for Testing and Materials*.

ASTM C403. (2016). "Standard Test Method for Time of Setting of Concrete Mixtures by Penetration Resistance." *American Society for Testing and Materials*.

ASTM C618. (2019). "Standard Specification for Coal Fly Ash and Raw or Calcined Natural Pozzolan for Use in Concrete" *American Society for Testing and Materials*.

Azari, H., and Nazarian, S. (2015). *Exploratory Study of Use of Surface Waves to Determine Defects in Concrete*.

Azenha, M., Faria, R., and Figueiras, H. (2011). "Thermography as a Technique for Monitoring Early Age Temperatures of Hardening Concrete." *Construction and Building Materials*, Elsevier Ltd, 25(11), 4232–4240.

Babu, K. G., and Apparao, C. V. (1996). "Strength Behaviour of Concretes Containing Metakaolin." *Design Quality in Higher Education Buildings*, R. K. Dhir, M. D. Newlands, and L. J. Csetenyi, eds., 231–239.

Badogiannis, E., Tsivilis, S., Papadakis, V. G., and Chaniotakis, E. (2002). "The Effect of Metakaolin on Concrete Properties." *Innovations and Developments In Concrete Materials And Construction*, R. K. Dhir, P. C. Hewlett, and L. J. Csetenyi, eds., 81–89.

Ballim, Y., and Graham, P. C. (2004). "Early-Age Heat Evolution of Clinker Cements in Relation to Microstructure and Composition: Implications for Temperature Development in Large Concrete Elements." *Cement and Concrete Composites*, 26(5), 417–426.

Benaicha, M., Burtschell, Y., and Alaoui, A. H. (2016). "Prediction of Compressive Strength at Early Age of Concrete - Application of Maturity." *Journal of Building Engineering*, 6, 119–125.

Bentz, D. P. (2008). "A Review of Early-Age Properties of Cement-Based Materials." *Cement and Concrete Research*, 38(2), 196–204.

Bertagnoli, G., Mancini, G., and Tondolo, F. (2009). "Numerical Modelling of Early-Age Concrete Hardening." *Magazine of Concrete Research*, 61(4), 299–307.

Burg, Ronald G. (1996), *The influence of Casting and Curing Temperature on the Properties of Fresh and Hardened Concrete,* Research and Development Bulletin RD113, Portland Cement Association, Skokie, Illlinois, U.S.A.

Büyüköztürk, O. (1998). "Imaging of Concrete Structures." *NDT & E International*, 31(4), 233–243.

Caldarone, M. A. (2009). *High-Strength Concrete: A Practical Guide*. Taylor & Francis.

Clark, M. ., McCann, D. ., and Forde, M. . (2003). "Application of Infrared Thermography to the Non-Destructive Testing of Concrete and Masonry Bridges." *NDT & E International*, 36(4), 265–275.

Collier, Z., Rupnow, T., and Raghavendra, A. (2017). *Implementation of Maturity for Concrete Strength Measurement and Pay*.

Dinakar, P., and Ganesh Babu, K. (2006). "Strength Efficiency of Metakaolin in Concrete." *Structural Concrete*, 7(1), 27–31.

Ding, J. T., and Li, Z. (2002). "Effects of Metakaolin and Silica Fume on Properties of Concrete." *ACI Materials Journal*, 99(4), 393–398.

Fournier, B., Berube, M.-A., Folliard, K. J., and Thomas, M. (2010). *Report on the Diagnosis, Prognosis, and Mitigation of Alkali-Silica Reaction (ASR) in Transportation Structures*.

Gams, M., and Trtnik, G. (2013). "A New US Procedure to Determine Setting Period of Cement Pastes, Mortars, and Concretes." *Cement and Concrete Research*, Elsevier Ltd, 53, 9–17.

Giannini, E. R., Folliard, K. J., Zhu, J., Bayrak, O., Kreitman, K., Webb, Z., and Hanson, B. (2013). *Non-Destructive Evaluation of In-Service Concrete Structures Affected by Alkali-Silica Reaction (ASR) or Delayed Ettringite Formation (DEF)—Final Report, Part I*.

Glisic, B., and Simon, N. (2000). "Monitoring of Concrete at Very Early Age Using Stiff SOFO Sensor." *Cement and Concrete Composites*, 22, 115–119.

Guo, L., Guo, L., Zhong, L., and Zhu, Y. (2011). "Thermal Conductivity and Heat Transfer Coefficient of Concrete." *Journal of Wuhan University of Technology-Mater. Sci. Ed.*, 26(4), 791–796.

Hiasa, S., Birgul, R., Watase, A., Matsumtot, M., Mitani, K., and Catbas, F. N. (2014). "A Review of Field Implementation of Infrared Thermography as a Non-destructive Evaluation

Technology." *International Conference on Computing in Civil and Building Engineering*, 1715–1722.

Ismael, N. S., and Ghanim, M. N. (2015). "Properties of Blended Cement Using Metakaolin and Hydrated Lime." *Advances in Cement Research*, 27(6), 1–8.

Khan, M. . (2002). "Factors Affecting the Thermal Properties of Concrete and Applicability of its Prediction Models." *Building and Environment*, 37(6), 607–614.

Kosmatka, S. H., Kerkhoff, B., and Panarese, W. C. (2002). *Design and Control of Concrete Mixtures*. Portland Cement Association, Skokie, IL.

Kreitman, K. L. (2011). "Nondestructive Evaluation of Reinforced Concrete Structures Affected by Alkali-Silica Reaction and Delayed Ettringite Formation." The University of Texas at Austin.

Langan, B. W., Weng, K., and Ward, M. A. (2002). "Effect of Silica Fume and Fly Ash on Heat of Hydration of Portland Cement." *Cement and Concrete Research*, 32(7), 1045–1051.

Lara, G. W. (2008). "Quality Evaluation of Portland Cement Concrete at Early Age with Free-Free Resonant Column." The University of Texas at El Paso.

Lee, Y., Choi, M. S., Yi, S. T., and Kim, J. K. (2009). "Experimental Study on The Convective Heat Transfer Coefficient of Early-Age Concrete." *Cement and Concrete Composites*, Elsevier Ltd, 31(1), 60–71.

Lin, F., and Meyer, C. (2009). "Hydration Kinetics Modeling of Portland Cement Considering the Effects of Curing Temperature and Applied Pressure." *Cement and Concrete Research*, Elsevier Ltd, 39(4), 255–265.

Maser, K. R., and Roddis, W. M. K. (1990). "Principles of Thermography and Radar for Bridge Deck Assessment." *Journal of Transportaion Engineering*, 116(5), 583–601.

Mehta, P. K., and Monteiro, P. J. M. (2006). *Concrete: Microstructure, Properties, and Materials*. McGraw-Hill.

Mindess, S., Young, J. F., and Darwin, D. (2003). *Concrete*. Prentice Hall.

Nazarian, S., Yuan, D., Smith, K., Ansari, F., and Gonzalez, C. (2006). *Acceptance Criteria of Airfield Concrete Pavement Using Seismic and Maturity Concepts*.

Nazarian, S., Yuan, D., Weissinger, E., and McDaniel, M. (1997). "Comprehensive Quality Control of Portland Cement Concrete With Seismic Methods." *Transportation Research Record*, 1575(1), 102–111.

Neville, A. M. (1996). *Properties of Concrete*. John Wiley & Sons.

Newman, J., and Choo, B. S. (Eds.). (2003a). *Advanced Concrete Technology: Constituent Materials*. Elsevier.

Newman, J., and Choo, B. S. (Eds.). (2003b). *Advanced Concrete Technology: Concrete Properites*. Elsevier.

Newman, J., and Choo, B. S. (Eds.). (2003c). *Advanced Concrete Technology: Processes*. Elsevier.

Nixon, P., Fournier, B., and Thomas, M. (2016). "Options for Minimising the Risk of Alkali – Aggregate Reactions." *Proceedings*, 169(CM4).

Papadakis, V. G., and Tsimas, S. (2002). "Supplementary Cementing Materials in Concrete. Part I: Efficiency and Design." *Cement and Concrete Research*, 32(10), 1525–1532.

Parande, A. K., Chitradevi, R. H., Thangavel, K., Kartikeyan, M. S., Ganesh, B., and Palaniswamy, N. (2009). "Metakaolin: A Versatile Material to Enhance the Durability of Concrete – An Overview." *Structural Concrete*, 10(3), 125–138.

Payá, J., Monzó, J., Peris-Mora, E., Borrachero, M. V., Tercero, R., and Pinillos, C. (1995). "Early-Strength Development of Portland Cement Mortars Containing Air Classified Fly Ashes." *Cement and Concrete Research*, 25(2), 449–456.

Pla-Rucki, G. F., and Eberhard, M. O. (1995). "Imaging of Reinforced Concrete: State-of-the-Art Review." *Journal of Infrastructure Systems*, 1(2), 134–141.

Popovics, S. (1982). *Fundamentals of Portland Cement Concrete: A Quantitaive Approach Volume 1: Fresh Concrete*. John Wiley & Sons.

Schindler, A. K., and Folliard, K. J. (2005). "Heat of Hydration Models for Cementitious Materials." *ACI Materials Journal*, 102(1), 24–33.

Swaddiwudhipong, S., Chen, D., and Zhang, M. H. (2002). "Simulation of the Exothermic Hydration Process of Portland Cement." *Advances in Cement Research*, 14(2), 61–69.

Targan, C. ¸ Olgun, A., Erdogan, Y., and Sevinc, V. (2002). "Effects of Supplementary Cementing Materials on the Properties of Cement and Concrete." *Cement and Concrete Research*, 32(10), 1551–1558.

"Thermal Conductivity of Common Materials and Gases." (2003). *Engineering ToolBox*, <https://www.engineeringtoolbox.com/thermal-conductivity-d_429.html> (Mar. 23, 2018).

Thomas, M. D. A., Fournier, B., and Folliard, K. J. (2012). *Selecting Measures to Prevent Deleterious Alkali-Silica Reaction in Concrete: Rationale for the AASHTO PP65 Prescriptive Approach*.

Thomas, M. D. A., Fournier, B., and Folliard, K. J. (2013). *Alkali-Aggregate Reactivity (AAR) Facts Book*.

Transportation, T. D. of. (2016). "Chemcial Admixtures for Concrete."

TxDOT. (2014). "Standard Specifications for Construction and Maintenance of Highways, Streets, and Bridges." *TxDOT*.

TxDOT Designation: Tex-426-A. (2010). *Estimating Concrete Strength by the Maturity Method. TxDOT*.

Weil, G. J. (1991). "Infrared Thermographic Techniques." *CRC Handbook on Nondestructive Testing of Concrete*, V. M. Malhotra and N. J. Carino, eds., CRC Press.

Yi, S. T., Moon, Y. H., and Kim, J. K. (2005). "Long-term strength prediction of concrete with curing temperature." *Cement and Concrete Research*, 35(10), 1961–1969.

Yikici, T. A., and Chen, H. L. (2015). "Use of Maturity Method to Estimate Compressive Strength of Mass Concrete." *Construction and Building Materials*, Elsevier Ltd, 95, 802–812.

Yuan, D., Nazarian, S., and Medichetti, A. (2003). *A Methodology for Optimizing Opening of PCC Pavements to Traffic*.

Yuan, D., Nazarian, S., Perea, A., and Zhang, D. (2005). *Relating Seismic Modulus to Strength Parameters of Portland Cement Concrete*.

# Appendix A: Internal Temperature Trends Based on Mix Changes
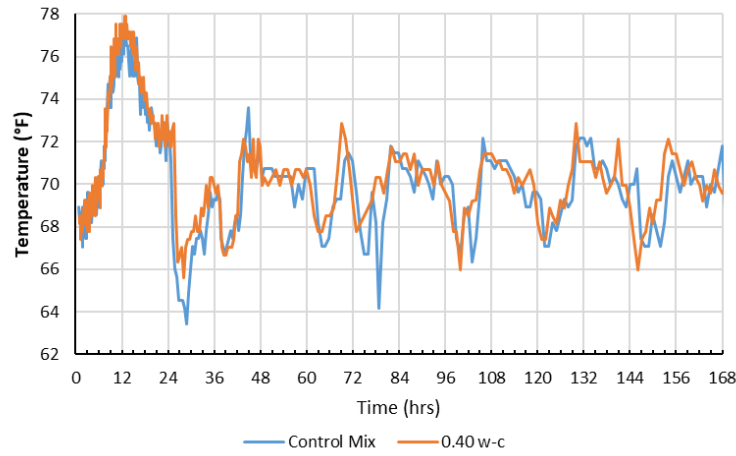


**Figure A.1 Internal Temperature Trends from Change in Water-Cement Ratio**
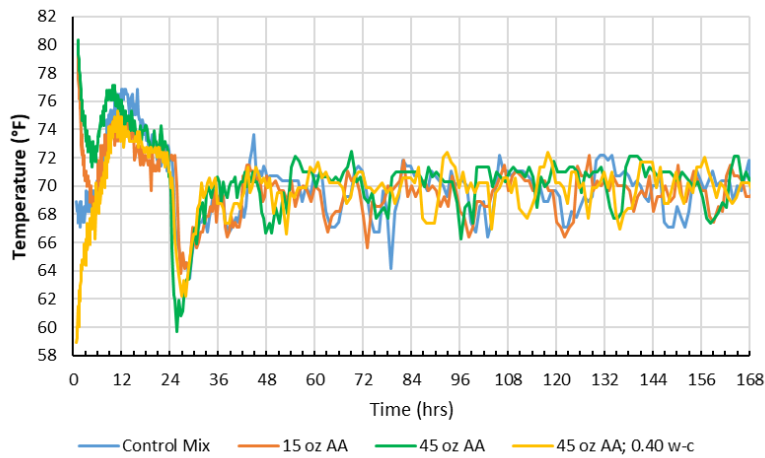


**Figure A.2 Internal Temperature Trends from Addition of Accelerating Agent**
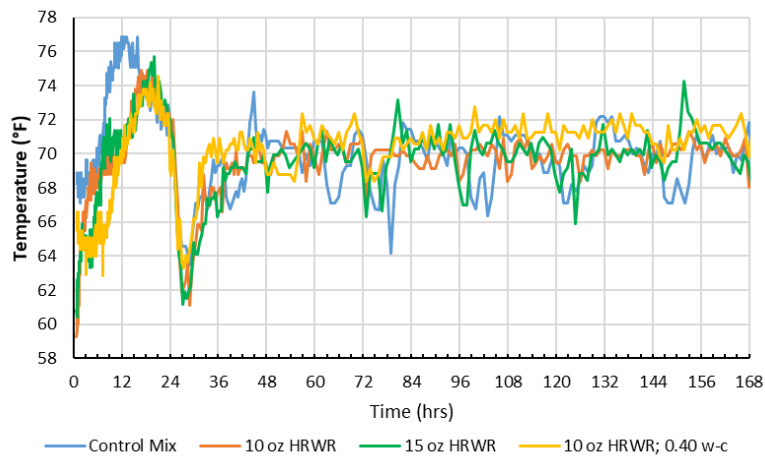


**Figure A.3 Internal Temperature Trends from Addition of HRWR**
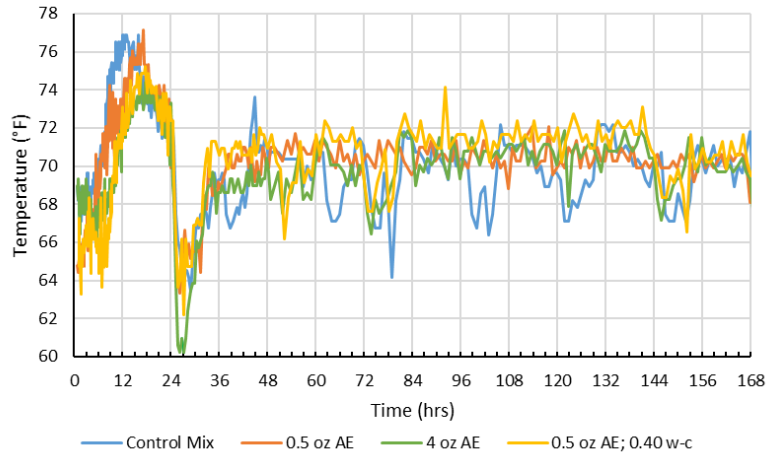
**Figure A.4 Internal Temperature Trends from Addition of AEA**
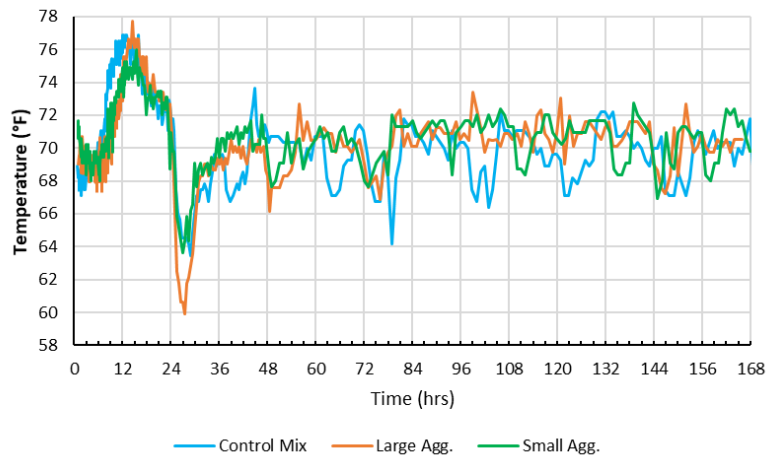


**Figure A.5 Internal Temperature Trends from Change in Coarse Aggregate**

# Appendix B: Alternative TTF Trends

**Dolomite Mix**

**Gravel Mix**



**Figure B.1 Alternative TTF at High Humidity**



**Figure B.2 Alternative TTF at Low Humidity**



**Figure B.3 Alternative TTF at 50°F Curing**
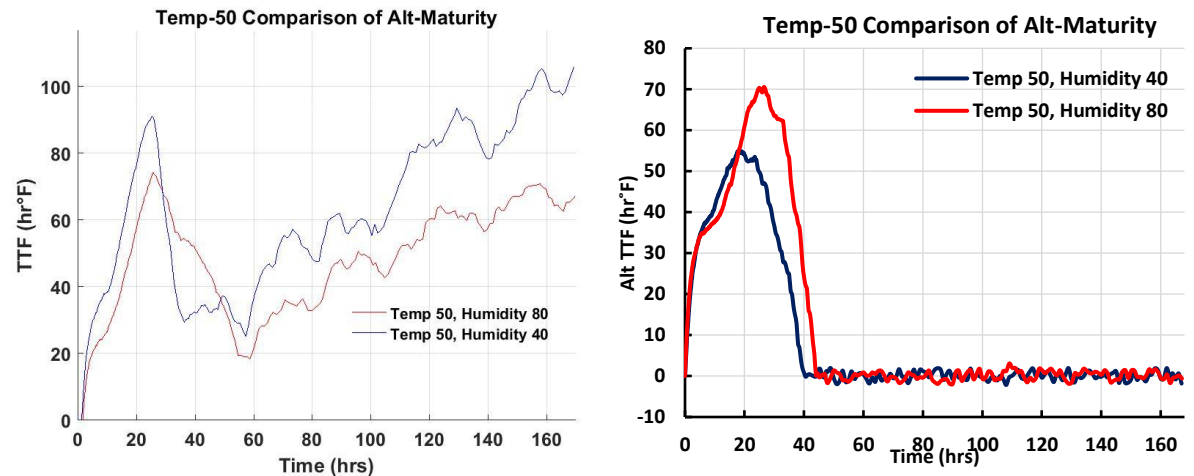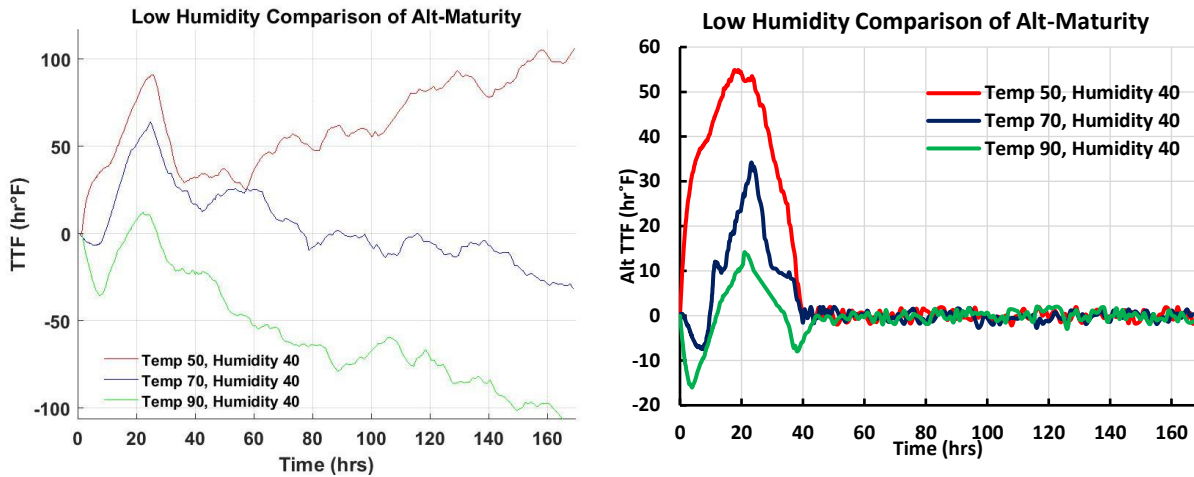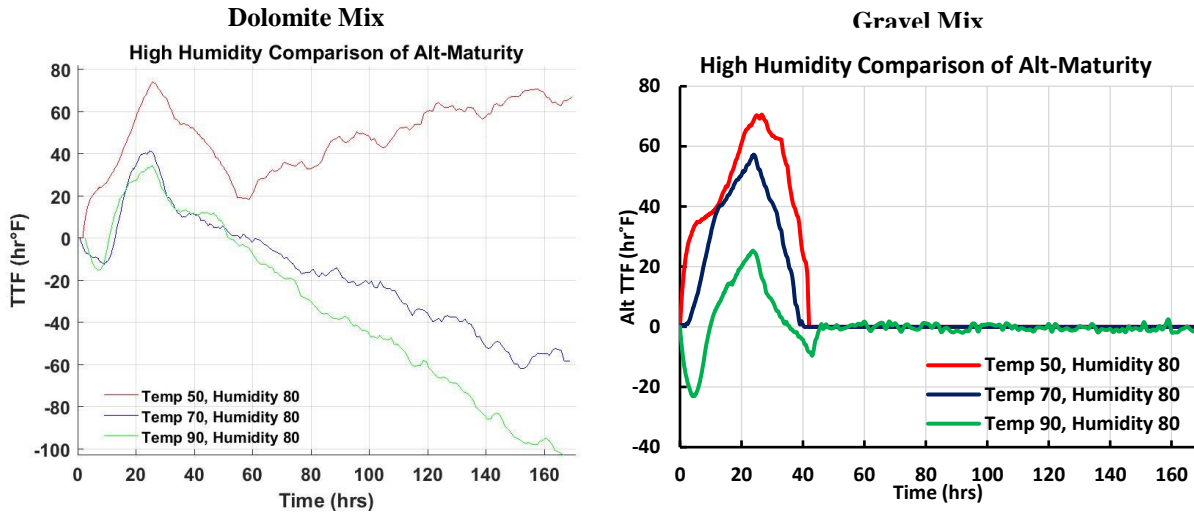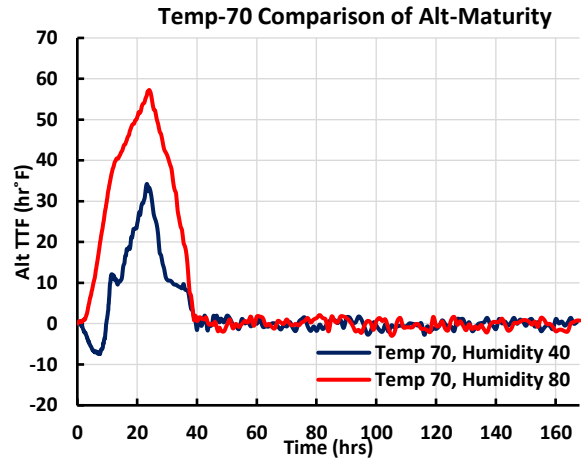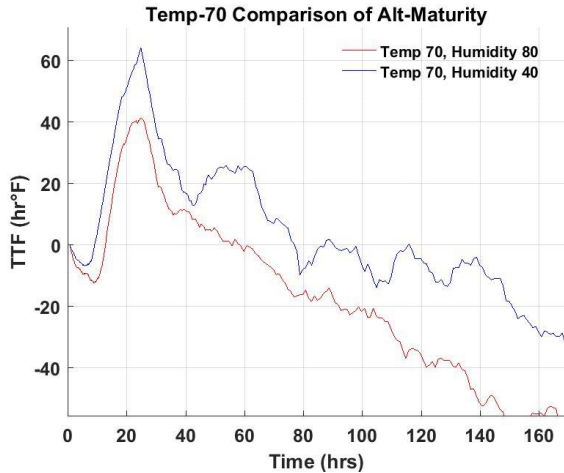
**Figure B.4 Alternative TTF at 70°F Curing**
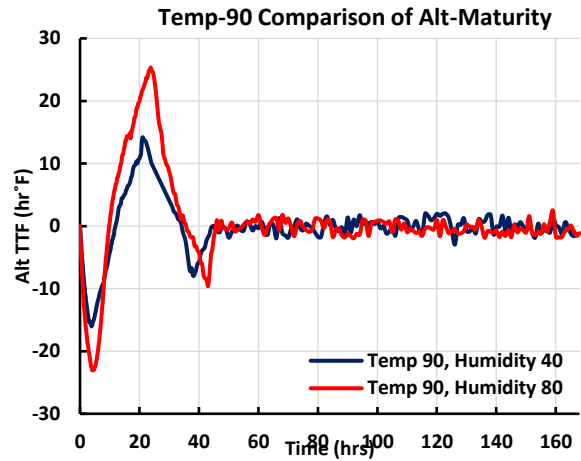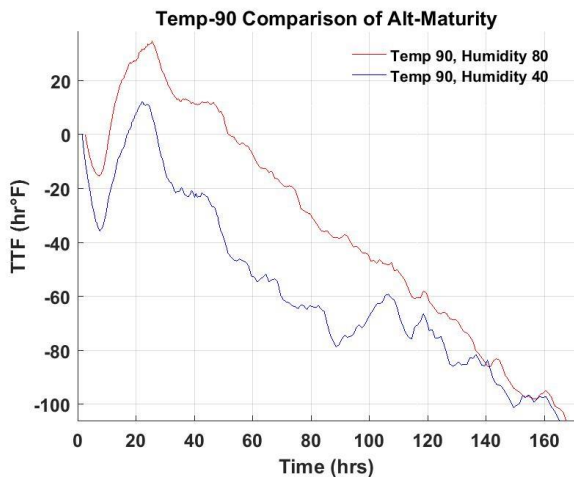


**Figure B.5 Alternative TTF at 90°F Curing**
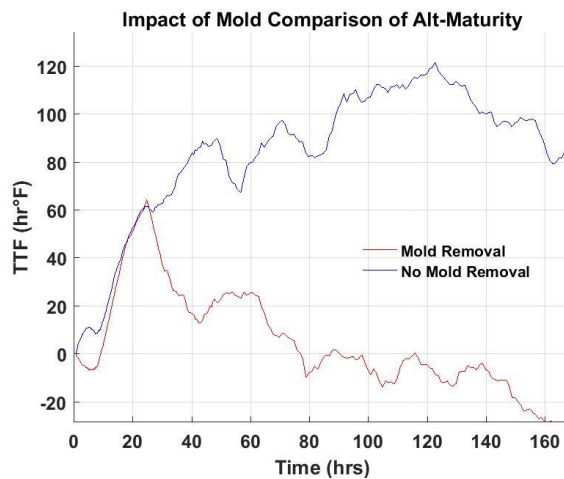


**Figure B.6 Alternative Maturity Impacts from Mold of Specimens Cured at 70°F and 40%**

**Humidity**

126
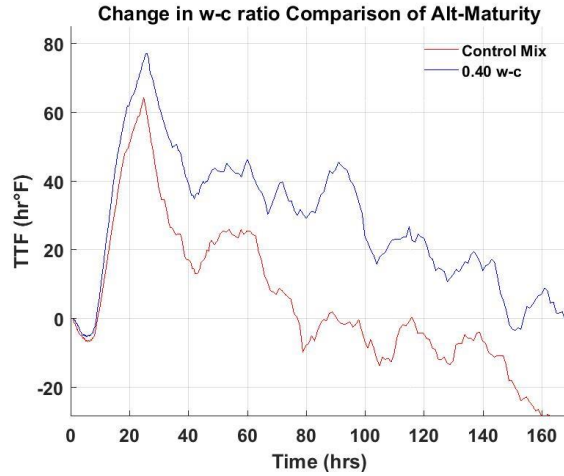
**Figure B.7 Alternative Maturity Impacts from Change in Water-Cement Ratio**
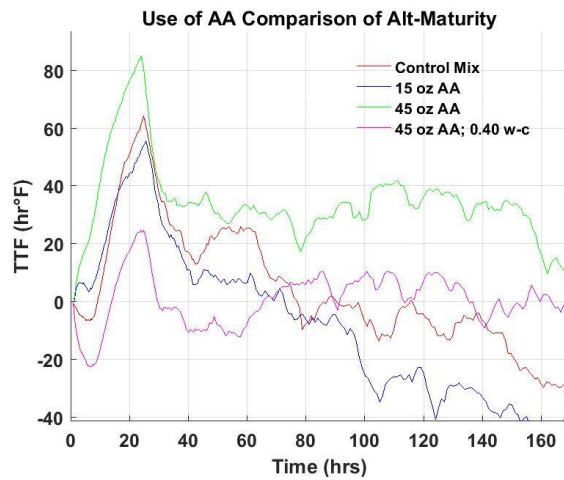


**Figure B.8 Alternative Maturity Impacts from Addition of Accelerating Agent**
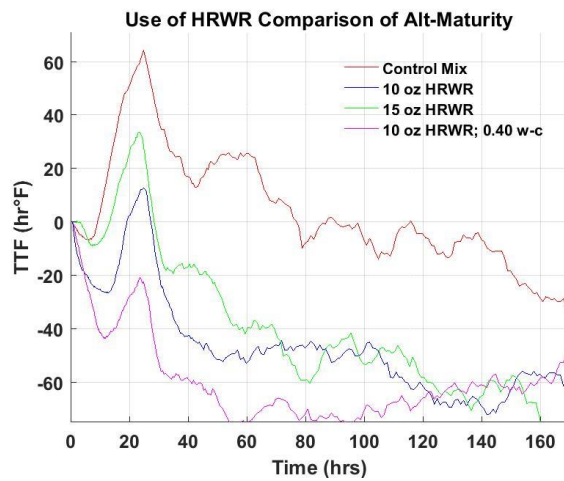


**Figure B.9 Alternative Maturity Impacts from Addition of HRWR**
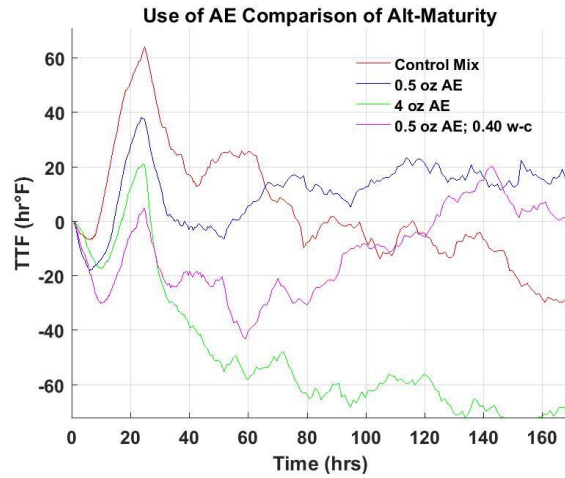
**Figure B.10 Alternative Maturity Impacts from Addition of AEA**
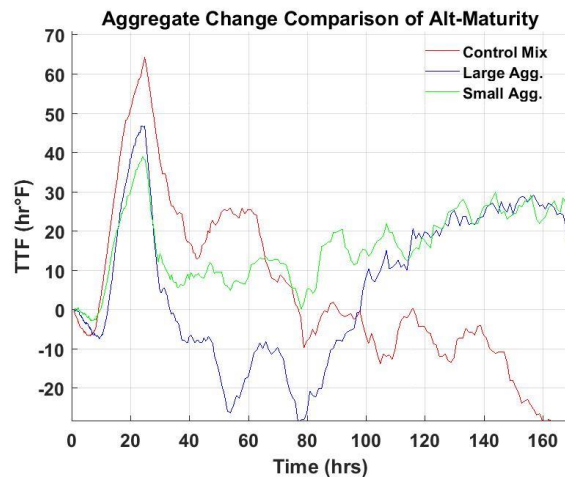


**Figure B.11 Alternative Maturity Impacts from Change in Coarse Aggregate Gradation**

128

# Appendix C: Thermal Profiles

Images on the left use penetration determined times of initial and final set while images on the right use the time based modulus approach to determine times of set
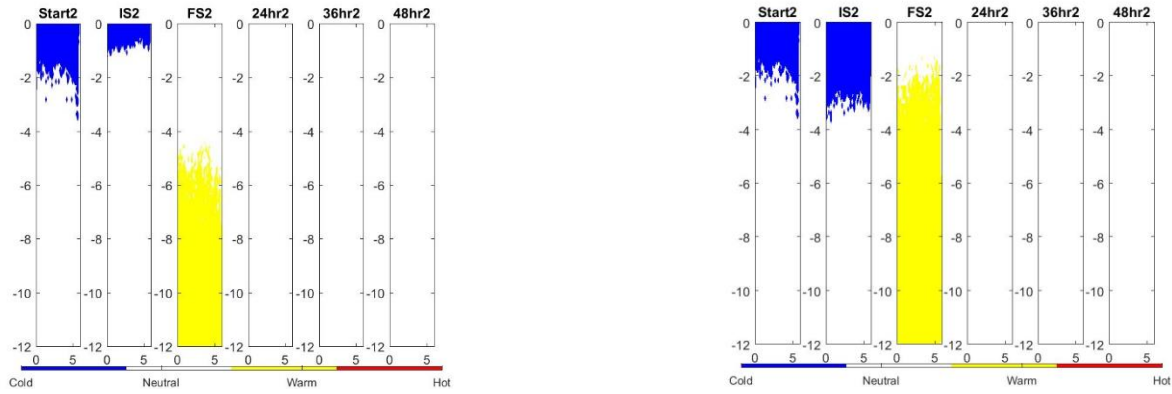


**Figure C.1 Thermal Profile of Reference Mix at 90°F and 40% RH**
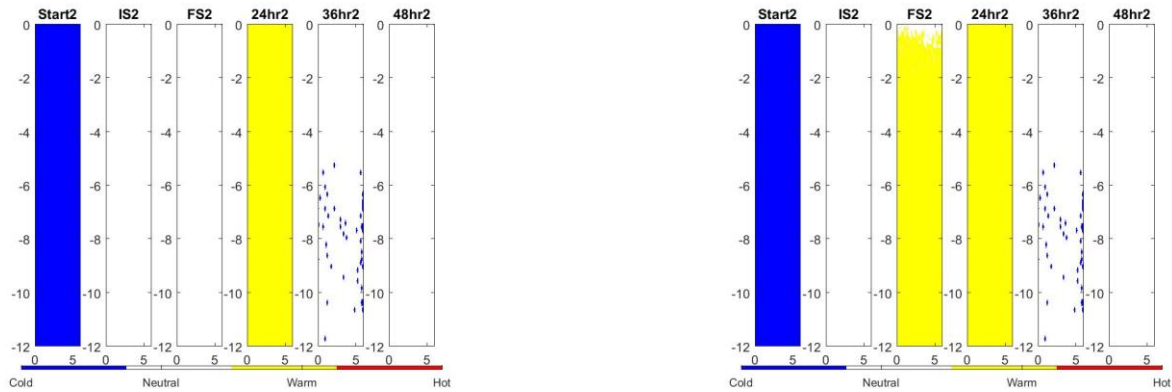


**Figure C.2 Thermal Profile of Reference Mix at 90°F and 80% RH**
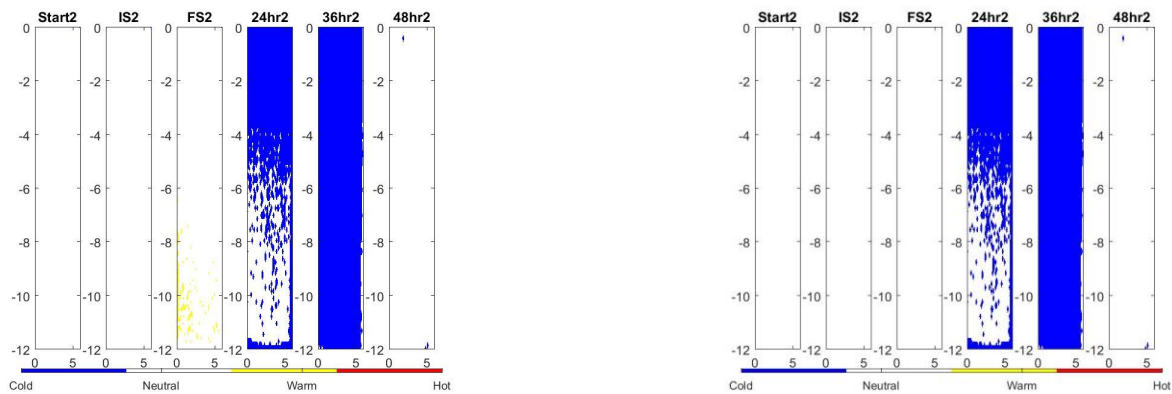


**Figure C.3 Thermal Profile of Reference Mix at 70°F and 40% RH**
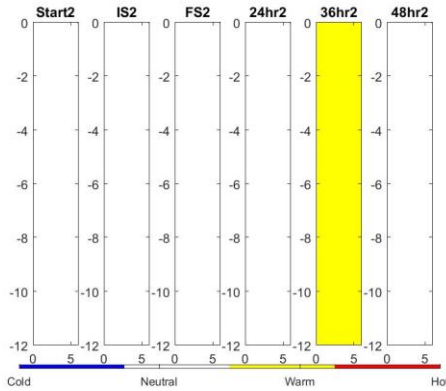
**Figure C.4 Thermal Profile of Reference Mix at 70°F and 80% RH**
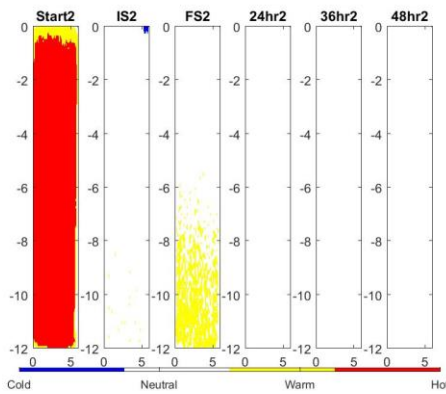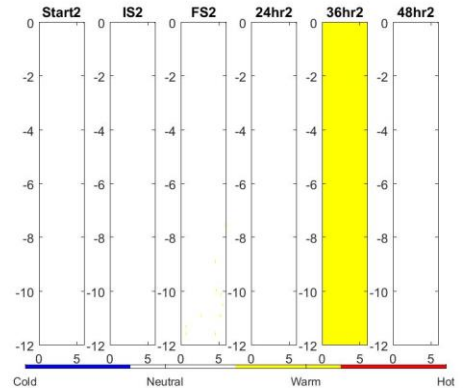

**Figure C.5 Thermal Profile of Reference Mix at 50°F and 40% RH**
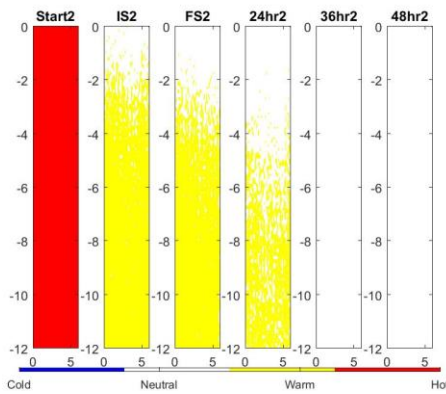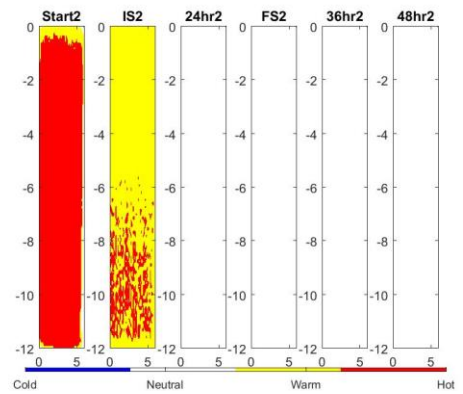

**Figure C.6 Thermal Profile of Reference Mix at 50°F and 80% RH**
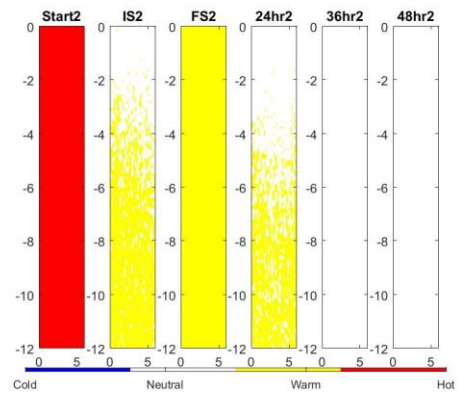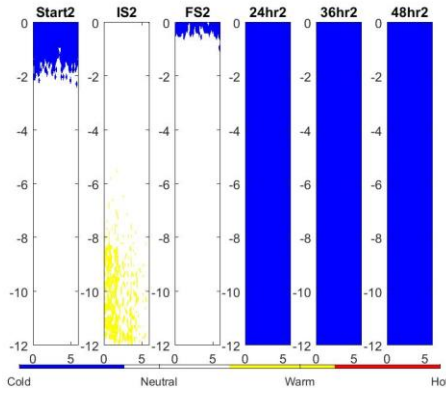
**Figure C.7 Thermal Profile of Mix with Water-Cement Ratio of 0.40**
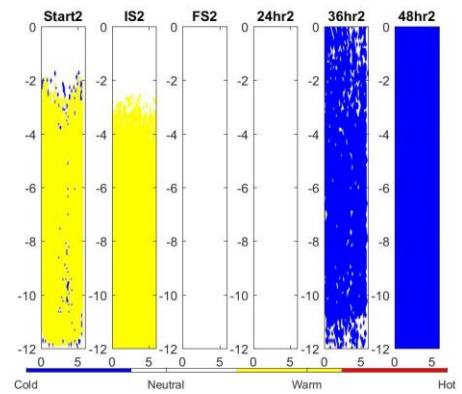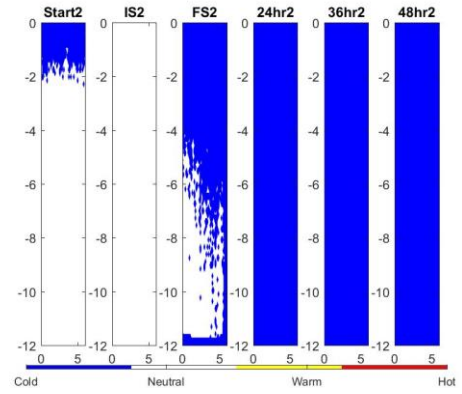


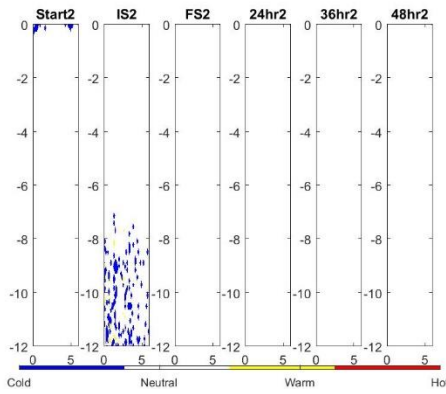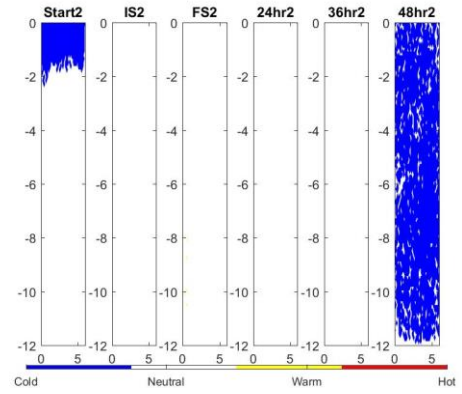**Figure C.8 Thermal Profile of Mix with 15 oz. of Accelerating Agent**
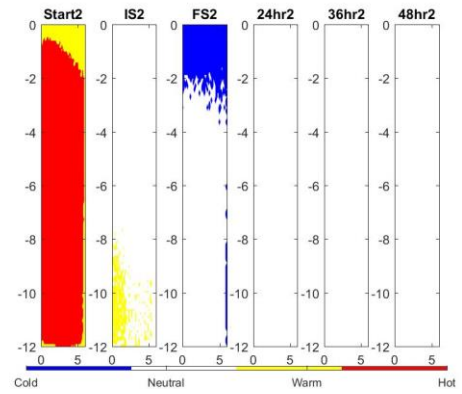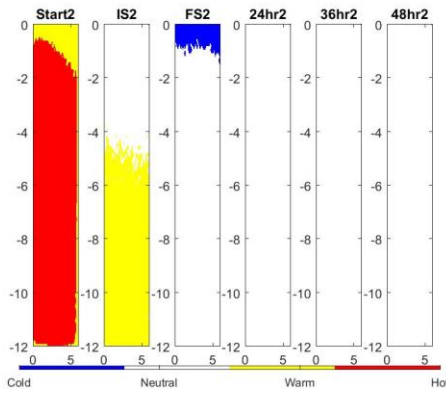


**Figure C.9 Thermal Profile of Mix with 45 oz. of Accelerating Agent**
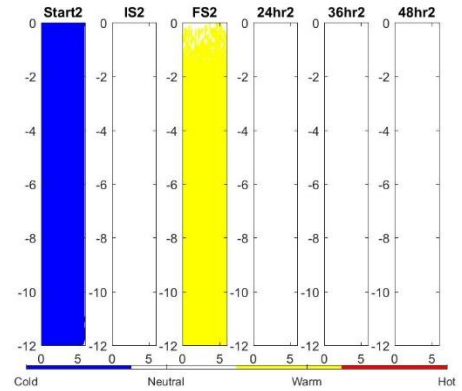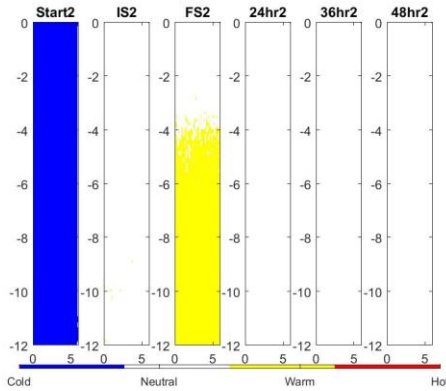
**Figure C.10 Thermal Profile of Mix with 45 oz. of Accelerating Agent and Water-Cement**

**Ratio of 0.40**
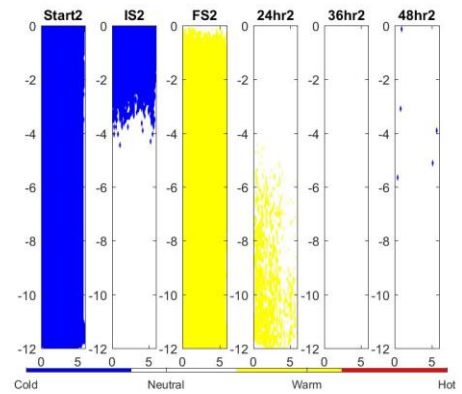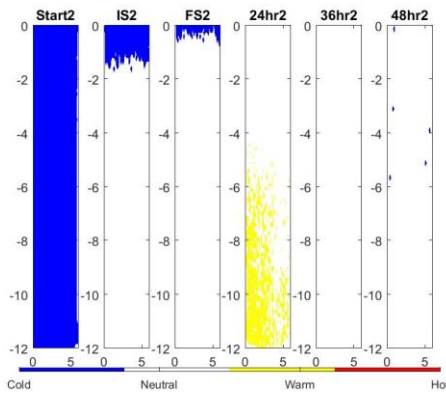


**Figure C.11 Thermal Profile of Mix with 10 oz. of HRWR**
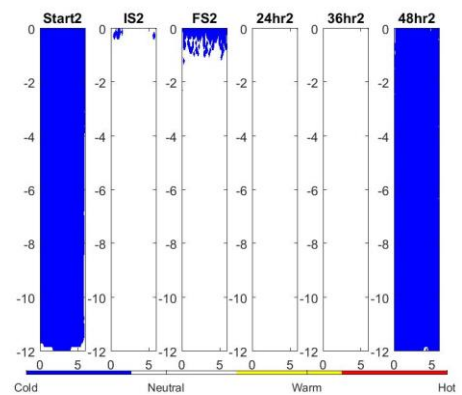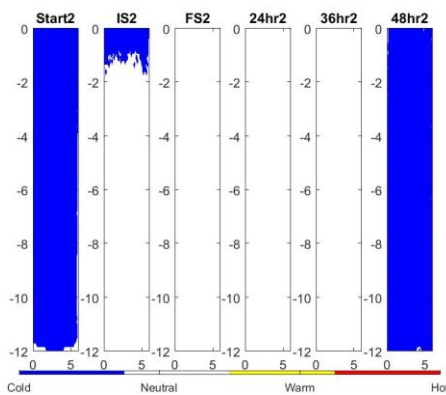


**Figure C.12 Thermal Profile of Mix with 15 oz. of HRWR**
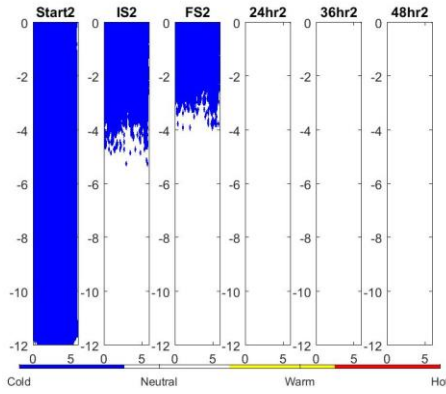
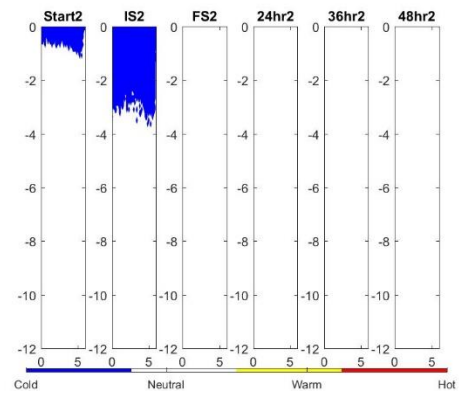**Figure C.13 Thermal Profile of Mix with 10 oz. of HRWR and Water-Cement Ratio of 0.40**
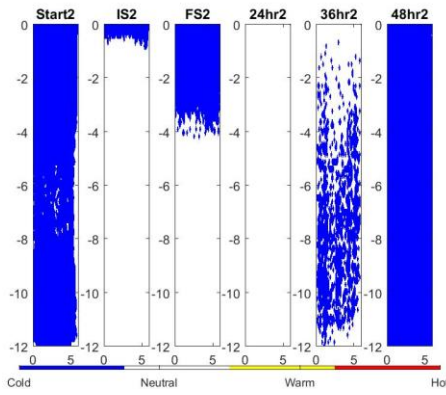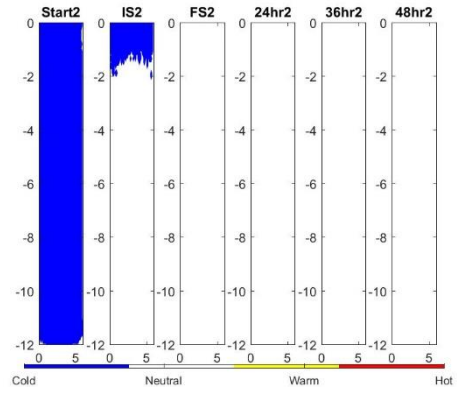


**Figure C.14 Thermal Profile of Mix with 0.5 oz. of AEA**
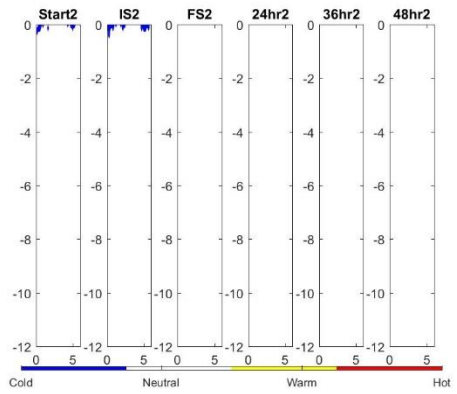


**Figure C.15 Thermal Profile of Mix with 4 oz. of AEA**
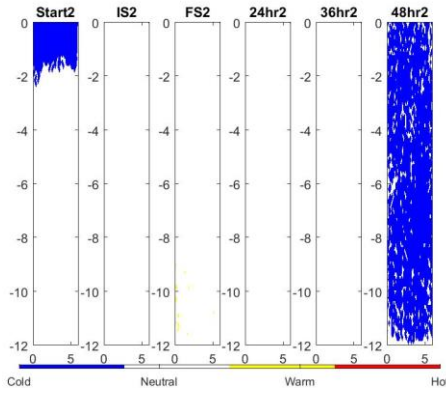
**Figure C.16 Thermal Profile of Mix with 0.5 oz. of AEA and Water-Cement Ratio of 0.40**
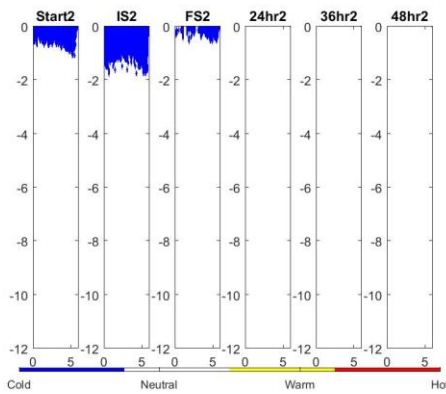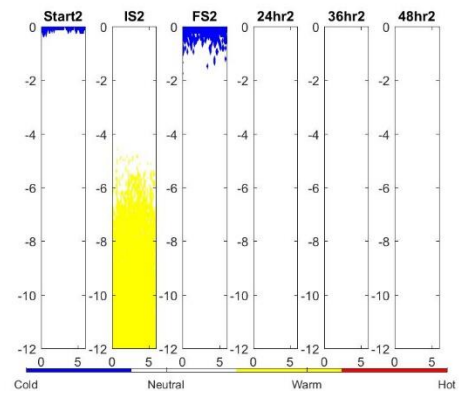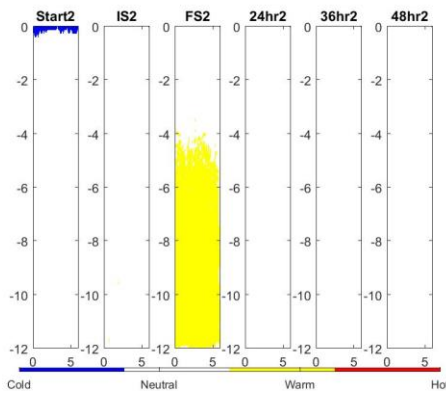

**Figure C.17 Thermal Profile of Mix with Large Aggregate**


**Figure C.18 Thermal Profile of Mix with Small Aggregate**